Osteosarcoma : searching for new treatment options

Baranski Madrigal, Z.

Osteosarcoma: searching for new treatment options

PROEFSCHRIFT

ter verkrijging van

de graad van Doctor aan de Universiteit Leiden,

op gezag van Rector Magnificus, prof. mr. C.J.J.M. Stolker,

volgens besluit van het College voor Promoties

te verdedigen op 26 Mei 2016

klokke 15:00 uur

door

Zuzanna Baranski Madrigal

geboren te San José, Costa Rica in 1981

Promotiecomissie

Promotor: Prof. Dr. B. van de Water
Promotor: Prof. Dr. P. Hogendoorn
Promotor: Prof. Dr. J. Bovée
Co-promotor: Dr. E.H.J. Danen
Overige leden: Prof. H. Gelderblom
Prof. H.J. Guchelaar
Prof. J. Bouwstra
Prof. P.H. van der Graaf
Prof. A. Flanagan

Cover By: Mónica Rodríguez
ISBN 9789462954434
An electronic version of this thesis can be found at
https://openaccess.leidenuniv.nl
Printed by: Uitgeverij BOXpress || proefschriftmaken.nl

This research was performed at the Division of Toxicology of the Leiden Academic Centre for Drug Research, Leiden University, Leiden, The Netherlands.

To my father and mother

Table of Contents

1

General introduction and outline of the thesis

1. What is Osteosarcoma?

Osteosarcoma is the most frequent high-grade primary malignant bone tumor that is thought to arise from mesenchymal stem cells with the capacity to produce osteoid.[1,2] The overall incidence is of three cases per million annually. Osteosarcoma occurs predominantly in children and adolescents, and in people over 50 years of age. It is located primarily in the metaphyseal region within the medullary cavity of long bones of the extremities (Fig. 1),[2,3] specifically in the knee area.[4] Other locations are the pelvis, ribs and spine, which are associated with worse outcome.[5,6]

Figure 1. Osteo-sarcoma of the distal femur

Osteosarcoma is classified into various histological subtypes: conventional, telangiectatic, small cell and other rare types. Conventional osteosarcoma is the most frequent, which originates in the medullary cavity of the metaphyseal region of long bones, and is mainly high grade. Telangiectatic represent less than 4% of the osteosarcomas. It is similar to conventional osteosarcoma in terms of clinical presentation, treatment and prognosis.[7] Small cell osteosarcoma is a rare entity with 1%-2% prevalence, and it resembles morphologically an Ewing sarcoma. However, small cell osteosarcoma has different genetic characteristics such as the absence of EWSR1 and FUS gene rearrangements, and the production of osteoid.[8–10]

Osteosarcoma diagnosis is only confirmed by the presence of osteoid in the biopsy. However, these malignant cells also have the capacity to produce cartilage matrix or fibrous tissue, which divides osteosarcoma in three categories: osteoblastic, chondroblastic and fibroblastic. Usually, a tumor shows all three matrix types, making it difficult to categorize it. The tumor will fall into one of these categories when it presents more than 50% of one of the histological types.[9]

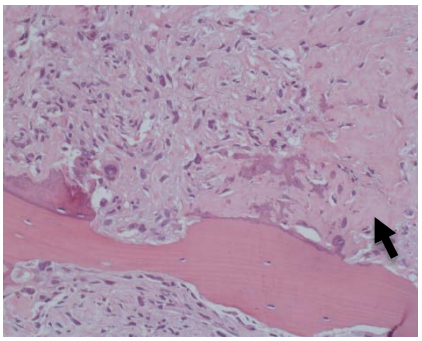

Figure 2. Primary osteosarcoma with osteoid (black arrow).

2. Etiology

2.1 Bone growth and turnover

Adolescent growth spurt coincides with the peak onset of osteosarcoma: girls show an earlier peak than boys which could be caused by their earlier growth spurt.[11] Research shows that there is higher incidence in boys (56%) compared to girls (42%).[12–14]

2.2 Predispositions

Paget's disease is characterized by a metabolic bone disorder leading to increased and disorganized bone formation.[15] It affects mainly people older than 50 years of age, and people with this disease present a 2% probability of developing osteosarcoma. Other predisposing factors are genetic disorders such as Li-Fraumeni syndrome, Rothmund-Thomson syndrome and Beckman-Wiederman syndrome.[11]

Li-Fraumeni syndrome is a hereditary disorder characterized by germline mutations in the *TP53* gene. This syndrome is characterized by the occurrence of sarcomas, among other cancers, in persons under the age of 45 years old.[16] These patients have a high risk of developing osteosarcoma. In fact, mice with $p53^{R172H/+}$ mutation showed 2 times increase in number of osteosarcomas compared to $p53^{+/-}$ mice,[17] and *p53*-null heterozygous mice present high numbers of osteosarcomas.[18,19]

Rothmund-Thomson syndrome is an autosomal recessive genodermatosis characterized by poikiloderma, short stature, premature aging and skeletal abnormalities among other features. Patients with this rare disease have a predisposition to develop osteosarcoma.[20,21] It was found that 60-65% of patients present mutations in the RECQL4 helicase gene suggesting a possible role of this gene in osteosarcoma development.[20]

Retinoblastoma is a hereditary disease that causes eye tumors in children. It is caused by mutations in *RB1* gene. Osteosarcoma is the most common secondary tumor that arises in these patients.[22,23]

Other rare genetic diseases such as Bloom, Werner, Rapadilino and Diamond blackfan are known for development of osteosarcoma among other malignancies.[22]

Finally, osteosarcomas arise secondary to radiation affecting mainly older patients. Studies show that sarcomas associated with radiation are uncommon. However, osteosarcomas are the main secondary tumor and represent 2.7-5.5% of osteosarcomas.[2,24,25]

3. Prognostic factors

There are several clinical characteristics that are predictors of clinical outcome. The outcome for patients that at the moment of diagnosis present with metastasis is still poor, and no improvement was observed with chemotherapy.[11,26,27] Additionally, the most common sites of recurrence are local and lung, presented in 20% and 62% of the cases respectively, and metastasis is correlated with poor survival.[28,29] Another important prognostic factor is the tumor site. Several studies report that tumors located in the axial skeleton have particularly poor outcome.[4–6,30] One of the requisites for a better control of the tumor is to achieve surgical excision with clean margins, and this is difficult for most of the axial tumors.[11] Response to chemotherapy is another variable that affects the outcome of these patients. Good responders are described as those with more than 90% of necrotic tissue after pre-operative chemotherapy. Several studies show that there is a correlation between good response to chemotherapy and prognosis.[31,32] Furthermore, tumor size is also considered a prognostic factor as indicated in a retrospective study of 331 osteosarcoma patients.[33–35] Finally, age is another prognostic factors. Older patients with osteosarcoma tend to have a worse prognosis than younger patients.[4,36,37]

4. Tumor Biology

Osteosarcoma cells are pleomorphic, anaplastic and hyperchromatic.[38] They are also characterized by complex karyotype as a result of chromosomal abnormalities that are different from cell to cell and from tumor to tumor (Fig. 2).[39,40] It was reported that copy number gains range from 7 to 190 and loses from 7 to 170 per sample. Gains are mainly located in chromosomes 6p, 8q/9p and 17p, and loses are in chromosomes 3q, 6q, 8p/9p, 11p, 15q and 17q among other aberrations.[41–43] These studies also show that genomic instability is correlated with poor prognosis and could be a cause of tumor initiation.[44] The fact that there is abundant genetic instability in osteosarcoma, makes it difficult to pinpoint genes involved in tumor progression, metastasis or response to chemotherapy. However, it is well established that genetic alterations in the tumor suppressor genes *Rb1* and *TP53* are consistent across osteosarcoma tumors.

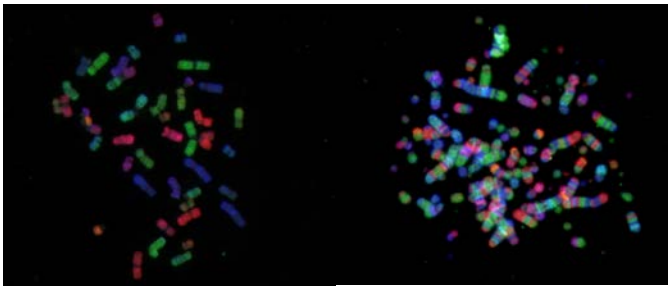

Figure 3. COBRA-FISH karyotype. Left) Normal human cell. Right) Osteosarcoma cell. Courtesy of Dr. Karolv Szuhai.

More than 70% of osteosarcomas have loss of heterozygosity (LOH) of the *TP53* gene, 20% present rearrangements, and 30% harbor mutations in *TP53*.[41,44,45] The *Rb1* gene was found to harbor LOH and mutations in more than 35% of osteosarcomas.[44,46,47] The establishment of a murine model with mutant or deleted p53 that leads to development of osteosarcomas spontaneously in more than 50% of the mice, confirms the role of p53 in osteosarcoma development.[19] Furthermore, MDM2 and COPS3, which are negative regulators of p53 that facilitate its proteasomal degradation, are amplified in 10% and 25% of osteosarcomas respectively.[48,49] The Rb protein binds to the E2F transcription factor, and this complex represses the transcription of genes necessary for cell cycle transition from G1 to S-phase.[50] The Rb protein is regulated by CDKN2A/p16 and CDK4/CDK6. CDK4/CDK6 phosphorylates Rb, thereby driving cell cycle progression, and CDKN2A/p16 inhibits the activation CDK4/CDK6.[51] It has been shown that in osteosarcoma *CDK4* is amplified in 10% of the tumors, and *CDKN2A/p16* is deleted in tumors that lack *Rb* mutations.[47,52–54] Deletion of *CDKN2A/p16* is correlated with poor prognosis.[1] Furthermore, a genome-wide expression study on a series of high-grade osteosarcomas compared to mesenchymal stem cells and osteoblasts, revealed significantly altered pathways in osteosarcoma such as upregulation of genes involved in mitosis and DNA replication.[55]

c-Myc and c-Fos are two proto-oncogenes that are regulators of cell cycle progression by modulating the cyclin-Cdk complex activity.[56,57] Expression of the *c-Myc* and *c-Fos* genes is increased in osteosarcoma.[58] One of the frequent genomic gains found in 34% of the cases is chromosome arm 8q, which contains the *c-Myc* proto-oncogene,[39,59] and its amplification is associated with poor overall survival and event-free survival.[47] In a genetic mouse model, 100% of transgenic mice overexpressing *c-Fos* were found to develop osteosarcoma.[58]

Receptor Tyrosine kinases (RTKs) are transmembrane receptors that are activated upon extracellular ligand binding such as growth factors, hormones and cytokines. They are mediators of the these environmental signals that lead to normal cellular processes like growth, proliferation, survival, differentiation and migration.[60] If these receptors are mutated or abnormally activated, they can be effective oncoproteins driving tumorigenesis.[61] The RTK family is composed of 58 members classified into 20 subfamilies[62] which include: epidermal growth factor receptors (EGFR), platelet-derived growth factor receptors (PDGFR), fibroblast growth factor receptors (FGFR), hepatocyte growth factor receptor (Met), insulin receptor (INSR), among others.[63]

The EGFR family is composed of EGFR, ERBB2, ERBB3 and ERBB4.[62] The *EGFR* gene was found to be amplified in 82% and expressed in 50% of osteosarcoma.[64,65] However, inhibition of EGFR in vitro had no effect on cell viability in vitro, and in osteosarcoma patients high EGFR expression is correlated with good prognosis.[66,67] There are contradicting results with respect to ERBB2 expression and its correlation with osteosarcoma prognosis, which could be due to study methodologies.[68–70] Inhibition of ERBB3 expression *in vitro* and *in vivo* reduces cell growth and invasiveness of osteosarcoma cells[71]. Studies on ERBB4 in osteosarcoma are limited but it was found to be paired with ERBB2 for its activation.[72]

PDGFR family is composed of CSF1R, KIT, FLT3, PDGFRα and PDGFRβ.[62] The *KIT* gene was found to be amplified in 57% of osteosarcoma patients.[73] PDGFRα/β were found to be expressed in osteosarcoma cell lines,[74] however, in osteosarcoma patients expression of PDGFRα is not correlated with overall survival.[75] No information is available on FLT3 and CSF1R in osteosarcoma.

The FGFR family includes FGFR1/2/3/4.[62] *FGFR1* gene has been reported to be amplified in 17% of the osteosarcoma cases, and it was significantly correlated with poor response to chemotherapy.[76] No studies have reported on the relation between FGFR2/3/4 expression and osteosarcoma.

Met is part of the Met family together with MST1R. Met is highly expressed in osteosarcoma, and it has been implicated in osteosarcomagenesis by inhibiting the differentiation of the osteo-progenitor cell population.[77,78] Additionally, Met expression was associated with ostesarcoma progression and aggressiveness.[79]

The INSR family groups the insulin receptor (IR) and the insulin-like growth factor 1 receptor (IGF-1R). IGF-1R is known to be expressed in osteosarcoma and its downstream signaling pathway was found to be altered in osteosarcoma.[80,81] However, IGF-1R expression is not proven to be a predictive marker for response to therapy with IGF-1R inhibitors.[82]

All these RTKs are activated by many different ligands, and to exert their effect they must activate downstream signaling pathways converting ligand binding into gene expression alterations. The pathway from cell surface to nucleus is mainly governed by: 1) the Ras/Raf/MEK/ERK cascade, 2) the PI3K/AKT pathway and 3) the Jak/STAT pathway.[83]

The Ras/Raf/MEK/ERK cascade is known to be involved in cell proliferation, apoptosis, differentiation and development. Activated cell surface receptors lead to ERK activation, which activates transcription factors such as c-Myc, c-Fos, Ets, and Elk-1.[84] This pathway is often deregulated in tumors caused by mutations or overexpression of upstream signaling components. *B-Raf* and *Ras* are frequently mutated in melanoma, colorectal cancer, ovarian cancer, lung cancer and pancreatic cancer among others.[85,86] In osteosarcoma, the ERK pathway was reported to be active in 67% of the cases analyzed, and mutations in B-RAF were only found in 13% of the cohort.[87] The PI3K pathway regulates processes such as proliferation, metabolism, apoptosis and cytoskeletal rearrangements.[88] In osteosarcoma, genetic screens have identified this pathway to be upregulated.[89–91] Recently, AKT2 was found to be overexpressed in osteosarcoma samples compared to normal tissue, and there was a positive correlation with shorter overall survival time.[92] Furthermore, it has been reported that STAT3 is overexpressed and constitutively active in osteosarcoma, and contributes to tumor progression.[93,94] Upstream of these three pathways is Src, a non-receptor tyrosine kinase that belongs to a family of 11 members.[95] It was shown that in osteosarcoma, Src expression and activity correlates with clinical stage and survival time.[96]

Finally, another important pathway involved in osteosarcoma development is Wnt/β-catenin. Active Wnt/β-catenin signaling stimulates osteogenic differentiation. This pathway was found to be inactive in osteosarcoma, thus facilitating dedifferentiation.[97]

5. Metastatic behavior

Osteosarcoma is a highly metastatic cancer. Approximately 20% of the patients present with pulmonary metastasis at the moment of diagnosis and when patients present with recurrence around 90% of the cases is in the lungs.[98] Ras/Raf/MEK/ERK activation downstream from IGF-1R has been shown to drive lung metastasis in an orthotopic mouse model.[99] The PI3K/AKT pathway is also involved in osteosarcoma metastasis. Several studies showed that this pathway is active in cell lines capable of forming metastatic lesions in mice[100] and that AKT activity is upregulated in anoikis-resistant cells.[101] As mentioned before, Src kinase activity can stimulate these pathways. Src regulates a variety of cellular processes such as cell morphology, migration, adhesion, survival and proliferation.[95] In cell-

matrix adhesions where integrin receptors connect the intracellular cytoskeleton to the extracellular matrix; Src forms a complex with focal adhesion kinase (Fak). Src phosphorylates Fak at multiple positions thereby creating a cell adhesion signaling platform that regulates cell-matrix adhesion dynamics and downstream signaling.[102] Fak is overexpressed in osteosarcoma, and it was shown to be involved in metastasis.[103] Another cytoskeleton-associated protein that influences the metastatic behavior of osteosarcoma is ezrin. Ezrin links the cytoskeleton to the plasma membrane allowing the cell to interact with the environment. In osteosarcoma, ezrin is necessary for initial survival once the cells metastasize, and this effect is dependent on ERK activity. Moreover, high expression of ezrin is correlated with poor survival.[104] Lastly, increased expression of vascular endothelial growth factor (VEGF), a factor that binds VEGF-R on endothelial cells and stimulates angiogenesis, has been reported as a prognostic marker in osteosarcoma[105].

6. Treatment options

Historically, osteosarcoma was treated with amputation of the limb, and the maximum 5-year survival rate was 20%. However, the majority of the patients died 2 years after diagnosis because of metastasis.[106] As surgical techniques advanced, resection of the tumor was possible with limb-salvage techniques, and it was proven to be as safe as amputation.[107] After the introduction of chemotherapy the disease survival rate increased to >50% with patients surviving more than 5 years.[108,109] Today, the treatment consists of preoperative chemotherapy followed by resection of the tumor. The most effective systemic chemotherapeutics are cisplatin,[110] doxorubicin[108] and methotrexate.[111] Despite extensive studies aimed at finding optimal combined chemotherapeutic strategies, overall 5-year survival rates have not increased above 70%. Furthermore, around 35-45% of the patients have tumors that do not respond to chemotherapy.[112–114] The mechanisms underlying such resistance are not well understood but may include p53 mutation as well as overexpression, rewiring of signaling pathways including PI3K/AKT and Ras/MAPK, and expression of ABC transporters.[115,116]

There is a clear need for alternatives to conventional chemotherapy or to drugs that suppress the resistance to chemotherapy. Genome-wide RNA interference (RNAi) screening to identify new drug targets and screening of chemical compound libraries hold the promise of identifying new strategies for molecularly targeted therapy. RNAi screens in osteosarcoma have identified the mTOR pathway (downstream from PI3K/AKT), CDK11, WEE1 as candidate

drug targets among others.[89,117–119] Other studies have reported that inhibition of Aurora A/B or polo-like kinase 1 sensitizes osteosarcoma cells to doxorubicin.[120,121]

Some of the candidate therapeutic targets have entered clinical testing in osteosarcoma patients. Recently, a clinical trial studying the effect of Alisertib (Aurora A inhibitor) was completed (NCT01154816). There are several ongoing clinical trials that are studying the inhibition of VEGFR in solid tumors (NCT02389244, NCT02432274, NCT02357810, NCT02243605). Others are studying the possibility of inhibiting Src with saracatinib (NCT00752206) and dasatinib in combination with chemotherapy (NCT00788125). Besides inhibiting kinases, other trials are investigating the effect of targeting the immune system (NCT02470091, NCT00743496, NCT00134030).

7. Aim and outline of this thesis

The aim of the studies described in this thesis was to discover new therapeutic options for osteosarcoma patients. I focused on finding candidate targets and pharmaceutical inhibitors for killing human osteosarcoma cells or for sensitizing osteosarcoma cells to the chemotherapeutical, doxorubicin. **Chapter 2** describes the role of Aven in cell cycle control in osteosarcoma cells. It shows that silencing Aven causes cell cycle arrest through downregulation of the checkpoint kinase, Chk1. It further explores the efficacy of small molecules targeting Chk1 in combination with doxorubicin. In **chapter 3**, the role of Bcl2 family members in osteosarcoma cell survival is studied using an RNAi library targeting members of this family. Identification of Bcl-xL and validation of this hit using small molecules is described for a panel of human osteosarcoma cell lines. In **Chapter 4** identification of MEK inhibitors in a chemical kinase inhibitor library screen is described. Results are presented pointing to MEK inhibitors as a candidate therapeutic option for osteosarcomas showing high MEK activity. **Chapter 5**, focuses on elucidating the effect of three Src inhibitors on osteosarcoma viability and cell migration using 2D cultures and validation in 3D culture systems. Lastly, **chapter 6** provides overall conclusions of the studies described in this thesis and describes future perspectives.

8. References

1. Mohseny, A. B. *et al.* Osteosarcoma originates from mesenchymal stem cells in consequence of aneuploidization and genomic loss of Cdkn2. *J. Pathol.* **219,** 294–305 (2009).

2. Rosenberg, A. . *et al.* in *WHO Classification of Tumours of Soft Tissue and Bone* (eds. Fletcher, C. D. M., Bridge, J. A., Hogendoorn, P. C. W. & Mertens, F.) 282–288 (2013).

3. Luetke, A., Meyers, P. A., Lewis, I. & Juergens, H. Osteosarcoma treatment - where do we stand? A state of the art review. *Cancer Treat. Rev.* **40,** 523–32 (2014).

4. Bielack, S. S. *et al.* Prognostic factors in high-grade osteosarcoma of the extremities or trunk: an analysis of 1,702 patients treated on neoadjuvant cooperative osteosarcoma study group protocols. *J. Clin. Oncol.* **20,** 776–90 (2002).

5. Ozaki, T. *et al.* Osteosarcoma of the spine: experience of the Cooperative Osteosarcoma Study Group. *Cancer* **94,** 1069–77 (2002).

6. Ozaki, T. *et al.* Osteosarcoma of the pelvis: experience of the Cooperative Osteosarcoma Study Group. *J. Clin. Oncol.* **21,** 334–41 (2003).

7. Sangle, N. A. & Layfield, L. J. Telangiectatic osteosarcoma. *Arch. Pathol. Lab. Med.* **136,** 572–6 (2012).

8. Kalil, R. K. & Squire, J. in *WHO Classification of Tumours of Soft Tissue and Bone* (eds. Fletcher, C. D. M., Bridge, J. A., Hogendoorn, P. C. W. & Mertens, F.) 291 (2013).

9. Klein, M. J. & Siegal, G. P. Osteosarcoma: anatomic and histologic variants. *Am. J. Clin. Pathol.* **125,** 555–81 (2006).

10. Righi, A. *et al.* Small Cell Osteosarcoma. *Am. J. Surg. Pathol.* **39,** 691–699 (2015).

11. Meyers, P. A. in *Pediatric Bone and Soft Tissue Sarcomas* (ed. Pappo, A.) 219–228 (Springer-Verlag, 2006).

12. Cotterill, S. J., Wright, C. M., Pearce, M. S. & Craft, A. W. Stature of young people with malignant bone tumors. *Pediatr. Blood Cancer* **42,** 59–63 (2004).

13. Longhi, A. *et al.* Height as a risk factor for osteosarcoma. *J. Pediatr. Hematol. Off. J. Am. Soc. Pediatr. Hematol.* **27,** 314–318 (2005).

14. Gelberg, K. H., Fitzgerald, E. F., Hwang, S. & Dubrow, R. Growth and development and other risk factors for osteosarcoma in children and young adults. *Int. J. Epidemiol.* **26,** 272–8 (1997).

15. Ralston, S. H. Pathogenesis of Paget's disease of bone. *Bone* **43,** 819–825 (2008).

16. Varley, J. M. Germline TP53 mutations and Li-Fraumeni syndrome. *Hum. Mutat.* **21,** 313–20 (2003).

17. Olive, K. P. *et al.* Mutant p53 gain of function in two mouse models of Li-Fraumeni syndrome. *Cell* **119,** 847–60 (2004).

18. Malkin, D. Li-fraumeni syndrome. *Genes Cancer* **2,** 475–84 (2011).

19. Donehower, L. a. The p53-deficient mouse: a model for basic and applied cancer studies. *Semin. Cancer Biol.* **7,** 269–278 (1996).

20. Larizza, L., Roversi, G. & Volpi, L. Rothmund-Thomson syndrome. 1–16 (2010).

21. Zils, K. *et al.* Osteosarcoma in Patients with Rothmund–Thomson Syndrome. *Pediatr. Hematol.* **32,** 32–40 (2015).

22. Calvert, G. T. *et al.* At-risk populations for osteosarcoma: the syndromes and beyond. *Sarcoma* **2012,** 152382 (2012).

23. Thériault, B. L., Dimaras, H., Gallie, B. L. & Corson, T. W. The genomic landscape of retinoblastoma: a review. *Clin. Experiment. Ophthalmol.* **42,** 33–52

24. Brady, M. S., Gaynor, J. J. & Brennan, M. F. Radiation-associated sarcoma of bone and soft tissue. *Arch. Surg.* **127,** 1379–85 (1992).

25. Sheppard, D. G. & Libshitz, H. I. Post-radiation sarcomas: a review of the clinical and imaging features in 63 cases. *Clin. Radiol.* **56,** 22–9 (2001).

26. Meyers, P. A. *et al.* Osteogenic sarcoma with clinically detectable metastasis at initial presentation. *J. Clin. Oncol.* **11,** 449–53 (1993).

27. Salah, S., Ahmad, R., Sultan, I., Yaser, S. & Shehadeh, a. Osteosarcoma with metastasis at initial diagnosis: Current outcomes and prognostic factors in the context of a comprehensive cancer center. *Mol. Clin. Onocology* **2,** 811–816 (2014).

28. Gelderblom, H. *et al.* Survival after recurrent osteosarcoma: data from 3 European Osteosarcoma Intergroup (EOI) randomized controlled trials. *Eur. J. Cancer* **47,** 895–902 (2011).

29. Ferrari, S. *et al.* Postrelapse survival in osteosarcoma of the extremities: prognostic factors for long-term survival. *J. Clin. Oncol.* **21,** 710–5 (2003).

30. Shives, T. C., Dahlin, D. C., Sim, F. H., Pritchard, D. J. & Earle, J. D. Osteosarcoma of the spine. *J. Bone Joint Surg. Am.* **68,** 660–8 (1986).

31. Hudson, M. *et al.* Pediatric osteosarcoma: therapeutic strategies, results, and prognostic factors derived from a 10-year experience. *J. Clin. Oncol.* **8,** 1988–97 (1990).

32. Picci, P. *et al.* Relationship of chemotherapy-induced necrosis and surgical margins to local recurrence in osteosarcoma. *J. Clin. Oncol.* **12,** 2699–705 (1994).

33. Bieling, P. *et al.* Tumor size and prognosis in aggressively treated osteosarcoma. *J. Clin. Oncol.* **14,** 848–58 (1996).

34. Lee, J. A. *et al.* Relative tumor burden predicts metastasis-free survival in pediatric osteosarcoma. *Pediatr. Blood Cancer* **50,** 195–200 (2008).

35. Kim, M. S. *et al.* Initial tumor size predicts histologic response and survival in localized osteosarcoma patients. *J. Surg. Oncol.* **97,** 456–61 (2008).

36. Hagleitner, M. M. *et al.* Age as prognostic factor in patients with osteosarcoma. *Bone* **49,** 1173–7 (2011).

37. Harting, M. T. *et al.* Age as a prognostic factor for patients with osteosarcoma: an analysis of 438 patients. *J. Cancer Res. Clin. Oncol.* **136,** 561–70 (2010).

38. Rozeman, L. B., Cleton-Jansen, A. M. & Hogendoorn, P. C. W. Pathology of primary malignant bone and cartilage tumours. *Int. Orthop.* **30,** 437–44 (2006).

39. Poos, K. *et al.* Genomic Heterogeneity of Osteosarcoma - Shift from Single Candidates to Functional Modules. *PLoS One* **10,** e0123082 (2015).

40. Squire, J. a. *et al.* High-resolution mapping of amplifications and deletions in pediatric osteosarcoma by use of CGH analysis of cDNA microarrays. *Genes Chromosom. Cancer* **38,** 215–225 (2003).

41. Kuijjer, M. L. *et al.* Identification of osteosarcoma driver genes by integrative analysis of copy number and gene expression data. *Genes. Chromosomes Cancer* **51,** 696–706 (2012).

42. Atiye, J. *et al.* Gene amplifications in osteosarcoma - CGH microarray analysis. *Genes Chromosom. Cancer* **42,** 158–163 (2005).

43. Ozaki, T. *et al.* Genetic imbalances revealed by comparative genomic hybridization in osteosarcomas. *Int. J. Cancer* **102,** 355–365 (2002).

44. Chen, X. *et al.* Recurrent somatic structural variations contribute to tumorigenesis in pediatric osteosarcoma. *Cell Rep.* **7,** 104–112 (2014).

45. Miller, C. W. *et al.* Frequency and structure of p53 rearrangements in human osteosarcoma. *Cancer Res.* **50,** 7950–7954 (1990).

46. Feugeas, O. *et al.* Loss of heterozygosity of the RB gene is a poor prognostic factor in patients with osteosarcoma. *J. Clin. Oncol.* **14,** 467–72 (1996).

47. Smida, J. *et al.* Genomic alterations and allelic imbalances are strong prognostic predictors in osteosarcoma. *Clin. Cancer Res.* **16,** 4256–4267 (2010).

48. Yan, T. *et al.* COPS3 amplification and clinical outcome in osteosarcoma. *Cancer* **109,** 1870–1876 (2007).

49. Lonardo, F., Ueda, T., Huvos, A. G., Healey, J. & Ladanyi, M. p53 and MDM2 alterations in osteosarcomas: Correlation with clinicopathologic features and proliferative rate. *Cancer* **79,** 1541–1547 (1997).

50. Giacinti, C. & Giordano, a. RB and cell cycle progression. *Oncogene* **25,** 5220–5227 (2006).

51. Malumbres, M. & Barbacid, M. Cell cycle, CDKs and cancer: a changing paradigm. *Nat. Rev. Cancer* **9,** 153–66 (2009).

52. Nielsen, G. P., Burns, K. L., Rosenberg, a E. & Louis, D. N. CDKN2A gene deletions and loss of p16 expression occur in osteosarcomas that lack RB alterations. *Am. J. Pathol.* **153,** 159–163 (1998).

53. Mohseny, A. B. *et al.* Small deletions but not methylation underlie CDKN2A/p16 loss of expression in conventional osteosarcoma. *Genes. Chromosomes Cancer* **49,** 1095–103 (2010).

54. Wei, G. *et al.* CDK4 gene amplification in osteosarcoma: Reciprocal relationship with INK4A gene alterations and mapping of 12q13 amplicons. *Int. J. Cancer* **80,** 199–204 (1999).

55. Cleton-Jansen, a-M. *et al.* Profiling of high-grade central osteosarcoma and its putative progenitor cells identifies tumourigenic pathways. *Br. J. Cancer* **101,** 1909–1918 (2009).

56. Sunters, A., Thomas, D. P., Yeudall, W. A. & Grigoriadis, A. E. Accelerated cell cycle progression in osteoblasts overexpressing the c-fos proto-oncogene: induction of cyclin A and enhanced CDK2 activity. *J. Biol. Chem.* **279,** 9882–91 (2004).

57. Mateyak, M. K., Obaya, A. J. & Sedivy, J. M. c-Myc regulates cyclin D-Cdk4 and -Cdk6 activity but affects cell cycle progression at multiple independent points. *Mol. Cell. Biol.* **19,** 4672–83 (1999).

58. Wu, J. X. *et al.* The proto-oncogene c-fos is over-expressed in the majority of human osteosarcomas. *Oncogene* **5,** 989–1000 (1990).

59. Bayani, J. *et al.* Spectral karyotyping identifies recurrent complex rearrangements of chromosomes 8, 17, and 20 in osteosarcomas. *Genes. Chromosomes Cancer* **36,** 7–16 (2003).

60. Rivera-Valentin, R. K., Zhu, L. & Hughes, D. P. M. Bone Sarcomas in Pediatrics: Progress in Our Understanding of Tumor Biology and Implications for Therapy. *Paediatr. Drugs* **17,** 257–71 (2015).

61. Gschwind, A., Fischer, O. M. & Ullrich, A. The discovery of receptor tyrosine kinases: targets for cancer therapy. *Nat. Rev. Cancer* **4,** 361–70 (2004).

62. Robinson, D. R., Wu, Y. M. & Lin, S. F. The protein tyrosine kinase family of the human genome. *Oncogene* **19,** 5548–57 (2000).

63. Hubbard, S. R. & Miller, W. T. Receptor tyrosine kinases: mechanisms of activation and signaling. *Curr. Opin. Cell Biol.* **19,** 117–23 (2007).

64. Freeman, S. S. *et al.* Copy number gains in EGFR and copy number losses in PTEN are common events in osteosarcoma tumors. *Cancer* **113,** 1453–61 (2008).

65. Wen, Y. H. *et al.* Epidermal growth factor receptor in osteosarcoma: expression and mutational analysis. *Hum. Pathol.* **38,** 1184–91 (2007).

66. Lee, J. A. *et al.* Epidermal growth factor receptor: is it a feasible target for the treatment of osteosarcoma? *Cancer Res. Treat.* **44,** 202–9 (2012).

67. Kersting, C. *et al.* Epidermal growth factor receptor expression in high-grade osteosarcomas is associated with a good clinical outcome. *Clin. Cancer Res.* **13,** 2998–3005 (2007).

68. Gorlick, S. *et al.* HER-2 expression is not prognostic in osteosarcoma; a Children's Oncology Group prospective biology study. *Pediatr. Blood Cancer* **61,** 1558–64 (2014).

69. Anninga, J. K. *et al.* Overexpression of the HER-2 oncogene does not play a role in high-grade osteosarcomas. *Eur. J. Cancer* **40,** 963–70 (2004).

70. Akatsuka, T. *et al.* ErbB2 expression is correlated with increased survival of patients with osteosarcoma. *Cancer* **94,** 1397–404 (2002).

71. Jullien, N. *et al.* ErbB3 silencing reduces osteosarcoma cell proliferation and tumor growth in vivo. *Gene* **521,** 55–61 (2013).

72. Hughes, D. P. M., Thomas, D. G., Giordano, T. J., Baker, L. H. & McDonagh, K. T. Cell surface expression of epidermal growth factor receptor and Her-2 with nuclear expression of Her-4 in primary osteosarcoma. *Cancer Res.* **64,** 2047–53 (2004).

73. Entz-Werle, N. *et al.* KIT gene in pediatric osteosarcomas: could it be a new therapeutic target? *Int. J. Cancer* **120,** 2510–6 (2007).

74. Hassan, S. E. *et al.* Cell surface receptor expression patterns in osteosarcoma. *Cancer* **118,** 740–9 (2012).

75. Sulzbacher, I., Birner, P., Dominkus, M., Pichlhofer, B. & Mazal, P. R. Expression of platelet-derived growth factor-alpha receptor in human osteosarcoma is not a predictor of outcome. *Pathology* **42,** 664–8 (2010).

76. Fernanda Amary, M. *et al.* Fibroblastic growth factor receptor 1 amplification in osteosarcoma is associated with poor response to neo-adjuvant chemotherapy. *Cancer Med.* **3,** 980–7 (2014).

77. Dani, N. *et al.* The MET oncogene transforms human primary bone-derived cells into osteosarcomas by targeting committed osteo-progenitors. *J. Bone Miner. Res.* **27,** 1322–34 (2012).

78. Patanè, S. *et al.* MET overexpression turns human primary osteoblasts into osteosarcomas. *Cancer Res.* **66,** 4750–7 (2006).

79. Oda, Y., Naka, T., Takeshita, M., Iwamoto, Y. & Tsuneyoshi, M. Comparison of histological changes and changes in nm23 and c-MET expression between primary and metastatic sites in osteosarcoma: a clinicopathologic and immunohistochemical study. *Hum. Pathol.* **31,** 709–16 (2000).

80. MacEwen, E. G. *et al.* IGF-1 receptor contributes to the malignant phenotype in human and canine osteosarcoma. *J. Cell. Biochem.* **92,** 77–91 (2004).

81. Kuijjer, M. L. *et al.* IR/IGF1R signaling as potential target for treatment of high-grade osteosarcoma. *BMC Cancer* **13,** 245 (2013).

82. Cao, Y. *et al.* Insulin-like growth factor 1 receptor and response to anti-IGF1R antibody therapy in osteosarcoma. *PLoS One* **9,** e106249 (2014).

83. Schlessinger, J. Receptor Tyrosine Kinases: Legacy of the First Two Decades. *Cold Spring Harb. Perspect. Biol.* **6,** a008912–a008912 (2014).

84. Zhang, W. & Liu, H. T. MAPK signal pathways in the regulation of cell proliferation in mammalian cells. *Cell Res.* **12,** 9–18 (2002).

85. Roberts, P. J. & Der, C. J. Targeting the Raf-MEK-ERK mitogen-activated protein kinase cascade for the treatment of cancer. *Oncogene* **26,** 3291–310 (2007).

86. McCubrey, J. A. *et al.* Roles of the Raf/MEK/ERK pathway in cell growth, malignant transformation and drug resistance. *Biochim. Biophys. Acta* **1773,** 1263–84 (2007).

87. Pignochino, Y. *et al.* Sorafenib blocks tumour growth, angiogenesis and metastatic potential in preclinical models of osteosarcoma through a mechanism potentially involving the inhibition of ERK1/2, MCL-1 and ezrin pathways. *Mol. Cancer* **8,** 118 (2009).

88. Vivanco, I. & Sawyers, C. L. The phosphatidylinositol 3-Kinase AKT pathway in human cancer. *Nat. Rev. Cancer* **2,** 489–501 (2002).

89. Moriarity, B. S. *et al.* A Sleeping Beauty forward genetic screen identifies new genes and pathways driving osteosarcoma development and metastasis. *Nat. Genet.* **47,** 615–624 (2015).

90. Kuijjer, M. L. *et al.* Kinome and mRNA expression profiling of high-grade osteosarcoma cell lines implies Akt signaling as possible target for therapy. *BMC Med. Genomics* **7,** 4 (2014).

91. Perry, J. A. *et al.* Complementary genomic approaches highlight the PI3K/mTOR pathway as a common vulnerability in osteosarcoma. *Proc. Natl. Acad. Sci. U. S. A.* **111,** E5564–73 (2014).

92. Zhu, Y., Zhou, J., Ji, Y. & Yu, B. Elevated expression of AKT2 correlates with disease severity and poor prognosis in human osteosarcoma. *Mol. Med. Rep.* **10,** 737–42 (2014).

93. Fossey, S. L. *et al.* Characterization of STAT3 activation and expression in canine and human osteosarcoma. *BMC Cancer* **9,** 81 (2009).

94. Ryu, K. *et al.* Activation of signal transducer and activator of transcription 3 (Stat3) pathway in osteosarcoma cells and overexpression of phosphorylated-Stat3 correlates with poor prognosis. *J. Orthop. Res.* **28,** 971–8 (2010).

95. Roskoski, R. Src protein-tyrosine kinase structure, mechanism, and small molecule inhibitors. *Pharmacol. Res.* **94,** 9–25 (2015).

96. Hu, C. *et al.* The prognostic significance of Src and p-Src expression in patients with osteosarcoma. *Med. Sci. Monit.* **21,** 638–45 (2015).

97. Cai, Y. *et al.* Inactive Wnt/beta-catenin pathway in conventional high-grade osteosarcoma. *J. Pathol.* **220,** 24–33 (2010).

98. Bacci, G. *et al.* High grade osteosarcoma of the extremities with lung metastases at presentation: treatment with neoadjuvant chemotherapy and simultaneous resection of primary and metastatic lesions. *J. Surg. Oncol.* **98,** 415–20 (2008).

99. Yu, Y., Luk, F., Yang, J.-L. & Walsh, W. R. Ras/Raf/MEK/ERK pathway is associated with lung metastasis of osteosarcoma in an orthotopic mouse model. *Anticancer Res.* **31,** 1147–52 (2011).

100. Fukaya, Y. *et al.* A role for PI3K-Akt signaling in pulmonary metastatic nodule formation of the osteosarcoma cell line, LM8. *Oncol. Rep.* **14,** 847–52 (2005).

101. Díaz-Montero, C. M., Wygant, J. N. & McIntyre, B. W. PI3-K/Akt-mediated anoikis resistance of human osteosarcoma cells requires Src activation. *Eur. J. Cancer* **42,** 1491–500 (2006).

102. McLean, G. W. *et al.* The role of focal-adhesion kinase in cancer - a new therapeutic opportunity. *Nat. Rev. Cancer* **5,** 505–15 (2005).

103. Feng, S., Shi, X., Ren, K. E., Wu, S. & Sun, X. Focal adhesion kinase is involved in the migration of human osteosarcoma cells. *Oncol. Lett.* **9,** 2670–2674 (2015).

104. Khanna, C. *et al.* The membrane-cytoskeleton linker ezrin is necessary for osteosarcoma metastasis. *Nat. Med.* **10,** 182–6 (2004).

105. Bajpai, J. *et al.* VEGF expression as a prognostic marker in osteosarcoma. *Pediatr. Blood Cancer* **53,** 1035–9 (2009).

106. Jenkin, R. D., Allt, W. E. & Fitzpatrick, P. J. Osteosarcoma. An assessment of management with particular reference to primary irradiation and selective delayed amputation. *Cancer* **30,** 393–400 (1972).

107. Simon, M. A., Aschliman, M. A., Thomas, N. & Mankin, H. J. Limb-salvage treatment versus amputation for osteosarcoma of the distal end of the femur. 1986. *J. Bone Joint Surg. Am.* **87,** 2822 (2005).

108. Cortes, E. P. *et al.* Amputation and adriamycin in primary osteosarcoma. *N. Engl. J. Med.* **291,** 998–1000 (1974).

109. Anninga, J. K. *et al.* Chemotherapeutic adjuvant treatment for osteosarcoma: Where do we stand? *Eur. J. Cancer* **47,** 2431–2445 (2011).

110. Gasparini, M. *et al.* Phase II study of cisplatin in advanced osteogenic sarcoma. European Organization for Research on Treatment of Cancer Soft Tissue and Bone Sarcoma Group. *Cancer Treat. Rep.* **69,** 211–3 (1985).

111. Jaffe, N. & Gorlick, R. High-dose methotrexate in osteosarcoma: let the questions surcease--time for final acceptance. *J. Clin. Oncol.* **26,** 4365–6 (2008).

112. Whelan, J. S. *et al.* EURAMOS-1, an international randomised study for osteosarcoma: results from pre-randomisation treatment. *Ann. Oncol.* **26,** 407–414 (2014).

113. Bielack, S. S. *et al.* Methotrexate, Doxorubicin, and Cisplatin (MAP) Plus Maintenance Pegylated Interferon Alfa-2b Versus MAP Alone in Patients With Resectable High-Grade Osteosarcoma and Good Histologic Response to Preoperative MAP: First Results of the EURAMOS-1 Good Respons. *J. Clin. Oncol.* **33,** 2279–87 (2015).

114. Ferrari, S. *et al.* Neoadjuvant chemotherapy with methotrexate, cisplatin, and doxorubicin with or without ifosfamide in nonmetastatic osteosarcoma of the extremity: an Italian sarcoma group trial ISG/OS-1. *J. Clin. Oncol.* **30,** 2112–8 (2012).

115. Chou, A. J. & Gorlick, R. Chemotherapy resistance in osteosarcoma: current challenges and future directions. *Expert Rev. Anticancer Ther.* **6,** 1075–85 (2006).

116. Pápai, Z. *et al.* P53 Overexpression as an Indicator of Overall Survival and Response to Treatment in Osteosarcomas. *Pathol. Oncol. Res.* **3,** 15–19 (1997).

117. Gupte, A. *et al.* Systematic Screening Identifies Dual PI3K and mTOR Inhibition as a Conserved Therapeutic Vulnerability in Osteosarcoma. *Clin. Cancer Res.* **21,** 3216–29 (2015).

118. Duan, Z. *et al.* Systematic kinome shRNA screening identifies CDK11 (PITSLRE) kinase expression is critical for osteosarcoma cell growth and proliferation. *Clin. Cancer Res.* **18,** 4580–8 (2012).

119. Yamaguchi, U. *et al.* Functional genome screen for therapeutic targets of osteosarcoma. *Cancer Sci.* **100,** 2268–74 (2009).

120. Tavanti, E. *et al.* Preclinical validation of Aurora kinases-targeting drugs in osteosarcoma. *Br. J. Cancer* **109,** 2607–18 (2013).

121. Sero, V. *et al.* Targeting polo-like kinase 1 by NMS-P937 in osteosarcoma cell lines inhibits tumor cell growth and partially overcomes drug resistance. *Invest. New Drugs* **32,** 1167–80 (2014).

2

Aven-mediated checkpoint kinase control regulates proliferation and resistance to chemotherapy in conventional osteosarcoma

Zuzanna Baranski, Tijmen H. Booij, Anne-Marie Cleton-Jansen, Leo Price, Bob van de Water, Judith V. M. G. Bovée, Pancras C.W. Hogendoorn, Erik H.J. Danen

Published in *J Pathol* **236**:348-359, 2015

ABSTRACT

Conventional high-grade osteosarcoma is the most common primary bone sarcoma with relatively high incidence in young people. Here, we found that expression of Aven is inversely correlated with metastasis-free survival in osteosarcoma patients and is increased in metastases compared to primary tumours. Aven is an adaptor protein that has been implicated in anti-apoptotic signaling and serves as an oncoprotein in acute lymphoblastic leukemia. In tumour cells, silencing Aven triggered a G2 cell cycle arrest. Chk1 protein levels were attenuated and ATR-Chk1 DNA damage response signaling in response to chemotherapy was abolished in Aven-depleted osteosarcoma cells while ATM, Chk2, and p53 activation remained intact. Osteosarcoma is notoriously difficult to treat with standard chemotherapy, and we examined whether pharmacological inhibition of the Aven-controlled ATR-Chk1 response could sensitize osteosarcoma cells to genotoxic compounds. Indeed, pharmacological inhibitors targeting Chk1/Chk2 or those selective for Chk1 synergized with standard chemotherapy in 2D cultures. Likewise, in 3D extracellular matrix-embedded cultures Chk1 inhibition led to effective sensitization to chemotherapy. Together, these findings implicate Aven in ATR-Chk1 signaling and point towards Chk1 inhibition as a strategy to sensitize human osteosarcomas to chemotherapy.

INTRODUCTION

Osteosarcoma is the most common primary malignant bone tumor occurring predominantly in children and adolescents, and a second peak at middle age. It is thought to arise from mesenchymal stem cells that are capable of producing osteoid [1,2]. At the moment of diagnosis, 10-20% of the patients present with metastasis. About 30-40% of the patients with localized osteosarcoma will relapse mainly by presenting lung metastasis. Patients with recurrence have very poor prognosis with 23-33% 5-year overall survival [3].

Aven is an adaptor protein that exerts anti-apoptotic activity by potentiating Bcl-xL and by interfering with the self-association of Apaf-1, thereby preventing the activation of caspase 9[4,5]. Aven has also been identified through bioinformatics analysis as a novel potential BH3-domain containing protein[6]. Besides being involved in apoptosis, Aven was reported to control the DNA damage response (DDR) by physically interacting with- and supporting the activity of “ataxia-telangiectasia mutated” (ATM)[7].

The DDR is evolutionary conserved and essential to ensure the faithful maintenance and replication of the genome. This elaborate integrated signaling cascade senses DNA damage and triggers repair, cell cycle arrest and, in case of severe damage, cell death. The serine/threonine protein kinases of the phosphatidylinositol 3-kinase-like family, ATM and “ATM and Rad3-related” (ATR) are crucial players in the DDR [8,9]. After DNA damage, ATM and ATR are activated and, in turn, they activate critical effectors, including components of the DNA damage repair machinery and the checkpoint kinases, Chk1 and Chk2 to arrest the cell cycle[10]. Combining cytotoxic chemotherapeutics with pharmacological Chk1/Chk2 inhibitors can prevent damaged cancer cells from arresting, causing increased tumor cell killing and thus, improved therapeutic efficacy [11].

In the context of cancer, Aven has thus far been exclusively implicated in hematopoietic malignancies. Aven mRNA levels have been associated with disease relapse and poor prognosis of acute lymphoblastic leukemia and Aven has been shown to act as an oncoprotein that drives proliferation and survival of leukemic cells [12-14]. Here, we analyze Aven mRNA, protein expression, and function in osteosarcoma, the most common primary bone malignancy that is very difficult to treat. We show that Aven expression is increased in metastatic lesions and inversely correlated with metastasis-free survival in osteosarcoma patients. We show that Aven is in fact dispensable for ATM-Chk2 (and p53) activation. Instead, Aven is required for ATR-Chk1 signaling and Aven silencing leads to G2 cell cycle

arrest. Moreover, in the absence of Aven osteosarcoma cells fail to activate Chk1 (but not Chk2) in response to DNA damaging chemotherapeutics. Finally, we show that targeting the Aven-controlled ATR-Chk1 activity using clinically relevant pharmacological inhibitors sensitizes osteosarcoma to chemotherapy.

MATERIALS AND METHODS

Reagents and antibodies. Doxorubicin was obtained from the Department of Clinical Pharmacology at LUMC, AZD7762 Chk1/Chk2 inhibitor. Ly2603618 and CHIR-124 selective Chk1 inhibitors were from SelleckChem (Huissen, Netherlands). Cisplatin and etoposide were from Sigma-Aldrich (Zwijndrecht, The Netherlands). Hoechst 33342 was purchased from Fischer Scientific (Bleiswijk, The Netherlands) and the pan-caspase inhibitor z-VAD-fmk was obtained from Bachem (Weil am Rhein, Germany). The Aven antibody (HPA020563) used for immunohistochemistry was from Sigma Aldrich (Zwijndrecht, The Netherlands) and the Aven antibody (2300S) used for Western blot was from Cell Signalling (Bioké, Leiden, The Netherlands). The antibody against phospho-ATR(Ser428) (2853) was from Cell Signaling (Bioké, Leiden, Netherlands). The antibody against tubulin (T-9026) was from Sigma-Aldrich (Zwijndrecht, Netherlands). Antibodies against phospho-H3(ser10) (9701), phospho-CHK2(Thr68) (2661P), phospho-H2Ax(Ser139) (9718), phospho-ATM(Ser1981) (5883), and CHK1 (2345) were from Cell Signaling (Bioké, Leiden, Netherlands). The antibody against phospho-CHK1(Ser317) (A300-163A) was from Bethyl Laboratories (Uithoorn, The Netherlands).

Microarray data analysis. Gene expression profiles were obtained from a previously published microarray data set [15]. Kaplan Meier curves were created from the entry “Mixed Osteosarcoma-Kuijer-127-vst-ilmnhwg6v2” in the web application R2 (http://r2.amc.nl).

Immunohistochemistry on tissue microarrays. Tissue microarrays used in this study were previously constructed and published [16]. All specimens in this study were handled according to the ethical guidelines described in ‘Code for Proper Secondary Use of Human Tissue in The Netherlands’ of the Dutch Federation of Medical Scientific Societies. The slide was deparaffinized, rehydrated and blocked of endogenouse peroxidase. Subsequently, antigen retrieval was performed with citrate pH 6.0. Incubation with antibody was overnight at 4°C at a 1:1000 dilution. As a second step we used Immunologic Poly-HRP-GAM/R/R IgG (DVPO110HRP) and Dako liquid DAB+ Substrate Chromogen System (K3468), after which it was counterstained with hematoxiline. Testis tissue was used as control. Slides were scored independently by two observers (JVMGB and ZB). Staining intensity (0 = absent, 1 = weak, 2

= moderate, 3 = strong) and extent of the staining (0 = 0%, 1 = 1-24%, 2 = 25-49%, 3 = 50-74% and 4 = 75-100%) were assessed. The two values were added to obtain the score sum. Cores where the tissue was lost were excluded from the analysis.

Cell culture. Human osteosarcoma cell lines MOS, U2OS, 143B, ZK58 and KPD used were previously described [17,18]. Cells were grown in RPMI1640 medium supplemented with 10% fetal bovine serum and 25 U/mL penicillin and 25 μg/mL of penicillin-streptomycin. All cells were cultured in a humidified incubator at 37°C with 5% CO_2.

siRNA transfection. Transient knockdown of individual genes was achieved using siGenome SMARTpool siRNAs from Dharmacon, Thermofisher Scientific (Landsmeer, Netherlands). The end concentration of siRNA was 20nM and it was delivered to the cells by INTERFERin siRNA transfection reagent according to the manufacturer's procedures (Polyplus transfection, Leusden, Netherlands). Medium was refreshed 24 hours post transfection and transfected cells were used in experiments 48 hours post transfection. The sequences of siRNA are *GAUUAGGGAUGCAGUUAAA, GAACAGGGAAAUUAUUCUA, UAACUGGGAUCGAUAUCAA* and *GUUAUUGGUUCGAGCCCUU*.

Cell cycle analysis. Cell cycle analysis was performed using the Click-iT® Edu Flow Cytometry Assay Kit from Invitrogen (Oregon, USA). Cells were exposed to 10μM 5-ethynyl-2-deoxyuridine (Edu) for 1 hour followed by fixation, permeabilization, and staining. RNAase was added to each sample to a final concentration of 20mg/mL. Edu was probed with Pacific Blue azide and DNA was stained with FxCycle™ Far Red Stain with a final concentration of 200nM.

Immunoblotting. Cells were lysed with SDS protein buffer (125mM Tris/HCl pH 6.8, 20% glycerol, 4% SDS and 0.2% bromophenol blue). Proteins were resolved by SDS-PAGE and transferred to polyvinylidine difluoride membrane. Membranes were blocked in 5% BSA-TBST (TRIS-0.05% Tween20), followed by overnight incubation with primary antibodies and 45 minutes incubation with HRP-conjugated secondary antibodies. Chemoluminescence was detected with a Typhoon 9400 imager (GE Healthcare).

Cell number, cell viability, and real time growth assays. Control or siRNA-transfected cells were treated with compounds for the indicated time points in black 96-well μ-clear plates (Greiner). To determine cell numbers, cells were fixed in 4% paraformaldehyde for 15 minutes and nuclei were stained with Hoechst 33342 for 15 minutes. Plates were imaged

using a BD Pathway 855 imager (Becton Dickinson). Images were processed using an Image-Pro Analyzer 7.0 algorithm, yielding the number of nuclei in each well. For cell viability, cells were processed using the ATPlite 1Step kit (Perkin Elmer) according to the manufacturer's instructions, followed by luminescence measurement on a plate reader. For real time cell growth analysis the RTCA xCELLigence system (Roche Applied Sciences, Almere, The Netherlands) was used. In this system cells are plated on a surface covered with electrodes that measures cell impedance displayed as cell index. Cell index is a quantitative measure of the number of cells present in the well. For the assay, the cells were seeded in an E-View 96 well plate and loaded into the RTCA station immediately. The cells were exposed to compounds 16 hours later, and further monitored for 72 hours. Measurements were taken every 15 minutes.

Real time qPCR. RNA was isolated from control or siRNA-transfected cells using RNeasy (Qiagen). cDNA was generated from 500 ng total RNA using RNeasy Plus Kit from Qiagen. Real time qPCR was performed in triplicate using the SYBRGreen PCRMasterMix (Applied Biosystems) on a 7900HT fast real-time PCRsystem (Applied Biosystems). Primer sequence for CHK1 employed were: forward *TGGTATTGGAATAACTCACAGGGA* and reverse *TGTTCAACAAACGCTCACGA.* Data were collected and analyzed using SDS2.3 software (Applied Biosystems). Relative mRNA levels after correction for GAPDH control mRNA were expressed using 2^(-ΔΔCt) method.

3D culture assay. U2OS and MOS cells were cultured in 384-well plates (Greiner μclear) in a hydrogel containing Matrigel (Beckton Dickinson) and collagen I, supporting invasive growth of both cell lines. Cells in culture were trypsinized and directly added to the cooled gel solution. Using a robotic liquid handler (CyBio Selma 96/60), 14.5μL of gel-cell suspension was transferred to each well of a 384-well plate (2000 cells/well). After polymerization for 30 minutes at 37°C in an atmosphere of 5% CO_2, growth medium was added on top of the gel. After three days, when the cells had formed a network structure, compounds were diluted and added in quadruplicate wells for a period of 72 hours. For measuring cell viability in 3D, a solution of 7g/L WST-1 (Serva Electrophoresis) and 8mg/L phenazinium methylsulfate (PMS; Sigma Aldrich) in 1x PBS were mixed in a 1:1 ratio and 5μL was added to each well. Plates were placed at 37°C for 5 hours, after which the absorbance at 450nm was measured using a FluoStar plate reader. Percentage viability was thereafter calculated by robust normalization (median) of the plates between positive control (no cells; 0% viability) and negative control (solvent; 100% viability) conditions. Results are presented as means ± SD.

For imaging, cells were fixed using 3.7% Formaldehyde (Sigma-Aldrich), permeabilized with 0.1% Triton-X100 and stained for F-actin using 50nM Rhodamine-Phalloidin (Sigma Aldrich) for 12 hours at 4˚C . Subsequently, the plates were washed in PBS for at least 24 hours at 4˚C. The plates were then imaged on a BD Pathway 855 inverted fluorescence microscope (BD Biosciences) using a 4x lens to capture Rhodamine-Phalloidin staining at focal planes spaced 50µm throughout the gel, capturing approximately 70% of a well. Subsequently, maximum intensity projections of the in-focus information of the Z-stacks was made using OcellO (OcellO B.V., Leiden, The Netherlands) image analysis tools.

Synergy assessment. To assess synergy, we used the Bliss independence model, which defines that the effect of a drug at certain concentration is independent of the presence of the other drug.[19] This model predicts the combined response *C* for two single compounds with effects *A* and *B*: $C = A + B - A \bullet B$ [20].

Statistical analysis. Dose response curve fitting and all statistical analyses were performed with GraphPad Prism 5.0 (GraphPad Software, La Jolla, CA). The unpaired two-tailed *t*-test was used to compare between groups. Significant difference between groups in the 3D assay was calculated using 2way ANOVA with Bonferroni posttest.

RESULTS

Aven expression in human osteosarcoma samples

We used a previously published microarray data set[21] with available follow-up data to search for mRNAs whose expression correlated with metastasis-free survival in osteosarcoma patients. We used 53 osteosarcoma samples for which associated survival data were available. These were arranged by Aven mRNA expression level, and the median was used to divide the set in cases with high and low expression. The cutoff set by R2 was 218.6 with a raw p-value of 0.03. Using this approach, high expression of Aven significantly correlated with a lower metastasis-free survival probability (Fig 1A). Next, we assessed Aven protein expression by immunohistochemistry in 31 human primary osteosarcomas and 8 osteosarcoma lung metastases by immunohistochemistry. Aven protein was detected in most samples and expression was significantly higher in metastases as compared to primary osteosarcoma biopsies (Fig 1B,C).

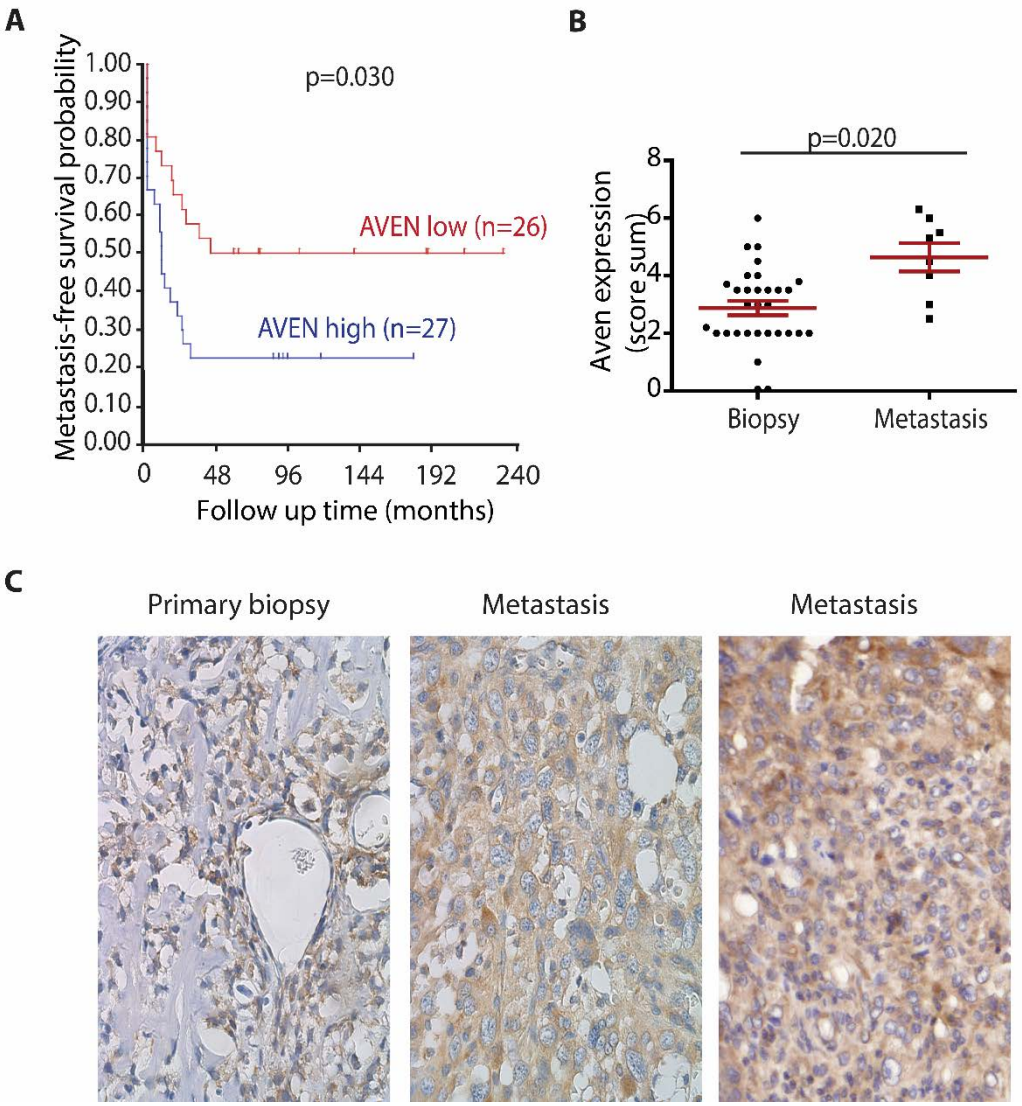

Figure 1. Aven expression in osteosarcoma biopsies. A) Kaplan Meier curve showing relation between Aven mRNA expression and metastasis-free survival. Expression of Aven mRNA was analyzed in 53 samples with survival data, and arranged by expression. The cohort was divided into high and low expression at the median. The curve was made using http://r2.amc.nl. p values were determined by Bonferroni testing. **B)** Sum score of Aven expression in all tumors included in the tissue microarrays. Average is shown in red; p values were determined by two-tailed t test. **C)** Representative images of Aven expression in primary biopsy and metastasis. Images made with 40x Lens.

Aven silencing attenuates growth of human osteosarcoma cells

To determine Aven's role in osteosarcoma cell viability and growth we silenced the *AVEN* gene in two human osteosarcoma cell lines: MOS and U2OS. We used a Smartpool of 4 siRNAs that led to a near complete loss of Aven protein at 48 hours after transfection in both cell lines (Fig 2A). In U2OS cells, transfection with this Smartpool or with any of the four individual siRNAs led to a 60-80% reduction in cell numbers as compared to control, GAPDH-silenced cells (Fig 2B). Likewise, MOS cells transfected with siAven showed a 60% reduction in cell numbers compared to controls (Fig 2C). Aven has been reported to suppress apoptosis in other cell types [4,5,22]. To test if increased apoptosis was responsible for the reduced cell numbers, MOS cells transfected with siAven were treated with the pan-caspase inhibitor, z-VAD-fmk. This led to a slight increase in cell numbers but did not restore growth to that of cells transfected with control siRNAs (Fig 2C). The same results were obtained with U2OS: treatment with z-VAD-fmk did not restore growth of Aven-silenced cells (Fig 2D).

Aven silencing in human osteosarcoma cells triggers G2 cell cycle arrest

We next made use of the RTCA XCelligence system for real time analysis of the effect of Aven silencing on human osteosarcoma cell populations. MOS cells that were MOCK (no siRNA) or siGAPDH transfected, expanded over approximately 24 hours followed by a plateau phase after reaching confluence, whereas siAven-transfected MOS cells stopped expanding at ~18 hours post transfection (Fig 3A). Similarly, a prolonged gradual increase in cell index that was observed for U2OS cells was terminated after 18 hours in response to Aven silencing. This indicated that Aven might be required for effective proliferation of osteosarcoma cells. Indeed, phosphorylation of Histone H3 Ser10 that is associated with mitosis was attenuated in siAven-transfected MOS and U2OS cells, indicating that Aven supported cell cycle progression (Fig 3B). Furthermore, FACS analysis of MOS and U2OS cells pulsed with Edu for 1 hour showed a reduction of cells in S-phase (*t*-test, $p<0.05$) and a concomitant increase in G2 (*t*-test, $p<0.05$) in response to Aven silencing (Fig 3C,D).

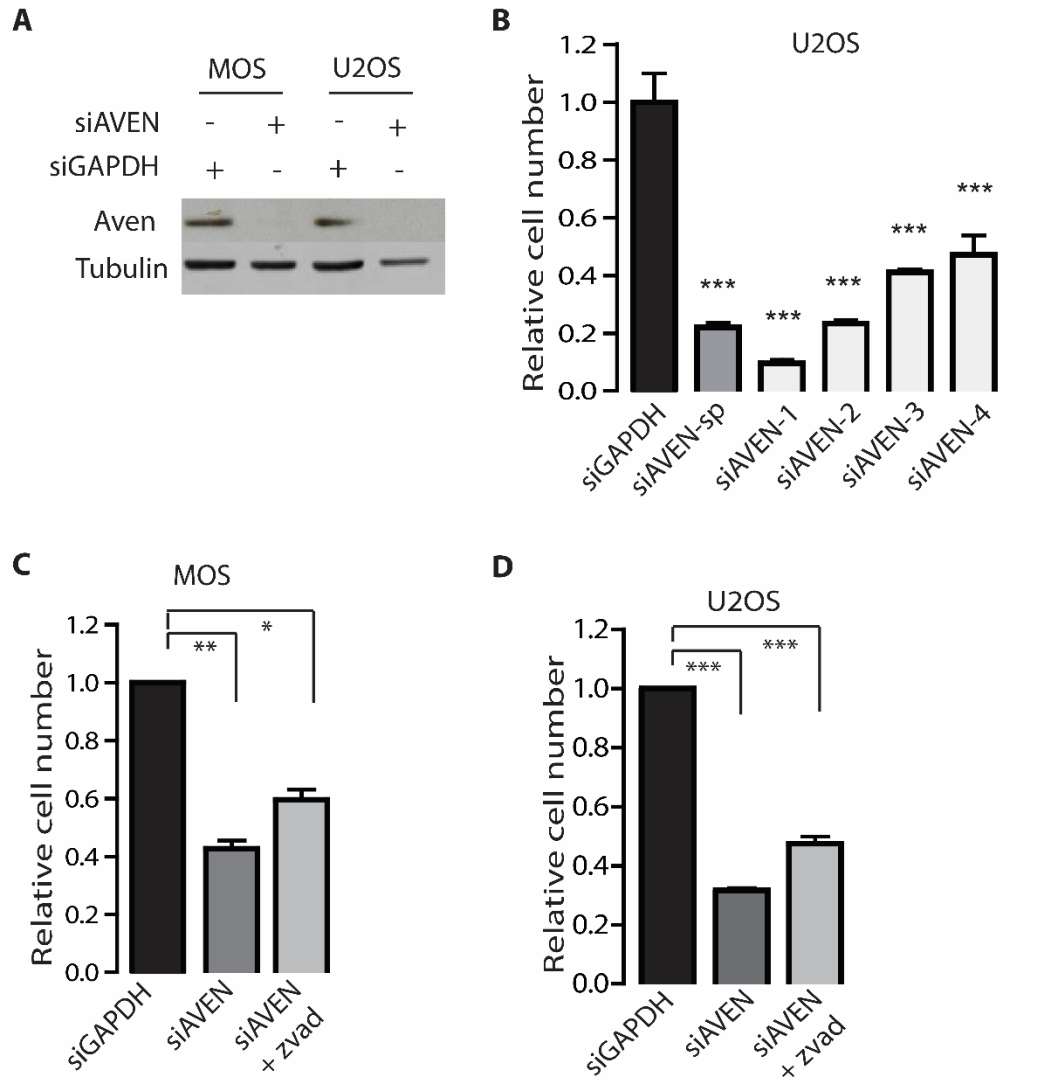

Figure 2. Effect of Aven silencing. A) Western blot analysis of Aven protein abundance and tubulin loading control in MOS and U2OS cells transfected for 48 hours with indicated siRNA Smartpools. **B)** Relative cell numbers based on Hoechst staining, 72 hours post transfection in U2OS cells transfected with GAPDH or Aven siRNA Smartpools or with Aven single siRNAs. Mean +/- SD for experiment performed in quadruplicate is shown. **C**,**D)** Relative cell numbers based on Hoechst staining for MOS and U2OS cell lines, 72 hours post-transfection with indicated siRNA Smartpools. Cells were treated with or without z-VAD-fmk during the last 24 hours (starting at 48 hours post transfection. Mean +/- SEM is shown for three independent experiments done in triplicate. *, $p<0.05$; **, $p<0.01$; ***, $p<0.005$.

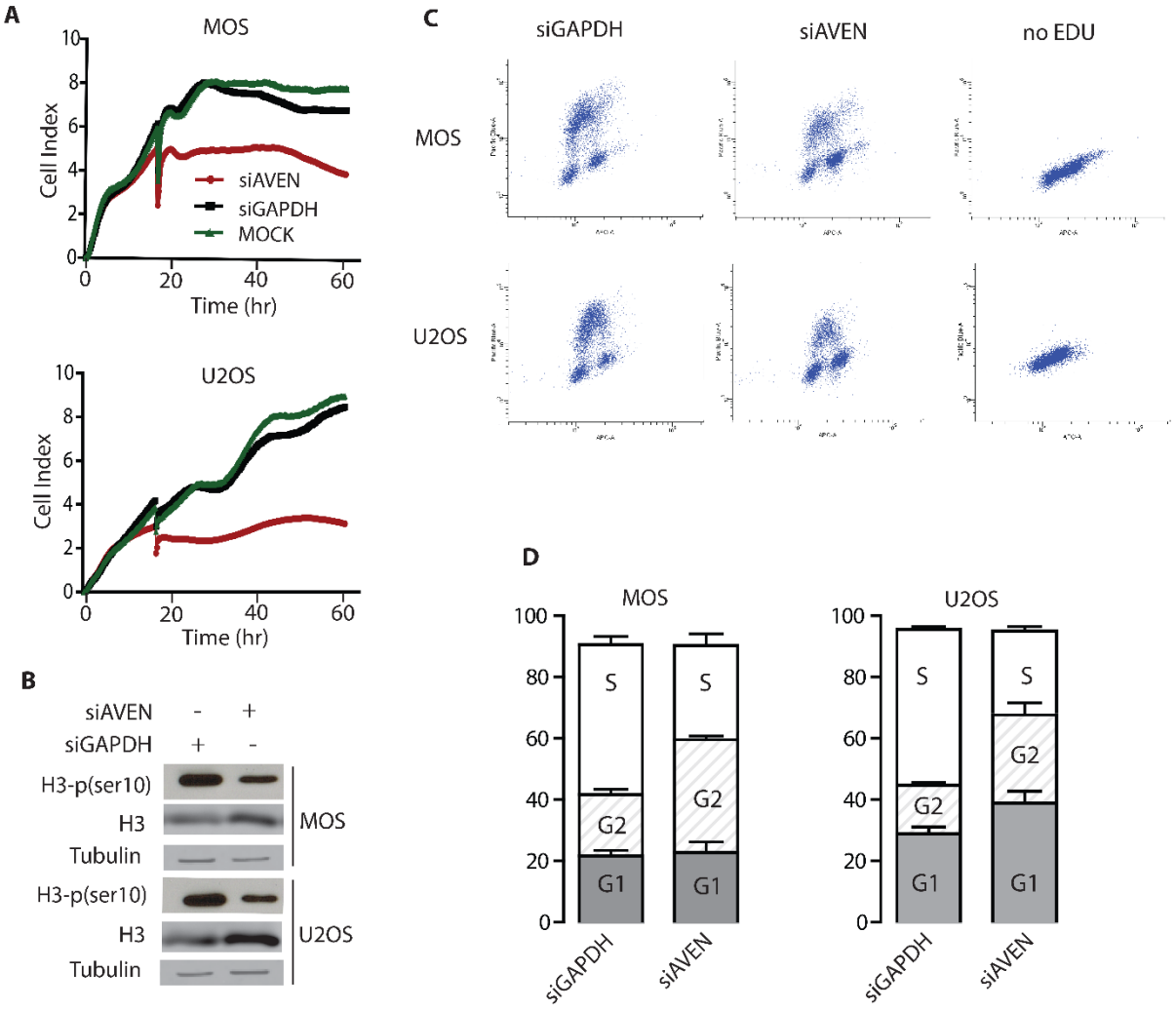

Figure 3. Aven silencing leads to cell cycle arrest. A) Subconfluent cultures of MOS and U2OS cells untransfected (MOCK, green) or transfected with control siGAPDH (black) or siAVEN (red) were monitored for 60 hours with RTCA Xcelligence System. Medium was refreshed at 18 hours post-transfection. Representative experiment of two biological replicates, performed in quadruplicate is shown. **B)** Western blot analysis of total and phospho(Ser10) histone H3 and tubulin loading control for MOS and U2OS cells transfected with siAVEN or siGAPDH for 48 hours. **C)** Flow cytometry analysis of DNA content (x-axis) and Edu incorporation (Y-axis) in MOS and U2OS cells transfected with siAVEN or control siGAPDH pulsed for 1 hour with 10µM Edu after 48 hours. Representative experiment from three biological replicates is shown. **D)** Quantification of data from C. Mean and SEM of three independent experiments is shown.

Aven silencing attenuates ATR-Chk1 DDR signaling in human osteosarcoma cells

The role of Aven in DDR signaling has been attributed to its interaction with ATM [7]. ATM senses double-strand breaks, becomes activated, and subsequently phosphorylates downstream substrates, including Chk2 and p53 [23]. We analyzed ATM activation in U2OS and MOS cells treated for 4 hours with 1 µM doxorubicin. Surprisingly, silencing Aven led to enhanced doxorubicin-induced ATM activation as measured by ATM auto-phosphorylation

at Ser1981 in MOS and U2OS cells (Fig 4A). Chk2 levels increased in response to Aven depletion in these cells (Fig 4B,C). Chk2 phosphorylation at the Thr68 ATM target site was not evident in U2OS cells and in MOS cells doxorubicin triggered ATM Thr68 phosphorylation irrespective of the absence or presence of Aven siRNAs (Fig 4B,C). Likewise, in MOS as well as U2OS cells doxorubicin treatment caused a strong phosphorylation of p53 at the ATM/ATR target site, Ser15 and this response was not affected by Aven silencing (Fig 4B,C).

ATR is activated in response to persistent single-stranded DNA, which is exposed at stalled replication forks and as an intermediate in several DNA damage repair pathways [23]. Doxorubicin treatment caused increased ATR phosphorylation at Ser428 in MOS and U2OS cells, a response that was abolished by Aven silencing (Fig 4A). Moreover, phosphorylation of Chk1 at the ATR target site Ser317 after exposure to doxorubicin was also prevented in Aven-depleted MOS and U2OS cells (Fig 4B,C). This was accompanied by a loss of Chk1 protein accumulation in response to doxorubicin. The role of Aven in the accumulation and phosphorylation of Chk1 was not restricted to doxorubicin but Aven was similarly required for this response in the context of treatment with 5µM cisplatin or 5µM etoposide (Fig 4D). qPCR analysis showed that changes in Chk1 protein abundance were not due to changes in mRNA (Fig S1). Notably, this also excluded a reduction of Chk1 levels through off-target Aven siRNA effects.

Together, these findings indicated that Aven supports ATR-Chk1, but not ATM-Chk2 DDR signaling in osteosarcoma cells. In contrast to ATM-Chk2 signaling, which is particularly important for the response to double strand breaks, ATR-Chk1 signaling is also required for mitotic progression in unperturbed cells [24]. We examined whether the slightly reduced levels of Chk1 (Fig 4B-D) could underlie the cell cycle arrest in Aven-depleted cells. In support of this, silencing Chk1, but not Chk2, impaired MOS cell growth to a similar extent as observed with Aven siRNAs (Fig 2C; S2).

Pharmacological inhibition of Chk1 sensitizes osteosarcoma cells to doxorubicin

Our findings thus far, suggested that Aven-controlled Chk1 signaling might represent an attractive target to sensitize osteosarcoma cells to chemotherapy. Aven inhibitors are not available, but novel Chk1/2 inhibitors that have already been tested in clinical trials are. Therefore, MOS and U2OS cells were treated with a concentration range of the Chk1/2 inhibitor, AZD7762, in combination with a concentration range of doxorubicin. Ranges were based on dose response curves determined for each drug individually (Fig S3,4). Treatment

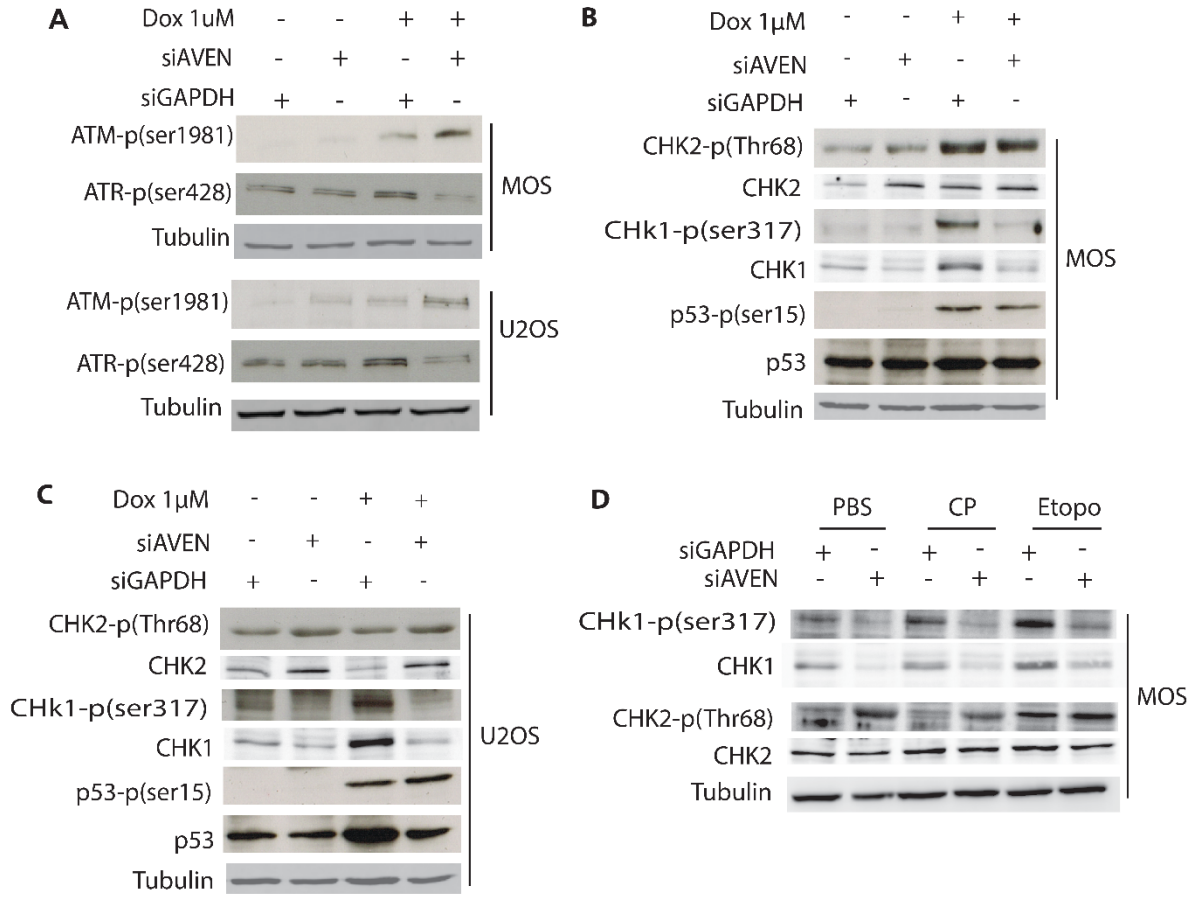

Figure 4. Aven silencing causes shift from ATR-Chk1 to ATM-Chk2 DDR signaling. A) Western blot analysis of total and phospho(Ser1981) ATM, total and phospho(Ser428) ATR, and tubulin loading control for MOS (top) and U2OS cells (bottom) transfected 48 hours with siGAPDH or siAVEN and subsequently treated with 1µM doxorubicin for 4 hours. One representative experiment of 3 is shown. **B**,**C)** Western blot analysis of total and phospho(Thr68) Chk2, total and phospho(Ser317) CHK1, total and phospho(ser15) p53, and tubulin loading control for MOS (**B**) and U2OS cells (**C**) transfected 48 hours with siGAPDH or siAVEN and subsequently treated with 1µM doxorubicin for 4 hours. One representative experiment of 3 is shown. **D)** Western blot analysis of total and phospho(Thr68) Chk2, total and phospho(Ser317) CHK1, and tubulin loading control for MOS cells transfected 48 hours with siGAPDH or siAVEN and subsequently treated with PBS, 5µM cisplatin (CP), or 5µM etoposide for 4 hours.

of MOS with 25-100 nM AZD7762 by itself did not affect cell viability but it led to a strong sensitization to low (50-100 nM) concentrations of doxorubicin (Fig 5A). Calculation of the deviation from additivity as predicted by Bliss independence [19], indicated synergy between AZD7762 and doxorubicin (Fig 5B). The same synergistic relationship between these two compounds was observed for U2OS cells (Fig 5C,D). We further explored the AZD7762-doxorubicin combination using three other human osteosarcoma cell lines, ZK58, KPD, and

143B. Again, 50 nM AZD7762 slightly increased the effect of doxorubicin on ZK58 and strongly sensitized KPD and 143B cells to doxorubicin treatment (Fig 5E).

We also examined the interaction of two clinically relevant selective CHK1 inhibitors, CHIR-124 and LY2603618 with doxorubicin in osteosarcoma cells. CHIR-124 by itself already affected viability at concentrations above 25 nM, especially in U2OS cells (Fig 5F,G). At 25 nM, CHIR-124 sensitized MOS and to a lesser extent, U2OS to doxorubicin (Fig 5F,G; S5). Up to 0.25 µM LY2603618 by itself did not affect either cell line but at this concentration LY2603618 strongly augmented the effect of low concentrations of doxorubicin in U2OS and, especially in MOS cells (Fig 5H,I; S5).

2D and 3D osteosarcoma cultures are chemosensitized by Chk1 inhibition

We confirmed chemosensitization by Chk inhibition by monitoring the cells over a period of 96 hours using the xCELLigence system. Growth of U2OS cells exposed to 0.1 µM doxorubicin was similar to growth under control conditions whereas treatment with 0.5 µM doxorubicin caused a loss of cells (Fig 6A). Again, exposure to 50 nM AZD7762 had no effect by itself but effectively sensitized U2OS cells to 0.1 µM doxorubicin (Fig 6A).

We further validated the possibility of chemosensitization by Chk1 inhibition using 3D osteosarcoma cell cultures. MOS and U2OS cells were suspended in a mixture of collagen and matrigel and allowed to grow for three days. Subsequently, cultures were exposed to a dose rage of doxorubicin in the absence or presence of 50 nM AZD7762, 25nM CHIR-124, or 0,125µM LY2603618 for 72 hours and viability was determined using a biochemical assay. Similar to the results in 2D cultures, MOS and to a lesser extent U2OS were sensitized in 3D to low doses of doxorubicin when Chk1/2 was inhibited using AZD7762 (Fig 6B,C).

Likewise, 3D cultures of U2OS and especially MOS were effectively sensitized to doxorubicin by the two selective Chk1 inhibitors CHIR-124 and LY2603618 (Fig 6B,C). Moreover, image-based analysis at the same time as biochemical viability assessment showed that combined exposure to 50nM AZD7762 and 0.05µM doxorubicin caused disruption of the multicellular network, which was not seen when either of these drugs was used alone (Fig 6D).

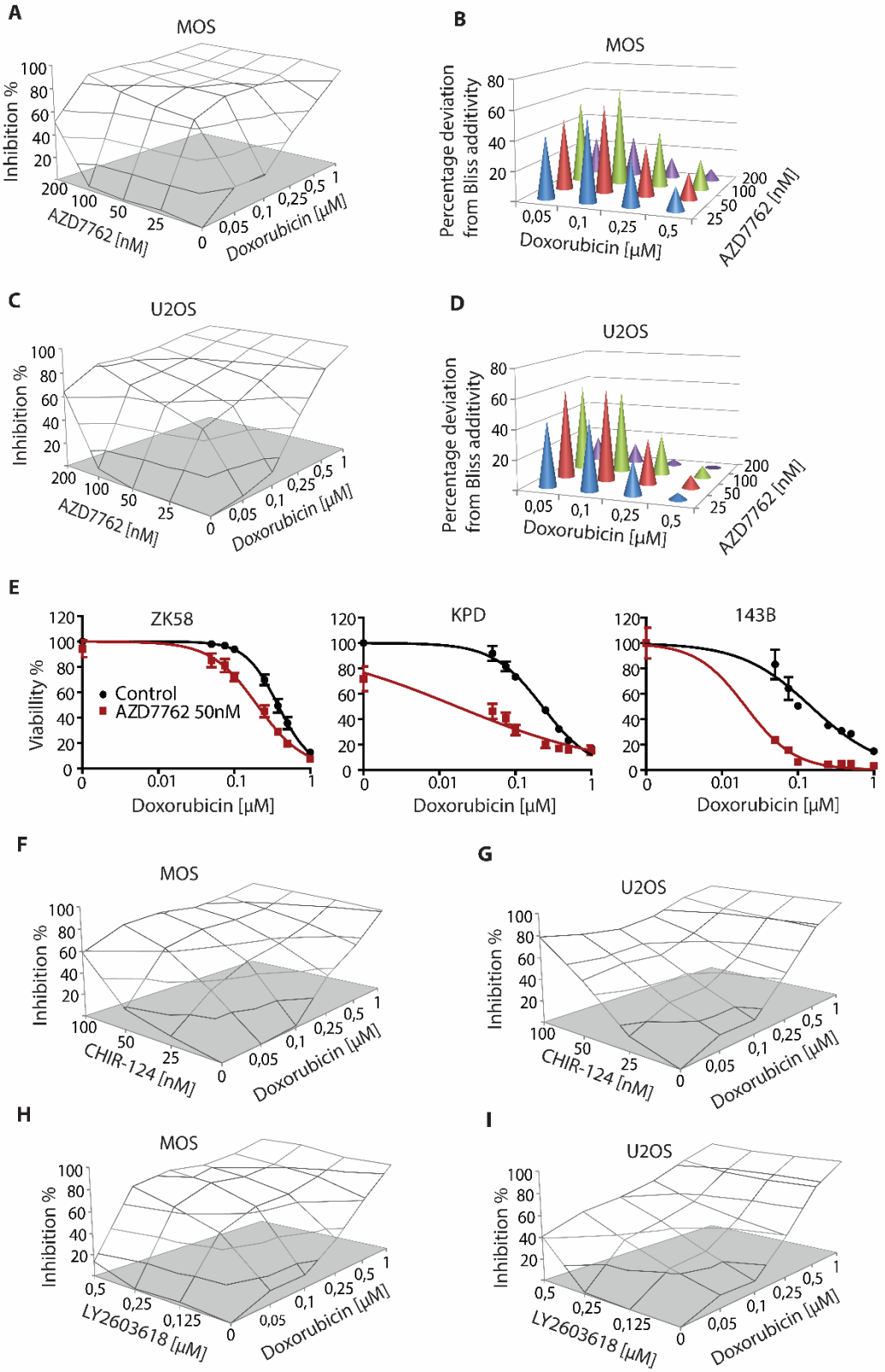

Figure 5. Treatment with Chk1 inhibitor sensitizes osteosarcoma cells to doxorubicin.

A,C) Combined effect of doxorubicin and AZD7762 dose ranges in MOS (**A**) and U2OS cell (**C**). Mean of triplicates is shown. Each graph shows one representative of three independent experiments. **B,D)** Needle graphs showing deviation from Bliss-predicted additivity based on data shown in A,C. Mean of triplicates is shown. Each graph shows one representative of three independent experiments. **E)** Doxorubicin dose response curves for three human osteosarcoma cell lines as indicated in absence or presence of 50nM of AZD7762. Cells were exposed for 72 hours. Each graph represents mean ± SEM. **F,G)** Combined effect of doxorubicin and CHIR-124 dose ranges in MOS (**F**) and U2OS (**G**) cells. Mean of triplicates is shown. Each graph shows one representative of three independent experiments. **H,I)** Combined effect of doxorubicin and LY2603618 dose ranges in MOS (**H**) and U2OS (**I**) cells. Mean of triplicates is shown. Each graph shows one representative of three independent experiments.

DISCUSSION

Our data point to a role for Aven in growth and therapy resistance of osteosarcomas. High expression of Aven mRNA correlates with low metastasis-free survival in conventional osteosarcoma patients and Aven protein expression is high in metastasis as compared to primary biopsies of osteosarcoma. Aven has been shown to suppress apoptosis through its ability to enhance the anti-apoptotic effect of BCL-xl and to interfere with Apaf-1-mediated apoptosome formation in leukemic and breast cancer cells [4,5,14]. In human osteosarcoma cells we find that depletion of Aven does not trigger cell death through apoptosis. Rather, it leads to a G2 cell cycle arrest and ultimately to loss of viability by a mechanism that is not caspase-dependent. Instead, our findings indicate that this is due to impaired checkpoint kinase signaling.

Checkpoint kinases Chk1 and Chk2 coordinate progression through the cell cycle[23,25] and Chk1 is expressed in S through M phase of the cell cycle [26]. Aven-depleted osteosarcoma cells have reduced phospho-Chk1(Ser317) and total Chk1 protein levels. Thus, Aven supports Chk1 protein synthesis or stability. As Ser317-phosphorylated Chk1 is required for DNA replication and mitotic progression [24], the important role we identify for Aven in osteosarcoma cell proliferation can be explained by its support of Chk1 abundance and phosphorylation.

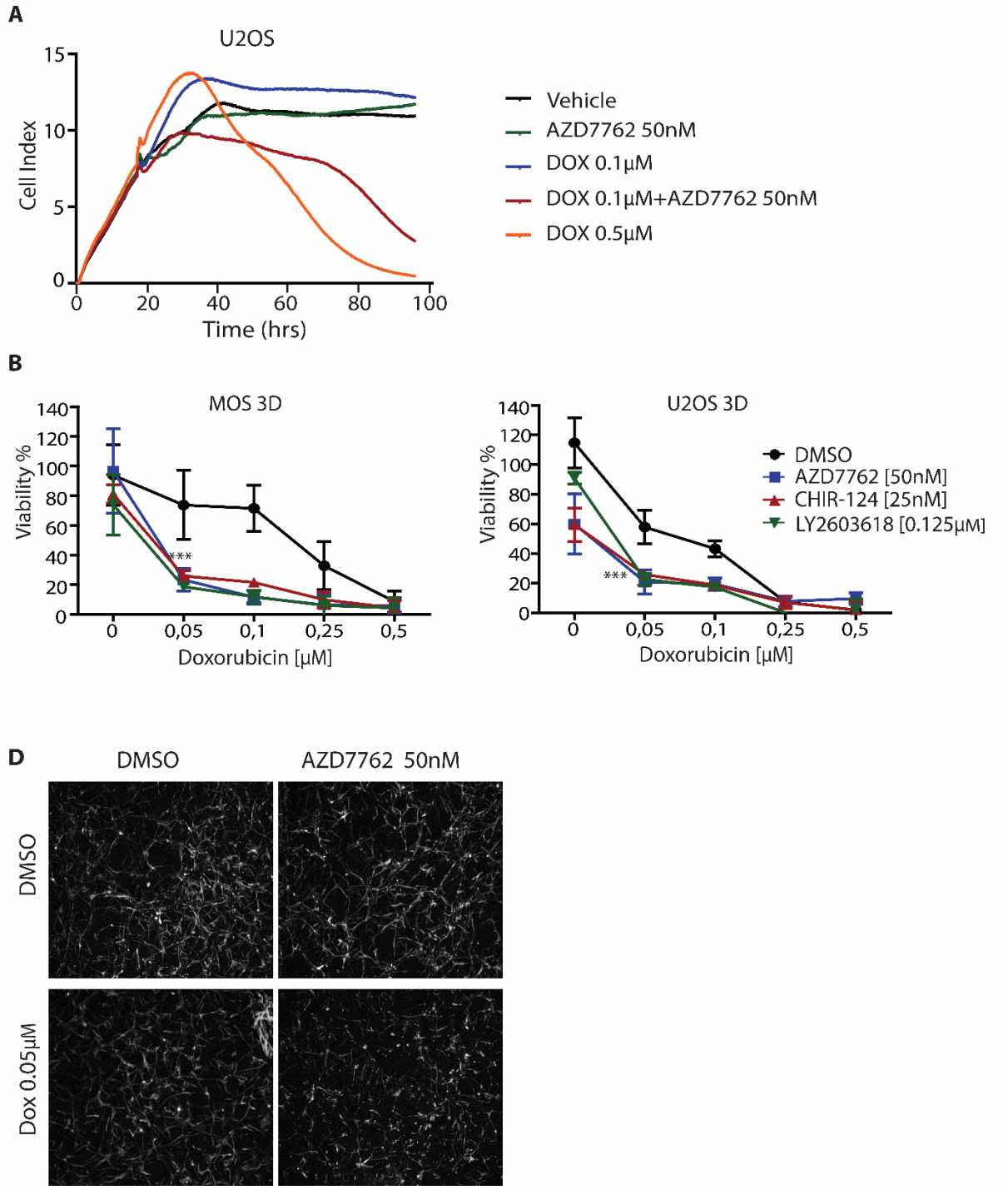

Figure 6. Osteosarcoma cells are sensitized to doxorubicin by Chk1 inhibition in a 2D and 3D environment. A) Subconfluent U2OS cultures were monitored for 90 hours with RTCA Xcelligence System. Cells were exposed 16 hours after seeding to vehicle (black line), 50nM AZD7762 (green line), 0.1µM doxorubicin (blue line), 0.5 µM doxorubicin (orange line), or 0.1µM doxorubicin in combination with 50nM AZD7762 (red line). One experiment of two independent experiments done in quadruplicate is shown. **B,C)** Cell viability measured by WST assay in 3D extracellular matrix-embedded MOS (**B**) and U2OS cultures (**C**) grown for 3 days and subsequently exposed to indicated compound concentrations for 72 hours. Mean ± SD of triplicates (MOS cells) or quadruplicates (U2OS cells) are shown. **D)** Representative images of 3D cultures of MOS cells exposed to DMSO, 50nM

AZD7762, 0.05µM doxorubicin, or the combination of the two drugs. Images are compressed z-stacks of actin cytoskeletal staining (Rhodamine-Phalloidin).

The anti-apoptotic role of Aven is especially prominent in the response to genotoxic therapy. Overexpression of Aven in leukemic and breast cancer cells promotes resistance to γ irradiation and DNA damaging agents such as UV, SN-38 and cisplatin [4,5]. In addition to its role in BCL-xl function and interference with Apaf-1-mediated apoptosome formation as discussed above, this may be related to its role in DDR signaling. Aven has been shown to support ATM activation in cycling *Xenopus* eggs and in HeLa cells treated with neocarzinostatin [7]. Remarkably, our findings demonstrate that ATM activation in response to doxorubicin is fully intact or even potentiated in Aven-silenced osteosarcoma cells. Instead, we show that ATR activation in response to genotoxic stress is abrogated in the absence of Aven.

ATM is mainly activated by double strand breaks, subsequently activating Chk2 to induce cell cycle arrest or apoptosis when the damage is extensive [9]. ATR is an essential regulator of genome integrity, responding to various types of DNA damage and it activates Chk1 [8]. However, crosstalk between ATM and ATR occurs and Chk1 activation by ATR in the context of double strand breaks is dependent on ATM [27,28]. Our data implicate Aven in ATR-Chk1 activation under conditions of genotoxic stress whereas baseline ATR Ser428 phosphorylation appears unaffected by Aven silencing. This suggests that Aven may facilitate the interaction between ATM and ATR, driving ATR signaling in response to double strand breaks.

We show that in osteosarcoma cells, the absence of Aven shifts the DDR from ATR-Chk1 to ATM-Chk2 signaling. This does not affect the activation of p53 in response to genotoxic stress. In U2OS cells expressing wild type p53 as well as in MOS cells expressing a mutant p53, silencing Aven does not affect phosphorylation of p53 at the ATM/ATR target site Ser15 in response to doxorubicin. Under these conditions, ATM, either directly or through Chk2 likely phosphorylates p53 at Ser15 in response to DNA damage [29].

As a potential scaffold protein without enzymatic activity, Aven is unlikely to represent a candidate drug target. However, our data show that Aven-controlled Chk1 signaling may well be an interesting drug target in osteosarcoma. Depletion of Chk1, but not Chk2, to some extent phenocopies the effect of Aven silencing and pharmacological inhibition of Chk1 at higher compound concentrations has the same effect. The use of Chk1

inhibitors for osteosarcoma appears most promising in a combination strategy. Chk1 inhibition is already used as a therapeutic approach to potentiate the efficacy of genotoxic chemotherapeutics in other cancer types [30].

The Chk1/Chk2 inhibitor, AZD7762, is known to potentiate the effect of cisplatin in ovarian clear cell carcinoma [31] as well as in multiple myeloma cells [32]. It was also reported to sensitize pancreatic tumor cells to radiation and to interfere with DNA repair in these cells [33]. However, recently it was reported that this drug would not be continued in clinical trials due to cardiac toxicity [34]. We have tested two selective Chk1 inhibitors, CHIR-124 and LY2603618. The latter drug was tested in a phase I dose-escalation study, and acceptable safety and pharmacokinetic profiles were reported [35,36]. Here, in 2D as well as 3D cultures of human osteosarcoma cells, low concentrations of Chk1 inhibitors cause effective sensitization to low concentrations of doxorubicin. Doxorubicin is routinely used in the treatment of osteosarcoma patients but resistance is a major obstacle [37]. Our findings indicate that abrogation of Chk1 signaling using clinically relevant drugs may be combined with chemotherapy to more effectively treat osteosarcoma.

ACKNOWLEDGEMENTS

The authors would like to thank Jan Koster for help with R2, Inge Briaire-de Bruijn for immunohistochemistry and technical advice, Yvonne de Jong for designing the qPCR primers for CHK1, and Laura Heitman for her introduction to the xCELLigence System. This project was granted by a university profile grant of Leiden University/LUMC titled “Translational Drug Discovery and Development”.

AUTHOR CONTRIBUTION

ZB conceived and carried out experiments, THB carried out and analyzed the 3D assay. All authors were involved in writing the paper and had final approval of the submitted and published versions.

REFERENCES

1. Anninga JK, Gelderblom H, Fiocco M*, et al.* Chemotherapeutic adjuvant treatment for osteosarcoma: where do we stand? *Eur J Cancer* 2011; **47**: 2431-2445.
2. Fletcher CDM, Bridge JA, Hogendoorn PCW*, et al.* Conventional osteosarcoma. In: WHO Classification of Tumours of Soft Tissue and Bone. (ed)^(eds). IARC: Lyon, 2013; 282-288.
3. Buddingh EP, Anninga JK, Versteegh MI*, et al.* Prognostic factors in pulmonary metastasized high-grade osteosarcoma. *Pediatric blood & cancer* 2010; **54**: 216-221.
4. Chau BN, Cheng EH, Kerr DA*, et al.* Aven, a novel inhibitor of caspase activation, binds Bcl-xL and Apaf-1. *Mol Cell* 2000; **6**: 31-40.
5. Kutuk O, Temel SG, Tolunay S*, et al.* Aven blocks DNA damage-induced apoptosis by stabilising Bcl-xL. *Eur J Cancer* 2010; **46**: 2494-2505.
6. Hawley RG, Chen Y, Riz I*, et al.* An Integrated Bioinformatics and Computational Biology Approach Identifies New BH3-Only Protein Candidates. *Open Biol J* 2012; **5**: 6-16.
7. Guo JY, Yamada A, Kajino T*, et al.* Aven-dependent activation of ATM following DNA damage. *Curr Biol* 2008; **18**: 933-942.
8. Mordes DA, Cortez D. Activation of ATR and related PIKKs. *Cell Cycle* 2008; **7**: 2809-2812.
9. Kurz EU, Lees-Miller SP. DNA damage-induced activation of ATM and ATM-dependent signaling pathways. *DNA Repair (Amst)* 2004; **3**: 889-900.
10. Bartek J, Lukas J. Chk1 and Chk2 kinases in checkpoint control and cancer. *Cancer Cell* 2003; **3**: 421-429.
11. Garrett MD, Collins I. Anticancer therapy with checkpoint inhibitors: what, where and when? *Trends Pharmacol Sci* 2011; **32**: 308-316.
12. Paydas S, Tanriverdi K, Yavuz S*, et al.* Survivin and aven: two distinct antiapoptotic signals in acute leukemias. *Ann Oncol* 2003; **14**: 1045-1050.
13. Choi J, Hwang YK, Sung KW*, et al.* Aven overexpression: association with poor prognosis in childhood acute lymphoblastic leukemia. *Leuk Res* 2006; **30**: 1019-1025.
14. Eissmann M, Melzer IM, Fernandez SB*, et al.* Overexpression of the anti-apoptotic protein AVEN contributes to increased malignancy in hematopoietic neoplasms. *Oncogene* 2013; **32**: 2586-2591.
15. Kuijjer ML, Rydbeck H, Kresse SH*, et al.* Identification of osteosarcoma driver genes by integrative analysis of copy number and gene expression data. *Genes Chromosomes Cancer* 2012; **51**: 696-706.
16. Mohseny AB, Szuhai K, Romeo S*, et al.* Osteosarcoma originates from mesenchymal stem cells in consequence of aneuploidization and genomic loss of Cdkn2. *J Pathol* 2009; **219**: 294-305.
17. Mohseny AB, Machado I, Cai Y*, et al.* Functional characterization of osteosarcoma cell lines provides representative models to study the human disease. *Lab Invest* 2011; **91**: 1195-1205.
18. Ottaviano L, Schaefer KL, Gajewski M*, et al.* Molecular characterization of commonly used cell lines for bone tumor research: a trans-European EuroBoNet effort. *Genes Chromosomes Cancer* 2010; **49**: 40-51.

19. Greco WR, Bravo G, Parsons JC. The search for synergy: a critical review from a response surface perspective. *Pharmacol Rev* 1995; **47**: 331-385.
20. Borisy AA, Elliott PJ, Hurst NW*, et al.* Systematic discovery of multicomponent therapeutics. *Proc Natl Acad Sci U S A* 2003; **100**: 7977-7982.
21. Kuijjer ML, Hogendoorn PC, Cleton-Jansen AM. Genome-wide analyses on high-grade osteosarcoma: making sense of a genomically most unstable tumor. *Int J Cancer* 2013; **133**: 2512-2521.
22. Figueroa B, Jr., Chen S, Oyler GA*, et al.* Aven and Bcl-xL enhance protection against apoptosis for mammalian cells exposed to various culture conditions. *Biotechnol Bioeng* 2004; **85**: 589-600.
23. Kastan MB, Bartek J. Cell-cycle checkpoints and cancer. *Nature* 2004; **432**: 316-323.
24. Wilsker D, Petermann E, Helleday T*, et al.* Essential function of Chk1 can be uncoupled from DNA damage checkpoint and replication control. *Proc Natl Acad Sci U S A* 2008; **105**: 20752-20757.
25. OncogeneBartek J, Falck J, Lukas J. CHK2 kinase--a busy messenger. *Nat Rev Mol Cell Biol* 2001; **2**: 877-886.
26. Kaneko YS, Watanabe N, Morisaki H*, et al.* Cell-cycle-dependent and ATM-independent expression of human Chk1 kinase. *Oncogene* 1999; **18**: 3673-3681.
27. Jazayeri A, Falck J, Lukas C*, et al.* ATM- and cell cycle-dependent regulation of ATR in response to DNA double-strand breaks. *Nat Cell Biol* 2006; **8**: 37-45.
28. Cuadrado M, Martinez-Pastor B, Murga M*, et al.* ATM regulates ATR chromatin loading in response to DNA double-strand breaks. *J Exp Med* 2006; **203**: 297-303.
29. Harper JW, Elledge SJ. The DNA damage response: ten years after. *Mol Cell* 2007; **28**: 739-745.
30. McNeely S, Beckmann R, Bence Lin AK. CHEK again: revisiting the development of CHK1 inhibitors for cancer therapy. *Pharmacol Ther* 2014; **142**: 1-10.
31. Itamochi H, Nishimura M, Oumi N*, et al.* Checkpoint kinase inhibitor AZD7762 overcomes cisplatin resistance in clear cell carcinoma of the ovary. *Int J Gynecol Cancer* 2014; **24**: 61-69.
32. Landau HJ, McNeely SC, Nair JS*, et al.* The checkpoint kinase inhibitor AZD7762 potentiates chemotherapy-induced apoptosis of p53-mutated multiple myeloma cells. *Mol Cancer Ther* 2012; **11**: 1781-1788.
33. Morgan MA, Parsels LA, Zhao L*, et al.* Mechanism of radiosensitization by the Chk1/2 inhibitor AZD7762 involves abrogation of the G2 checkpoint and inhibition of homologous recombinational DNA repair. *Cancer Res* 2010; **70**: 4972-4981.
34. Sausville E, Lorusso P, Carducci M*, et al.* Phase I dose-escalation study of AZD7762, a checkpoint kinase inhibitor, in combination with gemcitabine in US patients with advanced solid tumors. *Cancer Chemother Pharmacol* 2014; **73**: 539-549.
35. Weiss GJ, Donehower RC, Iyengar T*, et al.* Phase I dose-escalation study to examine the safety and tolerability of LY2603618, a checkpoint 1 kinase inhibitor, administered 1 day after pemetrexed 500 mg/m(2) every 21 days in patients with cancer. *Invest New Drugs* 2013; **31**: 136-144.
36. Calvo E, Chen VJ, Marshall M*, et al.* Preclinical analyses and phase I evaluation of LY2603618 administered in combination with Pemetrexed and cisplatin in patients with advanced cancer. *Invest New Drugs* 2014; **5**: 955-968.

37. Luetke A, Meyers PA, Lewis I*, et al.* Osteosarcoma treatment - where do we stand? A state of the art review. *Cancer Treat Rev* 2014; **40**: 523-532.

Supplementary Figures

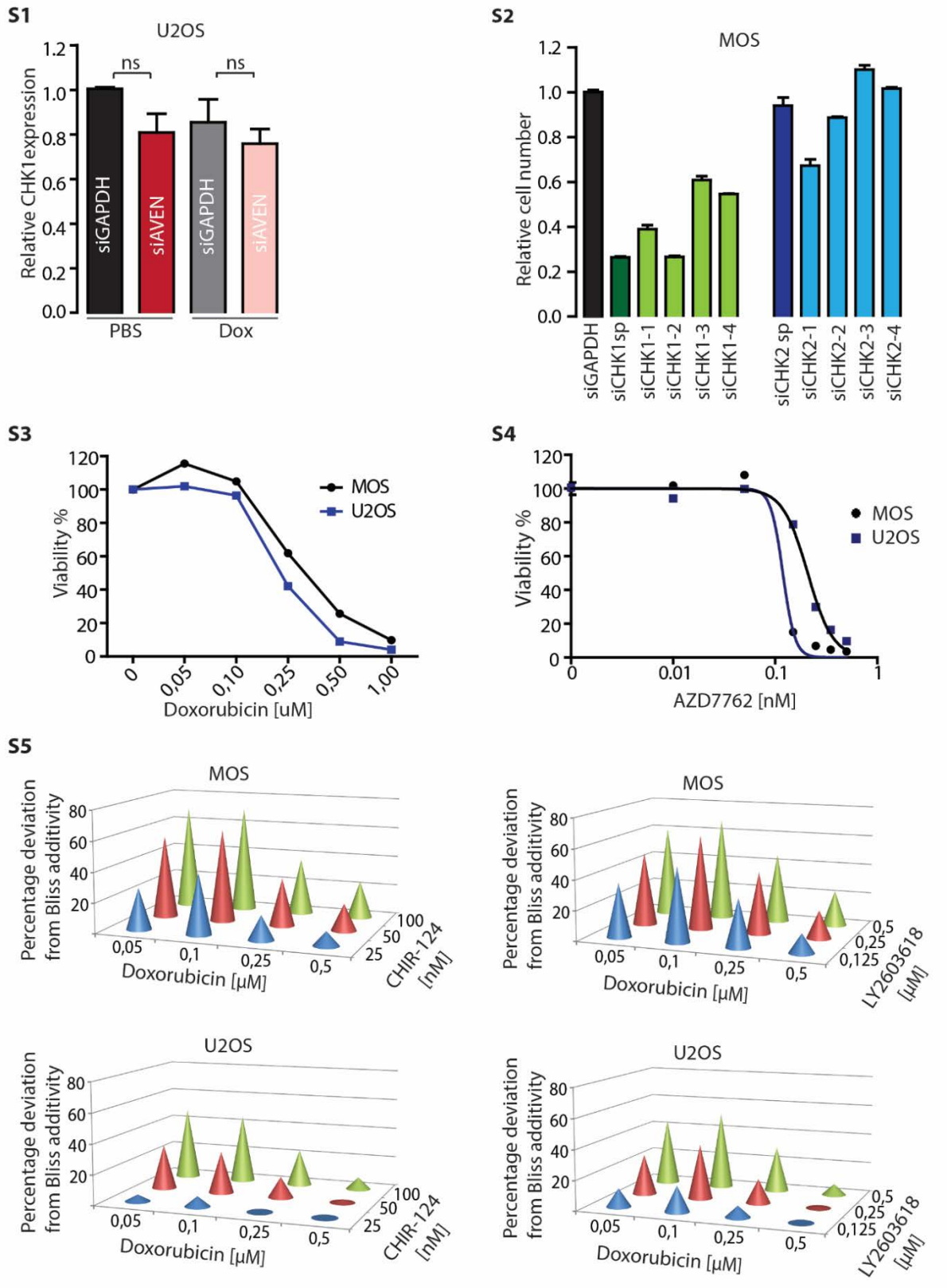

Figure S1) qPCR analysis showing Chk1 mRNA levels in U2OS cells transfected 48 hours with the indicated siRNAs. Mean +/- SEM of 3 independent experiments done in triplicate is shown.

Figure S2) MOS cells were transfected with siGAPDH, siChk1, siChk2 for 72 hours and cell numbers were determined by HOECHST staining and nuclei counting.
Figure S3) Dose response curve of Doxorubicin in MOS and U2OS cells; 72 hours exposure. Mean +/- S.D of one experiment done in triplicate.
Figure S4) Dose response curve of AZD7762 in MOS (black line) and U2OS cells (blue line); 72 hours exposure. Mean +/- SEM of 3 independent experiments done in triplicate is shown.
Figure S5) Needle graphs showing deviation from Bliss-predicted additivity in MOS (top) and U2OS cells (bottom) exposed to doxorubicin and CHIR-124 dose ranges (left) or doxorubicin and LY2603618 dose ranges (right). Each graph shows one representative of three independent experiments performed in triplicate.

3

Pharmacological inhibition of Bcl-xL sensitizes osteosarcoma to doxorubicin

Zuzanna Baranski, Yvonne de Jong, Trayana Ilkova, Elisabeth F.P. Peterse, Anne-Marie Cleton-Jansen, Bob van de Water, Pancras C.W. Hogendoorn, Judith V. M. G. Bovée, Erik H.J. Danen

Published in *Oncotarget* **6**:36113-36125, 2015

ABSTRACT

High-grade conventional osteosarcoma is the most common primary bone sarcoma. Prognosis for osteosarcoma patients is poor and resistance to chemotherapy is common. We performed an siRNA screen targeting members of the Bcl-2 family in human osteosarcoma cell lines to identify critical regulators of osteosarcoma cell survival. Silencing the anti-apoptotic family member Bcl-xL but also the pro-apoptotic member Bak using a SMARTpool of siRNAs as well as 4/4 individual siRNAs caused loss of viability. Loss of Bak impaired cell cycle progression and triggered autophagy. Instead, silencing Bcl-xL induced apoptotic cell death. Bcl-xL was expressed in clinical osteosarcoma samples but mRNA or protein levels did not significantly correlate with therapy response or survival. Nevertheless, pharmacological inhibition of a range of Bcl-2 family members showed that inhibitors targeting Bcl-xL synergistically enhanced the response to the chemotherapeutic agent, doxorubicin. Indeed, in osteosarcoma cells strongly expressing Bcl-xL, the Bcl-xL-selective BH3 mimetic, WEHI-539 potently enhanced apoptosis in the presence of low doses of doxorubicin. Our results identify Bcl-xL as a candidate drug target for sensitization to chemotherapy in patients with osteosarcoma.

INTRODUCTION

Osteosarcoma is the most common primary malignant bone tumor occurring predominantly in the second decade of life, and a second peak at middle age. It is thought to arise from mesenchymal stem cells that can produce osteoid [1-3]. About 30-40% of the patients with localized osteosarcoma will relapse mainly by presenting with lung metastasis. Approximately 10-20% of the patients present with metastasis at the moment of diagnosis. Since the introduction of chemotherapy patients with local disease have 50-60% long-term survival rate. There has been no significant further improvement over the past three decades [4]. Following disease relapse, prognosis is very poor with 23-33% 5-year overall survival despite repeated metastasectomies when feasible [5].

Apoptosis is a form of programmed cell death, which requires caspase-mediated proteolysis, and is governed by the Bcl-2 family. It is essential for development and tissue homeostasis, and can mediate cell death upon exposure to pathogens, cytotoxic agents, or oncogenic stress[6]. The Bcl-2 family includes BH3-only proteins (Bim, Puma, Bad, Noxa, Bik, Hrk, Bmf and tBid), pro-survival proteins (Bcl-2, Bcl-xL, Bcl-w, Mcl-1, Bfl-1, and Bcl-B) and pro-apoptosis proteins (Bax, Bak and Bok). Bok is primarily localized to ER and Golgi membranes where it was found to be important for a proper ER stress response. Its overexpression induces apoptosis in a manner that is dependent on Bax and Bak[7]. Bak is localized to mitochondria and Bax resides in the cytosol. Once Bak and Bax are activated, they undergo conformational changes and Bax localizes to the mitochondria. In the mitochondria, Bak and Bax form hetero and oligomers which lead to mitochondrial outer membrane permeabilization and cytochrome-c release, which is necessary for caspase activation[8]. Under normal conditions, the pro-survival Bcl-2 members form heterodimers with Bax or Bak inhibiting their activation. However, under cytotoxic stress the activated BH3-only proteins displace these proteins allowing Bax and Bak to cause cytochrome-c release from the mitochondria, caspase cascade activation, and ultimately cell death [8,9].

Impaired apoptosis is one of the hallmarks of cancer [10]. It allows cancer cells to tolerate oncogenic stress and survive in hostile environments such as hypoxic conditions. Furthermore, defects in apoptosis in cancer cells can hamper the response to chemotherapy [11]. In this study we used RNA interference and pharmacological inhibition to identify members of the Bcl-2 family that control osteosarcoma cell survival and resistance to chemotherapy.

MATERIALS AND METHODS

Reagents and antibodies. Doxorubicin was obtained from the Pharmacy at the Leiden University Academic Hospital, ABT-737, UMI-77 and HA14-1 were from SelleckChem (Huissen, Netherlands). WEHI-539 was from ApexBio (Texas, U.S.A.). The pan-caspase inhibitor z-VAD-fmk was obtained from Bachem (Weil am Rhein, Germany). The Bcl-xL antibody (clone 54H6) used for immunohistochemistry ,the Bcl-xL antibody (2762s) used for Western blot and Bak antibody were from Cell Signaling (Bioké, Leiden, The Netherlands). LC3 antibody was from Novus Biologics (Cambridge, England) and Ki67 was from Abcam (Cambridge, England). Chloroquine was bought from Sigma Aldrich (Zwijndrecht, The Netherlands). Hoechst 33342 was purchased from Fischer Scientific (Bleiswijk, The Netherlands).

Immunohistochemistry on tissue microarrays. Two tissue microarrays used in this study were previously constructed with one was previously published[3]. The second tissue microarray consisted of 73 FFPE biopsies, resections and metastases mainly from high grade conventional osteosarcomas. All specimens in this study were handled according to the ethical guidelines described in 'Code for Proper Secondary Use of Human Tissue in The Netherlands' of the Dutch Federation of Medical Scientific Societies. The slide was deparaffinized, rehydrated and blocked of endogenouse peroxidase. Subsequently, antigen retrieval was performed with citrate pH 6.0. Incubation with antibody was overnight at 4°C at a 1:1000 dilution. As a second step we used Immunologic Poly-HRP-GAM/R/R IgG (DVPO110HRP) and Dako liquid DAB+ Substrate Chromogen System (K3468), followed by counterstaining with hematoxylin. Testis tissue was used as control. Slides were scored independently by two observers (JVMGB and YJ). Staining intensity (0 = absent, 1 = weak, 2 = moderate, 3 = strong) and extent of the staining (0 = 0%, 1 = 1-24%, 2 = 25-49%, 3 = 50-74% and 4 = 75-100%) were assessed. The two values were added to obtain sum scores. Cores where the tissue was lost were excluded from the analysis. To assess response to chemotherapy, patients were divided among good and poor responders. The histological response was assessed by determining the amount of necrotic tissue in the resection specimen obtained after chemotherapy. Response was considered good when a patient presented more than 90% necrotic tissue in the tumor, and bad responders were those with less than 90% necrosis[51].

Cell culture. Human osteosarcoma cell lines MOS, U2OS, 143B, ZK58,KPD, MNNG, MG-63 and Saos-2 were previously described[52,53]. Cells were grown in RPMI1640 medium

supplemented with 10% fetal bovine serum and 25 U/mL penicillin and 25 µg/mL of penicillin-streptomycin. All cells were cultured in a humidified incubator at 37°C with 5% CO_2.

siRNA screen. Transient knockdown of individual genes in U2OS cells was achieved using siRNAs from Dharmacon, GE (Landsmeer, Netherlands). The end concentration of siRNA was 20nM and it was delivered to the cells with INTERFERin siRNA transfection reagent by reverse transfection according to the manufacturer's procedures (Polyplus transfection, Leusden, Netherlands). The transfection was performed in u-clear 96-well plates from Corning. Nineteen Bcl-2 family members were targeted with a SMARTpool comprised of 4 different siRNAs and with each single siRNA individually. After 24 hours of transfection the medium was refreshed and the cells were further incubated for 72 hours. Alamar Blue was acquired from Thermo Fisher Scientific (Bleiswijk, The Netherlands) and used to assess viability as specified by the manufacturer. Fluorescence was measured with a FluoStar Optima plate reader.

Microarray data analysis. Gene expression profiles were obtained from a previously published microarray data set[54]. Using the Bioconductor lumi package, data was transformed with the variance stabilizing transformation algorithm and normalized with the robust spline normalization algorithm. Probe_ID identifiers from the Illumina Annotation for Illumina human-6 v2.0 expression beadchip were used as reporters (Bcl-xL reporter = ILMN_1654118). Kaplan Meier curves were created from the entry "Mixed Osteosarcoma-Kuijer-127-vst-ilmnhwg6v2" in the web application R2 (http://r2.amc.nl).

Immunoblotting. Cells were lysed with SDS protein buffer (125mM Tris/HCl pH 6.8, 20% glycerol, 4% SDS and 0.2% bromophenol blue). Proteins were resolved by SDS-PAGE and transferred to polyvinylidine difluoride membrane. Membranes were blocked in 5% BSA-TBST (TRIS-0.05% Tween20), followed by overnight incubation with primary antibodies and 45 minutes incubation with HRP-conjugated secondary antibodies. Chemoluminescence was detected with the bioimager LAS400 (GE Healthcare).

Immunostaining. MOS and U2OS cells were transfected with siRNA as previously described. The cells were fixed 48 hours after transfection with ice cold methanol for 15 minutes, and were subsequently rinsed 3 times for 5 minutes with PBS. Afterwards, the cells were incubated with blocking solution [10% normal goat serum, 0.3%Triton100 in PBS] for 1 hour, rinsed 3 times for 5 minutes with PBS, and then incubated 1 hour with second

antibody(1:300). Nuclei stainig with Hoechst 33342 was performed as a final step together with the rinsing steps. The antibodies were diluted in antibody staining solution [1%BSA, 0.3%Triton100 in PBS]. The cells probed mitochondria, were exposed to 75nM of MitoTracker® Red CMX Ros (from Cell Signaling) for 45 minutes previous to fixation. All images were taken with confocal microscope Eclipse Ti-E from Nikon.

Cell viability, and real time apoptosis assays. For cell viability assays (excluding the siRNA screen), cells were processed using the ATPlite 1Step kit (Perkin Elmer) according to the manufacturer's instructions, followed by luminescence measurement in a Fluostar Optima plate reader. Apoptosis was assessed by Annexin V staining and Caspase Glo3/7 (Promega). For real time Annexin V binding assays, cells were co-exposed to drugs and Annexin V in a *u*-clear 96-well plate, and imaged every hour, for 66 hours. Images were obtained using a BD Pathway 855, then converted to videos, and Annexin V staining was quantified by an in-house macro for Image-Pro Analyzer 7.0 as previously described[20]. For caspase 3/7 activity measurements, cells were exposed to the drug for 24 hours after which the reagent was added 1:1. Luminescence was measured in a Fluostar Optima plate reader.

Synergy assessment. To assess synergy, we used the Bliss independence model, which defines to what extent the effect of a drug at a certain concentration is independent of the presence of the other drug at a certain concentration[55]. This model predicts the combined response *C* for two single compounds with effects *A* and *B*: $C = A+B-A*B$[56].

Statistical analysis. Dose response curve fitting and all statistical analyses were performed with GraphPad Prism 5.0 (GraphPad Software, La Jolla, CA). The unpaired and paired two-tailed *t*-test used to compare groups in Figure 3B and 3D was performed with IBM SPSS statistics 20. Event free survival was computed from the date of diagnosis until first recurrence, either local or metastatic. Tumors were divided into two groups, having low (mean sum score ≤3) or high Bcl-xL expression (mean sum score >3). Event free survival in both groups was compared using the Kaplan-Meier method and the Log-rank test with IBM SPSS statistics 20.

RESULTS

Identification of Bcl-xL as a critical pro-survival factor in osteosarcoma cells

An siRNA screen was performed in U2OS cells to identify Bcl-2 family members required for osteosarcoma cell viability (See Fig. S1 for screen layout and results). The screen was

performed in duplicate with two negative controls, siGapdh and MOCK (only transfection reagent), and siKif11 as positive control (all controls were present in triplicate in each plate). Each value was normalized to siGapdh, which was set as 100% viability. MOCK transfected cells showed the same viability as siGapdh. To select hits causing loss of viability we calculated the standard deviation across each plate, and determined that a gene was a hit if the SMARTpool (comprised of 4 single siRNAs targeting the same gene) and the 4 single siRNAs tested individually, each were two standard deviations separated from siGapdh. Using this criteria 7 genes were selected, which included Bcl-B, Bak, Bid, Bfl-1, Mcl-1, Bok and Bcl-xL (Fig. 1A and B). To assess whether loss of viability was due to apoptosis, a caspase 3/7 assay was performed. Caspase 3 and 7 are effector caspases that once activated, lead to cell death by cleaving important structural proteins, and causing DNA fragmentation and membrane blebbing[12]. Bcl-xL knockdown caused the highest caspase3/7 activity after 48 hours of transfection indicating that it effectively triggered apoptosis (Fig. 1C).

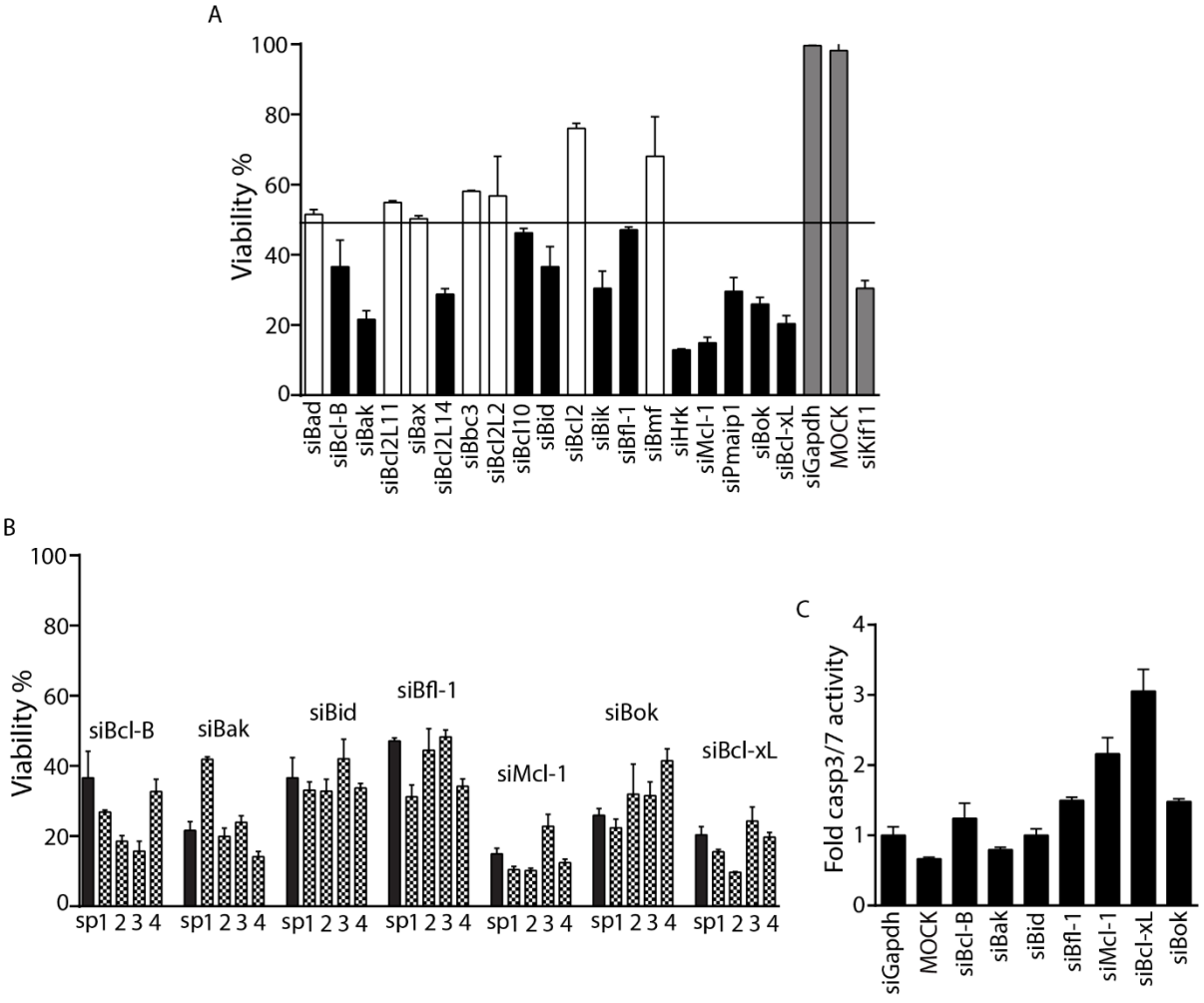

Figure 1. Identification of Bcl-xL as a candidate target for sensitization to doxorubicin.

A) Average U2OS viability in wells transfected with siRNA SMARTpools targeting the indicated genes relative to siGapdh. Mean and standard deviation is shown. Horizontal line marks 2 SD threshold (<48.4% viability), hits are indicated in black, positive and negative controls in grey. **B)** Validated hits where all 4 single siRNAs mimic the SMARTpool and are below the threshold. Black bars represent the SMARTpool and grey patterned bars represent the single siRNAs. **C)** Caspase3/7 activity in U2OS cells transfected with SMARTpool siRNAs targeting the indicated genes. Values were normalized to control siGapdh. One representative experiment of two performed in quadruplicate is shown. Error bars represent standard deviation.

Silencing Bak leads to autophagy in osteosarcoma cells

Surprisingly, the screen also identified pro-apoptotic Bcl-2 family members, including Bak, Bid and Bok (Fig 1A-B). A caspase activity assay indicated that the loss of cell viability caused by siRNAs targeting these genes was not due to apoptosis (Fig 1C). It has been described that failure to activate apoptosis in Bak/Bax double knockout cells is accompanied by increased autophagy[13,14]. Autophagy is a recycling process that provides building blocks and energy during cell stress while unlimited autophagy leads to cell death[15].. We first assessed the knockdown efficiency of Bak in U2OS cells and confirmed a ~100% efficacy (Fig. 2A). Since there was no caspase 3/7 activation in response to Bak knockdown, we next determined if the observed loss of cells was due to slower proliferation. Phospho(ser10)-HistoneH3, a marker for cells in mitosis and Ki67, a marker for proliferating cells were analyzed in cell lysates and by immunocytochemistry, respectively. Silencing Bak in U2OS or MOS cells caused a reduction in phospho(ser10)-HistoneH3 levels (Fig. 2B) and attenuated proliferation was confirmed by reduced Ki67 staining in si-Bak treated cells (Fig. 2C).

To assess if Bak depletion triggered autophagy as shown in other systems[11,12], we determined the conjugation of the LC3 protein to phosphatidylethanolamine. This conjugation represents a critical step in the formation of the autophagosome, a double-membrane organelle that engulfs cellular components during autophagy and subsequently fuse with the lysosome[16]. Silencing Bak in U2OS and in MOS cells led to accumulation of the conjugated form of LC3, termed LC3-II (Fig 2D). Moreover, treatment of U2OS cells in which Bak was silenced with 10µM chloroquine for 4 hours (chloroquine acidifies the phagosome inhibiting its fusion with the lysosome leading to autophagosome accumulation[17]) led to further accumulation of LC3 II (Fig 2E). In addition, immunocytochemistry showed that mitochondria no longer distributed throughout the cytoplasm but clustered perinuclearly in Bak-depleted cells where they colocalized with LC3-marked autophagosomes (Fig. 2F). Together, these findings indicate that depletion of Bak in

osteosarcoma cells induces altered mitochondrial distribution, decreased proliferation, and autophagy.

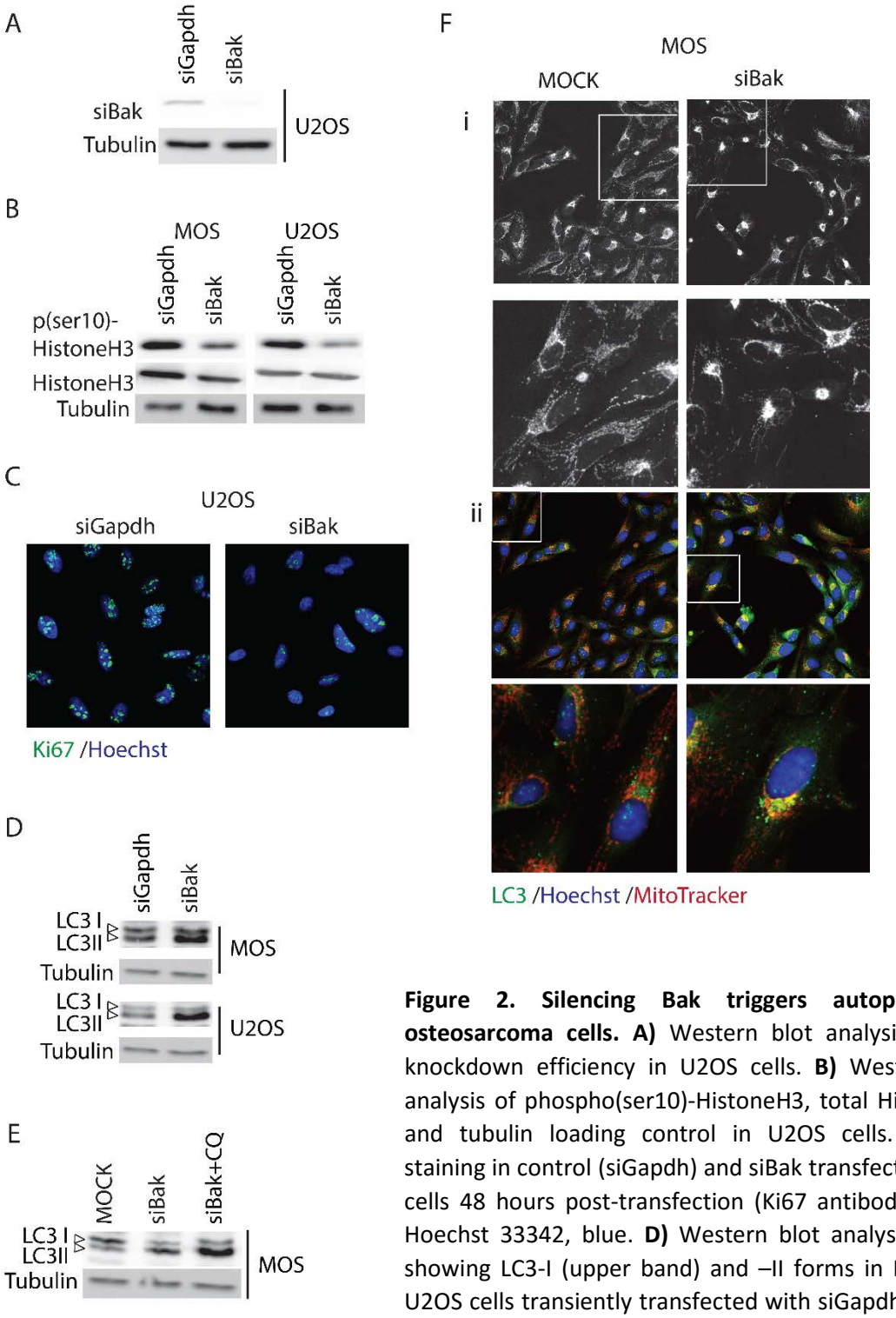

Figure 2. Silencing Bak triggers autophagy in osteosarcoma cells. A) Western blot analysis of Bak knockdown efficiency in U2OS cells. **B)** Western blot analysis of phospho(ser10)-HistoneH3, total HistoneH3, and tubulin loading control in U2OS cells. **C)** Ki67 staining in control (siGapdh) and siBak transfected U2OS cells 48 hours post-transfection (Ki67 antibody, green; Hoechst 33342, blue. **D)** Western blot analysis of LC3 showing LC3-I (upper band) and –II forms in MOS and U2OS cells transiently transfected with siGapdh or siBak SMARTpools. **E)** Western blot analysis of LC3 in control

siBak SMARTpool and treated with or without 10µM chloroquine for 4 hours. **F)** Control MOS cells (MOCK) or MOS cells transiently transfected with siBak for 48 hours, exposed to MitoTracker® (red) for 45 min, fixed and stained with anti-LC3 (green), and Hoechst 33342 (blue). i, MitoTracker only; ii, merge of all three channels.

Bcl-xL is expressed in osteosarcoma lung metastasis

As Bcl-xL silencing caused severe loss of viability and led to the strongest induction of caspase 3/7 activity, we decided to further study its role in osteosarcoma. Others have reported that high Bcl-xL mRNA expression in osteosarcoma patients is correlated with lower overall survival rate [18]. We analyzed Bcl-xL mRNA expression using a previously published microarray data set of a cohort of 88 osteosarcoma patients but did not observe significant association with overall survival (Fig 3A). We next analyzed the expression of Bcl-xL by immunohistochemistry in 60 human primary osteosarcomas and 23 osteosarcoma lung metastases. Expression of Bcl-xL was detected in the majority of osteosarcoma samples and expression was higher in metastases compared to primary tumors (Fig. 3B,C). However, contrary to our expectations, high Bcl-xL protein expression levels (SUM score of intensity and % positive cells) in primary biopsies correlated with good response to therapy in this study (>90% necrosis post-chemotherapy) (Fig. 3D). Furthermore, event-free survival rates did not significantly differ between patients with high and low Bcl-xL expression in diagnostic biopsies (Fig. 3E). These results indicate that Bcl-xL is expressed in advanced osteosarcomas, but its expression is not correlated with poor therapy response or survival.

Pharmacological inhibition of Bcl-xL sensitizes osteosarcoma cells to chemotherapy

Although we could not confirm earlier observations correlating Bcl-xL expression to patient survival, our siRNA screen indicated that Bcl-xL inhibition might enhance tumor killing in cases where it is expressed. Therefore, we assessed whether Bcl-xL represents a relevant target for osteosarcoma alone or in the context of conventional chemotherapy. First, four human osteosarcoma cell lines were treated with ABT-737, a BH3 mimetic that inhibits Bcl-w, Bcl-xL and Bcl-2; of which only Bcl-xL was identified in the siRNA screen (Fig 1A). In addition, HA14-1, a selective Bcl-2 inhibitor was tested. All the cell lines showed loss of cell viability in the 10µM range for ABT-737 and at higher concentrations for HA14-1 (Fig. 4A and B). Subsequently, we asked if these inhibitors, when used at lower concentrations, could sensitize osteosarcoma cells to chemotherapy. The four osteosarcoma cell lines were co-treated with a suboptimal concentration of ABT-737 and a dose range of doxorubicin for 72 hours. At a concentration of 2.5 µM of ABT-737, viability of the cells was close to 100%. MOS, U2OS and to a lesser extent KPD and ZK58 showed increased sensitivity to treatment

with 50-500 nM doxorubicin under these conditions (Fig. 4C). By contrast, treatment with up to 10 µM of the Bcl-2 selective inhibitor, HA14-1 did not affect sensitivity to doxorubicin. Indeed, calculation of the deviation from additivity as predicted by Bliss independence model[19] indicated synergy between ABT-737 and doxorubicin (Fig. 4D).

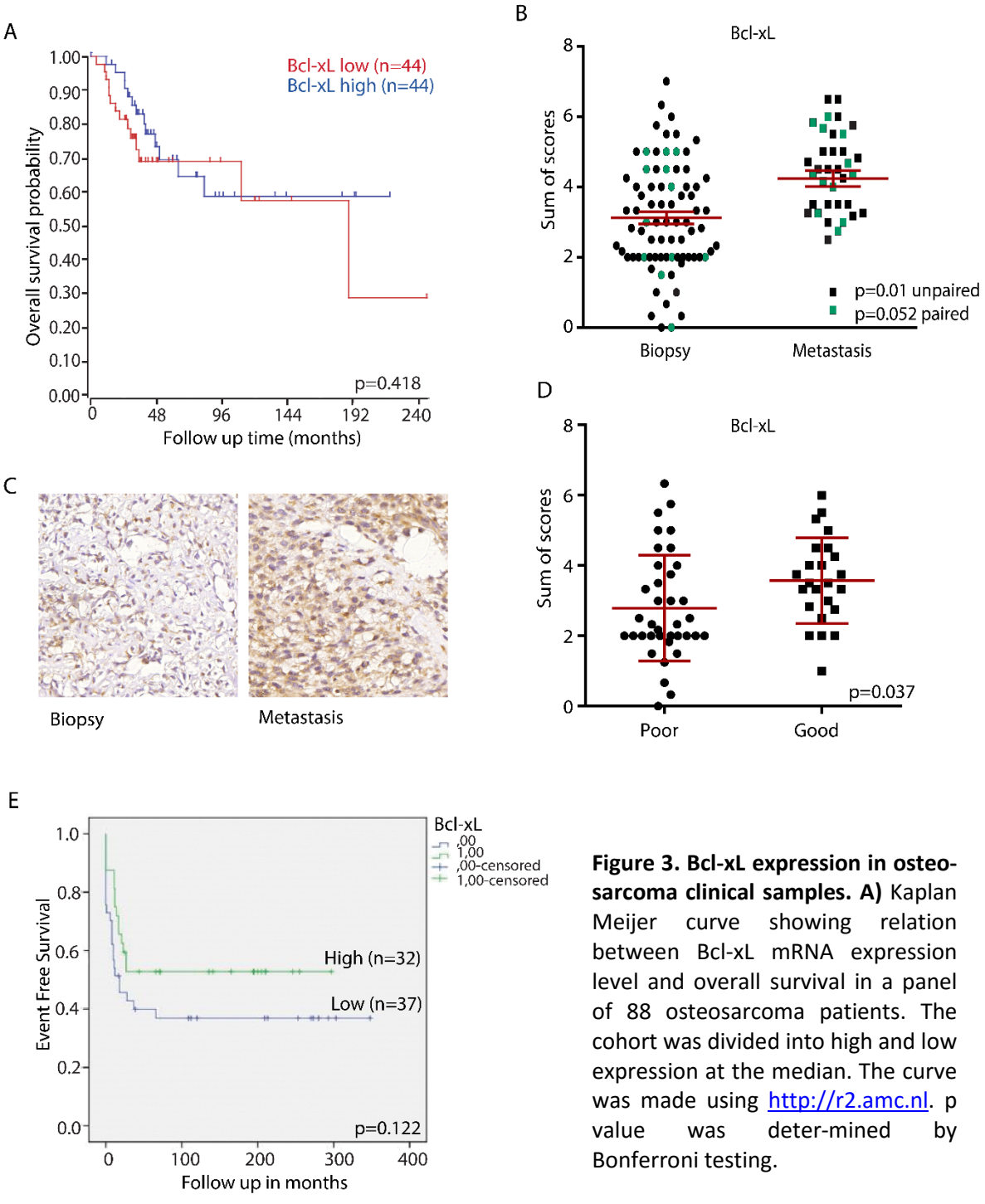

Figure 3. Bcl-xL expression in osteosarcoma clinical samples. A) Kaplan Meijer curve showing relation between Bcl-xL mRNA expression level and overall survival in a panel of 88 osteosarcoma patients. The cohort was divided into high and low expression at the median. The curve was made using http://r2.amc.nl. p value was deter-mined by Bonferroni testing.

B) Sum score (% plus intensity of staining) of Bcl-xL expression in all tumors included in the tissue microarray; average is shown in red. Biopsies and metastases from the same patient are indicated in green (n=12); p-value determined by paired *t*-test. Unpaired biopsies (n=59) and metastases (n=7) are indicated in black; p-value determined by unpaired *t*-test. **C)** Representative images of Bcl-xL expression in primary osteosarcoma biopsy and metastasis. Images made with 40x Lens. **D)** Bcl-xL expression in biopsies of poor and good responders to chemotherapy. P-value determined by unpaired two-tailed *t*-test. **E)** Event free survival related to Bcl-xL expression in tissue microarray. Tumors were divided according to low (mean sum score ≤3; blue line (n=40)) or high Bcl-xL expression (mean sum score >3; green line (n=29)). p-value determined by Log-rank test.

We next determined if synergy was due to enhanced apoptosis in the presence of the combination of ABT-737 and doxorubicin. For this purpose, real time imaging was used to detect labeled Annexin V binding to phosphatidylserine, a phospholipid that translocates to the outer lipid layer of the membrane when cells enter apoptosis [20]. In agreement with the viability assays (Fig 4C), ZK58 cells showed significant Annexin V labeling already in response to 2.5μM ABT-737 alone (Fig 5). However, in U2OS and KPD cells exposed to 2.5μM ABT-737 or 0.1μM doxorubicin alone, Annexin V labeling was absent or appeared at late time points after exposure whereas the combination of 2.5μM ABT-737 and 0.1μM doxorubicin caused rapid, strong Annexin V labeling. Moreover, this enhanced response to the combination of ABT-737 and chemotherapy was abolished in the presence of the pan-caspase inhibitor z-VAD-fmk (Fig. 5). These results indicate that ABT-737, but not the Bcl-2 selective inhibitor HA 14-1 can sensitize human osteosarcoma cells to chemotherapy leading to enhanced apoptosis.

Inhibition of Bcl-xL with WEHI-539 sensitizes osteosarcoma to doxorubicin

To further pinpoint the sensitization to chemotherapy to inhibition of Bcl-xL, we made use of a recently developed Bcl-xL-selective BH3 mimetic, WEHI-539[21]. Exposing U2OS and MOS cells to this compound caused loss of viability at concentrations between 1-10μM and a similar response was seen in KPD and ZK58 cells at concentrations >10 μM (Fig 6A).

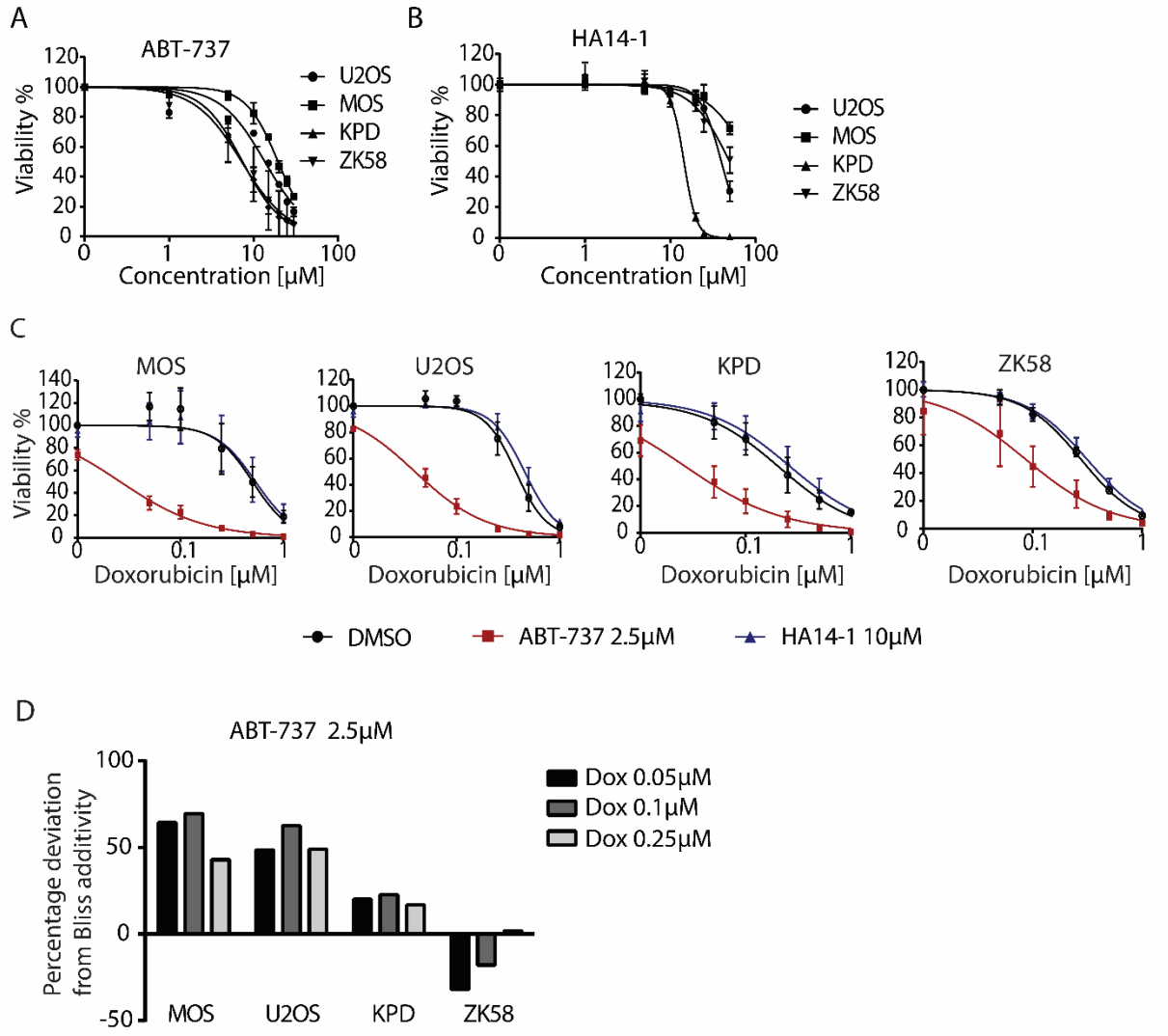

Figure 4. **Pharmacological inhibition of Bcl-xL sensitizes osteosarcoma cells to chemotherapy. A,B)** Dose response curve for ABT-737 (A) and HA14-1 (B) in the indicated human osteosarcoma cell lines. Error bars represent the standard deviation of two experiments performed in triplicate. Cells were exposed for 72 hours. **C)** Dose response curves for doxorubicin in the indicated osteosarcoma cell lines in absence (black circle) or presence of 2.5μM ABT-737 (red square) or 10μM HA14-1 (blue triangle). Cells were exposed for 72 hours. Error bars represent mean ± SEM of three experiments. **D)** Bar graph presenting the percentage of deviation from Bliss additivity based on data shown in C. One representative of three independent experiments is shown.

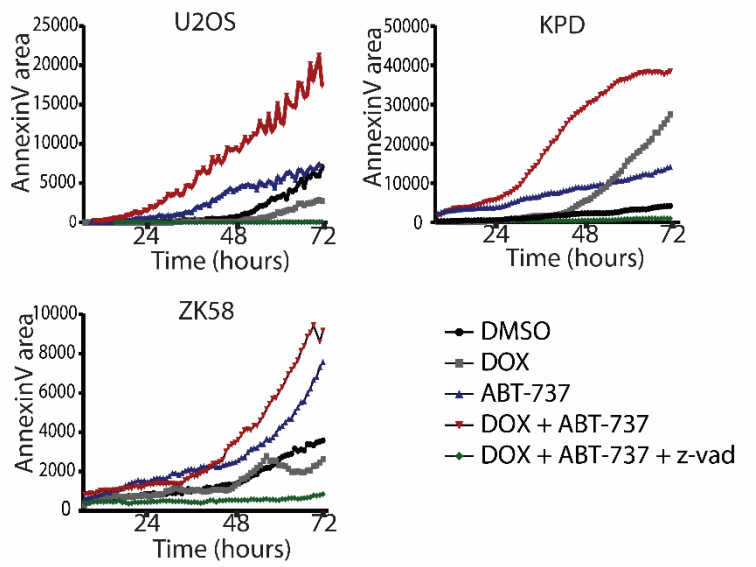

Figure 5. Inhibition of Bcl-xL in combination with doxorubicin leads to enhanced apoptosis. Live imaging of Annexin V accumulation in MOS, U2OS and ZK58 cells. Cells were treated with DMSO, 0.1µM Doxorubicin, 2.5µM ABT-737, or the combination with or without zvad-fmk as indicated. Graphs represent one of three independent experiments. Annexin V was quantified with ImagePro Analyzer 7.0.

Moreover, a suboptimal dose of 1µM WEHI-539 effectively enhanced the response to low doses of doxorubicin in U2OS and MOS cells but showed no effect in KPD,ZK58, MNNG, MG-63 and Saos-2. (Fig 6B). This difference could be attributed to differences in Bcl-xL expression: Bcl-xL protein levels were high in U2OS and MOS as compared to the other cell lines. (Fig 6C). Lastly, we investigated whether sensitization to doxorubicin in the presence of WEHI-539 was due to enhanced apoptosis. Indeed, MOS and U2OS cells exposed to 1µM WEHI-539 showed 2-3-fold higher induction of caspase 3/7 activity in response to 0.1µM doxorubicin, which by itself had little or no effect (Fig 6D). In agreement with the absence of synergy observed in KPD and ZK58 (Fig 6B), WEHI-539 failed to increase caspase activation in response to doxorubicin in these cells (Fig. 6D). Altogether, these findings demonstrate that osteosarcoma cells expressing Bcl-xL can be sensitized to chemotherapy through pharmacological Bcl-xL inhibition.

DISCUSSION

Patients with metastatic or recurrent osteosarcoma present low probability of survival mainly due to resistance to standard chemotherapy [22,23]. Bcl-2 family proteins play a crucial role in regulating cell survival/cell death pathways, and aberrations in their expression or function mediates tumor development and progression [24]. Our siRNA screen identifies anti-apoptosis genes such as Bcl-xL, Mcl-1 and Bfl-1, but interestingly, it also identified pro-apoptosis genes such as Bak, Bok and Bid. Autophagy was reported to be enhanced in Bak/Bax double

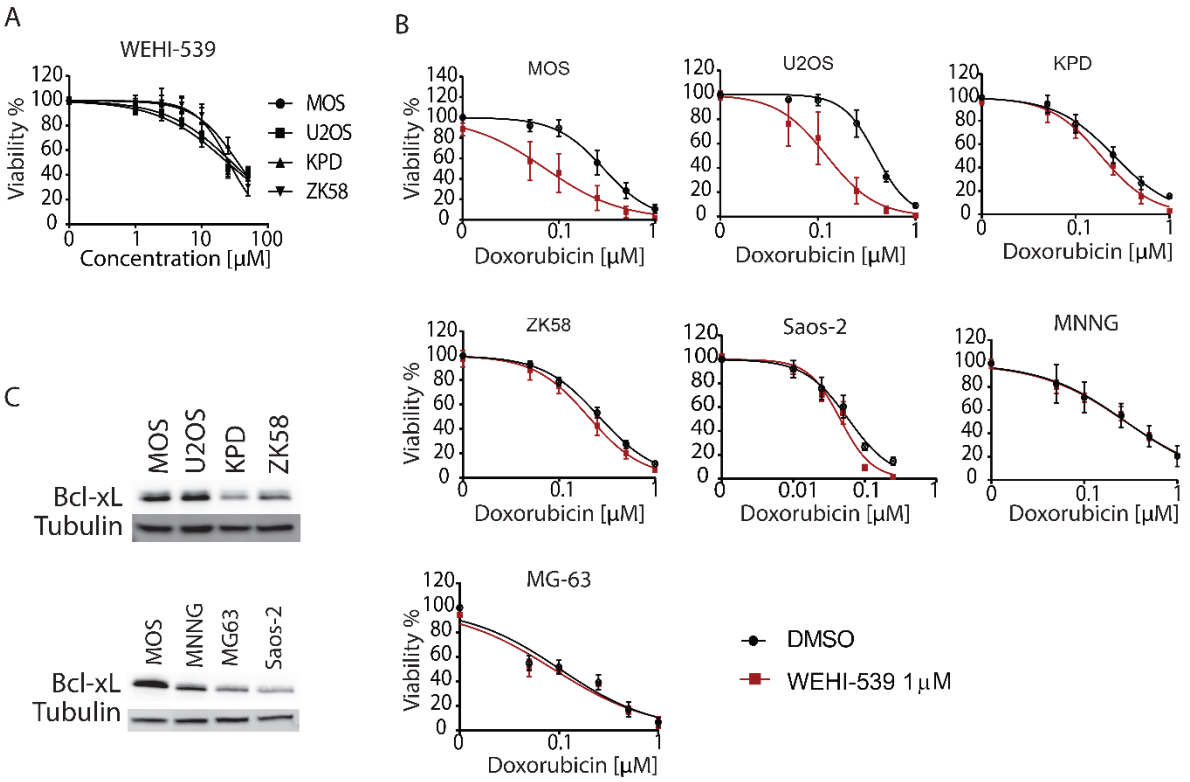

Figure 6. Inhibition of Bcl-xL with WEHI-539 sensitizes osteosarcoma to doxorubicin. A) WEHI-539 dose response curves for the indicated human osteosarcoma cell lines. Cells were exposed for 72 hours. Error bars represent standard deviation of two experiments performed in triplicate. **B)** Doxorubicin dose response curves for the indicated osteosarcoma cell lines in absence (black circles) or presence of 1µM WEHI-539 (red squares). Cells were exposed for 72 hours. Mean ± SEM of three experiments is shown. **C)** Western blot analysis of Bcl-xL expression in the indicated osteosarcoma cell lines. **D)** Caspase 3/7 activity in the indicated osteosarcoma cell lines exposed to DMSO, 0.1µM doxorubicin, 1µM WEHI539 or the combination (mix). Mean ± SEM of three experiments is shown.

knockout cells in response to death stimuli such as radiation and cytotoxic drugs [25,26]. Others have associated cell cycle arrest with Bak/Bax double knockout conditions [27,28]. We identify both aspects in Bak-silenced osteosarcoma cells: the cells proliferate slower and autophagy is activated. We also notice a recruitment of mitochondria to the perinuclear area where they colocalize with autophagosomes, which may point to mitoautophagy.

Alternatively, this may reflect the recent demonstration that mitochondria can in fact contribute to the formation of the autophagosome membrane [29].

Bcl-xL expression has been associated with poor prognosis for patients with colorectal cancer[30] and hepatocellular carcinoma [31]. In colorectal cancer, high expression of Bcl-xL correlates with lymph node metastasis and poorer survival [32]. In melanoma the expression of Bcl-xL is correlated with tumor thickness and disease free survival [33], and in follicular lymphoma it is correlated with overall survival [34]. Bcl-xL expression has also been associated with resistance to cytotoxic agents in ovarian cancer [35]. Furthermore, the correlation between Bcl-xL expression and chemoresistance has been demonstrated in the NCI panel of 60 cell lines to be independent of p53 status [36].

In osteosarcoma, patients with high Bcl-xL mRNA levels have been reported to have a lower probability of 5-year overall survival [18]. We were not able to reproduce such a correlation in our dataset. Moreover, although in our study Bcl-xL protein was expressed in osteosarcoma biopsies and levels were higher in metastases, no correlation with poor response to chemotherapy was observed. The reason for this difference between our own observation and that of others[18] is currently unknown. Nevertheless, in line with the common role of anti-apoptotic Bcl-2 family members in cancer resistance to cytotoxic therapy [37,38] we find that Bcl-xL inhibition can sensitize osteosarcoma cells to low dose chemotherapy.

ABT-737, a small molecule inhibitor of Bcl-xL, Bcl-2 and Bcl-w, was discovered in 2005 and found to enhance the cytotoxic effect of chemotherapy and radiation [39]. Studies in myeloma cells [40], myeloid leukemias[41], neck-squamous cell carcinoma[42], gastrointestinal stromal tumor cells[43], and chondrosarcoma[38] indicated that ABT-737 treatment sensitizes to chemotherapy and other cytotoxic agents [44]. We show that a similar strategy may be relevant in the context of human osteosarcoma. However, a major limitation for translation to the clinic is the fact that ABT-737 is not orally bioavailable, which limits flexibility of dosing regimens. ABT-263 is an analogue of ABT-737 with oral bioavailability, which also potently inhibits Bcl-xL, Bcl-2 and Bcl-w [45]. It has been demonstrated to have little activity as a single agent in a phase II clinical trial[46] but to enhance the effect of other cytotoxic agents [47-49]. The Bcl-xL-selective BH3 mimetic, WEHI-539 used in our current study has shown in vivo toxicity that hinders further clinical studies. Recently, a related Bcl-xL-selective inhibitor, A-1155463, has been synthesized lacking the toxic moiety [50]. Based on our current study, it will be of particular interest to

assess how such a pharmacological inhibitor affects the sensitivity of chemoresistant osteosarcomas. High Bcl-xL protein expression as detected by IHC may serve as a biomarker for treatment with Bcl-xL inhibitors alone or in the presence of chemotherapy. Such a strategy, would potentially allow reduced dosage of doxorubicin, thereby decreasing toxicity. Follow up preclinical studies, for instance using xenograft models, will have to determine efficacy and toxicity associated with different concentrations of Bcl-xL inhibitors, doxorubicin, and combinations. Our findings suggest that such studies are warranted to open the possibility for further clinical studies in patients with osteosarcoma.

ACKNOWLEDGEMENTS

The authors would like to thank Inge Briaire-de Bruijn and Marek Soltes for technical assistance.

FUNDING

This project was granted by a university profile grant of Leiden University/LUMC titled “Translational Drug Discovery and Development”.

CONFLICT OF INTEREST

The authors declare no conflict of interest

REFERENCES

1. Ottaviani G, Jaffe N. Cancer Treatment and Research. In. Norman Jaffe OSB, Stefan S. Bielack, (ed)^(eds). Springer, 2009; 3-13.
2. Federman N, Bernthal N, Eilber FC*, et al.* The multidisciplinary management of osteosarcoma. *Curr Treat Options Oncol* 2009; **10**: 82-93.
3. Mohseny AB, Szuhai K, Romeo S*, et al.* Osteosarcoma originates from mesenchymal stem cells in consequence of aneuploidization and genomic loss of Cdkn2. *The Journal of pathology* 2009; **219**: 294-305.
4. Anninga JK, Gelderblom H, Fiocco M*, et al.* Chemotherapeutic adjuvant treatment for osteosarcoma: where do we stand? *European journal of cancer* 2011; **47**: 2431-2445.
5. Buddingh EP, Anninga JK, Versteegh MI*, et al.* Prognostic factors in pulmonary metastasized high-grade osteosarcoma. *Pediatric blood & cancer* 2010; **54**: 216-221.
6. Czabotar PE, Lessene G, Strasser A*, et al.* Control of apoptosis by the BCL-2 protein family: implications for physiology and therapy. *Nature reviews Molecular cell biology* 2014; **15**: 49-63.
7. Echeverry N, Bachmann D, Ke F*, et al.* Intracellular localization of the BCL-2 family member BOK and functional implications. *Cell death and differentiation* 2013; **20**: 785-799.
8. Tait SW, Green DR. Mitochondria and cell death: outer membrane permeabilization and beyond. *Nature reviews Molecular cell biology* 2010; **11**: 621-632.
9. Shamas-Din A, Kale J, Leber B*, et al.* Mechanisms of action of Bcl-2 family proteins. *Cold Spring Harbor perspectives in biology* 2013; **5**: a008714.
10. Hanahan D, Weinberg RA. Hallmarks of cancer: the next generation. *Cell* 2011; **144**: 646-674.
11. Cory S, Adams JM. The Bcl2 family: regulators of the cellular life-or-death switch. *Nature reviews Cancer* 2002; **2**: 647-656.
12. McIlwain DR, Berger T, Mak TW. Caspase functions in cell death and disease. *Cold Spring Harbor perspectives in biology* 2013; **5**: a008656.
13. Ullman E, Fan Y, Stawowczyk M*, et al.* Autophagy promotes necrosis in apoptosis-deficient cells in response to ER stress. *Cell death and differentiation* 2008; **15**: 422-425.
14. Lindqvist LM, Heinlein M, Huang DC*, et al.* Prosurvival Bcl-2 family members affect autophagy only indirectly, by inhibiting Bax and Bak. *Proceedings of the National Academy of Sciences of the United States of America* 2014; **111**: 8512-8517.
15. Maiuri MC, Zalckvar E, Kimchi A*, et al.* Self-eating and self-killing: crosstalk between autophagy and apoptosis. *Nature reviews Molecular cell biology* 2007; **8**: 741-752.
16. Mizushima N, Yoshimori T. How to interpret LC3 immunoblotting. *Autophagy* 2007; **3**: 542-545.
17. Barth S, Glick D, Macleod KF. Autophagy: assays and artifacts. *The Journal of pathology* 2010; **221**: 117-124.
18. Wang ZX, Yang JS, Pan X*, et al.* Functional and biological analysis of Bcl-xL expression in human osteosarcoma. *Bone* 2010; **47**: 445-454.
19. Greco WR, Bravo G, Parsons JC. The search for synergy: a critical review from a response surface perspective. *Pharmacological reviews* 1995; **47**: 331-385.

20. Puigvert JC, de Bont H, van de Water B*, et al.* High-throughput live cell imaging of apoptosis. *Current protocols in cell biology / editorial board, Juan S Bonifacino [et al]* 2010; **Chapter 18**: Unit 18 10 11-13.
21. Lessene G, Czabotar PE, Sleebs BE*, et al.* Structure-guided design of a selective BCL-X(L) inhibitor. *Nature chemical biology* 2013; **9**: 390-397.
22. Whelan JS, Bielack SS, Marina N*, et al.* EURAMOS-1, an international randomised study for osteosarcoma: results from pre-randomisation treatment. *Annals of oncology : official journal of the European Society for Medical Oncology / ESMO* 2015; **26**: 407-414.
23. Whelan JS, Jinks RC, McTiernan A*, et al.* Survival from high-grade localised extremity osteosarcoma: combined results and prognostic factors from three European Osteosarcoma Intergroup randomised controlled trials. *Annals of oncology : official journal of the European Society for Medical Oncology / ESMO* 2012; **23**: 1607-1616.
24. Yip KW, Reed JC. Bcl-2 family proteins and cancer. *Oncogene* 2008; **27**: 6398-6406.
25. Moretti L, Attia A, Kim KW*, et al.* Crosstalk between Bak/Bax and mTOR signaling regulates radiation-induced autophagy. *Autophagy* 2007; **3**: 142-144.
26. Buytaert E, Callewaert G, Vandenheede JR*, et al.* Deficiency in apoptotic effectors Bax and Bak reveals an autophagic cell death pathway initiated by photodamage to the endoplasmic reticulum. *Autophagy* 2006; **2**: 238-240.
27. Janumyan Y, Cui Q, Yan L*, et al.* G0 function of BCL2 and BCL-xL requires BAX, BAK, and p27 phosphorylation by Mirk, revealing a novel role of BAX and BAK in quiescence regulation. *The Journal of biological chemistry* 2008; **283**: 34108-34120.
28. Cui Q, Valentin M, Janumyan Y*, et al.* Bax-/- bak-/- cells exhibit p27 Thr198 phosphorylation and autophagy. *Autophagy* 2009; **5**: 263-264.
29. Hailey DW, Rambold AS, Satpute-Krishnan P*, et al.* Mitochondria supply membranes for autophagosome biogenesis during starvation. *Cell* 2010; **141**: 656-667.
30. Fucini C, Messerini L, Saieva C*, et al.* Apoptotic proteins as prognostic markers and indicators of radiochemosensitivity in stage II/III rectal cancers. *Colorectal disease : the official journal of the Association of Coloproctology of Great Britain and Ireland* 2012; **14**: e64-71.
31. Watanabe J, Kushihata F, Honda K*, et al.* Prognostic significance of Bcl-xL in human hepatocellular carcinoma. *Surgery* 2004; **135**: 604-612.
32. Jin-Song Y, Zhao-Xia W, Cheng-Yu L*, et al.* Prognostic significance of Bcl-xL gene expression in human colorectal cancer. *Acta histochemica* 2011; **113**: 810-814.
33. Zhuang L, Lee CS, Scolyer RA*, et al.* Mcl-1, Bcl-XL and Stat3 expression are associated with progression of melanoma whereas Bcl-2, AP-2 and MITF levels decrease during progression of melanoma. *Modern pathology : an official journal of the United States and Canadian Academy of Pathology, Inc* 2007; **20**: 416-426.
34. Zhao WL, Daneshpouy ME, Mounier N*, et al.* Prognostic significance of bcl-xL gene expression and apoptotic cell counts in follicular lymphoma. *Blood* 2004; **103**: 695-697.
35. Rogers PM, Beale PJ, Al-Moundhri M*, et al.* Overexpression of BclXL in a human ovarian carcinoma cell line: paradoxic effects on chemosensitivity in vitro versus in vivo. *International journal of cancer Journal international du cancer* 2002; **97**: 858-863.

36. Amundson SA, Myers TG, Scudiero D*, et al.* An informatics approach identifying markers of chemosensitivity in human cancer cell lines. *Cancer research* 2000; **60**: 6101-6110.
37. Eom YW, Kim MA, Park SS*, et al.* Two distinct modes of cell death induced by doxorubicin: apoptosis and cell death through mitotic catastrophe accompanied by senescence-like phenotype. *Oncogene* 2005; **24**: 4765-4777.
38. van Oosterwijk JG, Herpers B, Meijer D*, et al.* Restoration of chemosensitivity for doxorubicin and cisplatin in chondrosarcoma in vitro: BCL-2 family members cause chemoresistance. *Annals of oncology : official journal of the European Society for Medical Oncology / ESMO* 2012; **23**: 1617-1626.
39. Oltersdorf T, Elmore SW, Shoemaker AR*, et al.* An inhibitor of Bcl-2 family proteins induces regression of solid tumours. *Nature* 2005; **435**: 677-681.
40. Trudel S, Stewart AK, Li Z*, et al.* The Bcl-2 family protein inhibitor, ABT-737, has substantial antimyeloma activity and shows synergistic effect with dexamethasone and melphalan. *Clinical cancer research : an official journal of the American Association for Cancer Research* 2007; **13**: 621-629.
41. Kuroda J, Kimura S, Andreeff M*, et al.* ABT-737 is a useful component of combinatory chemotherapies for chronic myeloid leukaemias with diverse drug-resistance mechanisms. *British journal of haematology* 2008; **140**: 181-190.
42. Li R, Zang Y, Li C*, et al.* ABT-737 synergizes with chemotherapy to kill head and neck squamous cell carcinoma cells via a Noxa-mediated pathway. *Molecular pharmacology* 2009; **75**: 1231-1239.
43. Reynoso D, Nolden LK, Yang D*, et al.* Synergistic induction of apoptosis by the Bcl-2 inhibitor ABT-737 and imatinib mesylate in gastrointestinal stromal tumor cells. *Molecular oncology* 2011; **5**: 93-104.
44. Fulda S. Targeting apoptosis pathways in childhood malignancies. *Cancer letters* 2013; **332**: 369-373.
45. Tse C, Shoemaker AR, Adickes J*, et al.* ABT-263: a potent and orally bioavailable Bcl-2 family inhibitor. *Cancer research* 2008; **68**: 3421-3428.
46. Rudin CM, Hann CL, Garon EB*, et al.* Phase II study of single-agent navitoclax (ABT-263) and biomarker correlates in patients with relapsed small cell lung cancer. *Clinical cancer research : an official journal of the American Association for Cancer Research* 2012; **18**: 3163-3169.
47. Chen J, Jin S, Abraham V*, et al.* The Bcl-2/Bcl-X(L)/Bcl-w inhibitor, navitoclax, enhances the activity of chemotherapeutic agents in vitro and in vivo. *Molecular cancer therapeutics* 2011; **10**: 2340-2349.
48. Ackler S, Mitten MJ, Chen J*, et al.* Navitoclax (ABT-263) and bendamustine +/- rituximab induce enhanced killing of non-Hodgkin's lymphoma tumours in vivo. *British journal of pharmacology* 2012; **167**: 881-891.
49. Leung EL, Tam IY, Tin VP*, et al.* SRC promotes survival and invasion of lung cancers with epidermal growth factor receptor abnormalities and is a potential candidate for molecular-targeted therapy. *Molecular cancer research : MCR* 2009; **7**: 923-932.
50. Tao ZF, Hasvold L, Wang L*, et al.* Discovery of a Potent and Selective BCL-XL Inhibitor with in Vivo Activity. *ACS medicinal chemistry letters* 2014; **5**: 1088-1093.
51. Bielack SS, Kempf-Bielack B, Delling G*, et al.* Prognostic factors in high-grade osteosarcoma of the extremities or trunk: an analysis of 1,702 patients treated on

neoadjuvant cooperative osteosarcoma study group protocols. *Journal of clinical oncology : official journal of the American Society of Clinical Oncology* 2002; **20**: 776-790.
52. Mohseny AB, Machado I, Cai Y*, et al.* Functional characterization of osteosarcoma cell lines provides representative models to study the human disease. *Lab Invest* 2011; **91**: 1195-1205.
53. Ottaviano L, Schaefer KL, Gajewski M*, et al.* Molecular characterization of commonly used cell lines for bone tumor research: a trans-European EuroBoNet effort. *Genes Chromosomes Cancer* 2010; **49**: 40-51.
54. Kuijjer ML, Rydbeck H, Kresse SH*, et al.* Identification of osteosarcoma driver genes by integrative analysis of copy number and gene expression data. *Genes, chromosomes & cancer* 2012; **51**: 696-706.
55. Greco WR, Bravo G, Parsons JC. The search for synergy: a critical review from a response surface perspective. *Pharmacol Rev* 1995; **47**: 331-385.
56. Borisy AA, Elliott PJ, Hurst NW*, et al.* Systematic discovery of multicomponent therapeutics. *Proc Natl Acad Sci U S A* 2003; **100**: 7977-7982.

Supplementary Figure

Figure S1: siRNA screen layout and results

exp 1 PLATE1_1

A	1078	1056	743	660	587	2047	862	543	404	364	723	mean siGAPDH	2053 μ_n
B	480	849	443	519	312	2048	1122	665	1302	1561	640	mean siKif11	629 μ_p
C	1044	414	457	797	645	2064	614	302	1531	514	322	s.d siGAPDH	9,539392 σ_n
D	1189	1384	1135	935	497	2035	1331	1404	972	2030	385	s.d siKif11	41,01219 σ_p
E	969	449	1197	636	320	2088	836	714	723	782	672		
F	1582	828	947	1957	831	658	696	1340	1178	945	1146	**Z'-factor**	**0,893501**
G	957	690	1002	961	732	600	1562	1437	1653	1761	1415		
H													

PLATE1_2

A	1459	1719	1045	913	1006	2875	904	788	504	396	873	mean siGAPDH	2888 μ_n
B	576	1224	528	656	378	2876	1597	987	1879	2377	852	mean siKif11	823 μ_p
C	1436	626	674	1000	1021	2913	797	408	2122	825	336	s.d siGAPDH	21,65641 σ_n
D	1684	2121	1707	1387	838	2834	1410	1905	1221	3233	477	s.d siKif11	17,67767 σ_p
E	1310	618	1291	1019	373	2736	940	909	877	1329	1001		
F	2166	1237	1190	3157	1164	835	778	1815	1607	1533	1831	**Z'-factor**	**0,94287**
G	1378	833	1160	1436	946	810	1737	2067	2391	2826	2645		
H													

exp 2 PLATE2_1

A	403	1695	700	663	694	3145						mean siGAPDH	3158 μ_n
B	438	311	307	646	369	3171						mean siKif11	653 μ_p
C	848	913	1522	1189	1133	642						s.d siGAPDH	18,38478 σ_n
D	777	652	816	907	1235	661						s.d siKif11	10,01665 σ_p
E	592	506	301	857	593	657							
F												**Z'-factor**	**0,965982**
G													
H													

PLATE2_2

A	396	1942	842	655	692	3074						mean siGAPDH	3019 μ_n
B	485	336	323	761	397	2964						mean siKif11	651 μ_p
C	978	1038	1841	1136	1307	663						s.d siGAPDH	77,78175 σ_n
D	824	730	1148	1035	1324	635						s.d siKif11	14,57166 σ_p
E	665	455	297	645	624	656							
F												**Z'-factor**	**0,882982**
G													
H													

PLATE 1 layout

	1	2	3	4	5	6	7	8	9	10	11	12
A		BAD_sp	BAD_1	BAD_2	BAD_3	BAD_4	siGAPDH	BCL2L10_sp	BCL2L10_1	BCL2L10_2	BCL2L10_3	BCL2L10_4
B		BAK1_sp	BAK1_1	BAK1_2	BAK1_3	BAK1_4	siGAPDH	BCL2L11_sp	BCL2L11_1	BCL2L11_2	BCL2L11_3	BCL2L11_4
C		BAX_sp	BAX_1	BAX_2	BAX_3	BAX_4	siGAPDH	BCL2L14_sp	BCL2L14_1	BCL2L14_2	BCL2L14_3	BCL2L14_4
D		BBC3_sp	BBC3_1	BBC3_2	BBC3_3	BBC3_4	MOCK	BCL2L2_sp	BCL2L2_1	BCL2L2_2	BCL2L2_3	BCL2L2_4
E		BCL10_sp	BCL10_1	BCL10_2	BCL10_3	BCL10_4	MOCK	BID_sp	BID_1	BID_2	BID_3	BID_4
F		BCL2_sp	BCL2_1	BCL2_2	BCL2_3	BCL2_4	Kif11	BIK_sp	BIK_1	BIK_2	BIK_3	BIK_4
G		BCL2A1_sp	BCL2A1_1	BCL2A1_2	BCL2A1_3	BCL2A1_4	Kif11	BMF_sp	BMF_1	BMF_2	BMF_3	BMF_4
H												

PLATE 2 layout

	1	2	3	4	5	6	7	8	9	10	11	12
A		HRK_sp	HRK_1	HRK_2	HRK_3	HRK_4	siGAPDH					
B		MCL1_sp	MCL1_1	MCL1_2	MCL1_3	MCL1_4	siGAPDH					
C		PMAIP1_sp	PMAIP1_1	PMAIP1_2	PMAIP1_3	PMAIP1_4	Kif11					
D		BOK_sp	BOK_1	BOK_2	BOK_3	BOK_4	Kif11					
E		BCL2L1_sp	BCL2L1_1	BCL2L1_2	BCL2L1_3	BCL2L1_4	Kif11					
F												
G												
H												

Figure S1. Characterization of the siRNA screen. Raw values and plate layouts for siRNA screen using SMARTpool (sp) and single siRNAs (_1, _2, _3, _4) are shown. Mean and SD for positive (si-Kif11) and negative controls (siGapdh) are shown on the right and these values were used to calculate the indicated Z' factors according to: $Z' = 1 - 3*(\sigma_p + \sigma_n) / |\mu_p - \mu_n|$.

4

MEK inhibition induces apoptosis in osteosarcoma cells with constitutive ERK1/2 phosphorylation

Zuzanna Baranski, Tijmen H. Booij, Marieke L. Kuijjer, Yvonne de Jong, Anne-Marie Cleton-Jansen, Leo S. Price, Bob van de Water, Judith V. M. G. Bovée, Pancras C.W. Hogendoorn, Erik H.J. Danen

Published in *Genes and Cancer.* 2015 Nov;6(11-12):503-12

ABSTRACT

Background: Conventional high-grade osteosarcoma is the most common primary bone sarcoma with relatively high incidence in young people. Recurrent and metastatic tumors are difficult to treat. **Methods:** We performed a kinase inhibitor screen in two osteosarcoma cell lines, which identified MEK1/2 inhibitors. These inhibitors were further validated in a panel of six osteosarcoma cell lines. Western blot analysis was performed to assess ERK activity and efficacy of MEK inhibition. A 3D culture system was used to validate results from 2D monolayer cultures. Gene expression analysis was performed to identify differentially expressed gene signatures in sensitive and resistant cell lines. Activation of the AKT signaling network was explored using Western blot and pharmacological inhibition.

Results: In the screen, Trametinib, AZD8330 and TAK-733 decreased cell viability by more than 50%. Validation in six osteosarcoma cell lines identified three cell lines as resistant and three as sensitive to the inhibitors. Western blot analysis of ERK activity revealed that sensitive lines had high constitutive ERK activity. Treatment with the three MEK inhibitors in a 3D culture system validated efficacy in inhibition of osteosarcoma viability.

Conclusions: MEK1/2 inhibition represents a candidate treatment strategy for osteosarcomas displaying high MEK activity as determined by ERK phosphorylation status.

INTRODUCTION

Osteosarcoma is the most common primary malignant bone tumor occurring predominantly in children and adolescents, as well as in people older than 40 years of age. It is thought to arise from mesenchymal stem cells that are capable of producing osteoid(Anninga *et al*, 2011; Rosenberg *et al*, 2013). At the moment of diagnosis, 10-20% of the patients present with metastasis. About 30-40% of the patients with localized osteosarcoma will present with relapse mainly as lung metastasis. Patients with recurrence have very poor prognosis with 23-33% 5-year overall survival(Buddingh *et al*, 2010). Therefore, new effective therapies are urgently needed to improve the prognosis of osteosarcoma patients.

Screening a kinase inhibitor library of pre-clinical or clinically approved drugs provides the possibility of identifying novel candidate treatments for osteosarcoma that can be translated to the clinic. In this study, we performed a kinase inhibitor screen in two osteosarcoma cell lines, and identified MEK inhibitors as possible therapeutic targets in cells with constitutive ERK activation.

MATERIALS AND METHODS

Reagents and antibodies. The kinase inhibitor library (L1200), Trametinib, AZD8330 and TAK-733 inhibitors were purchased from SelleckChem (Huissen, Netherlands). The ERK (9102), phospho(44/42)-ERK (137F5), phospho(Ser2448)-mTOR (D9C2), phospho(Ser473)-AKT (#9271) and AKT (#9272) antibodies were from Cell Signaling (Bioké, Leiden, Netherlands). The antibody against tubulin (T-9026) was from Sigma Aldrich (Zwijndrecht, The Netherlands).

Cell culture. Human osteosarcoma cell lines MOS, U2OS, 143B, ZK58, KPD and Saos-2 were previously described(Mohseny *et al*, 2011; Ottaviano *et al*, 2010). Cells were grown in RPMI1640 medium supplemented with 10% fetal bovine serum and 25 U/mL penicillin and 25 µg/mL of penicillin-streptomycin. All cells were cultured in a humidified incubator at 37°C with 5% CO_2.

Immunoblotting. Cells were lysed with SDS protein buffer (125mM Tris/HCl pH 6.8, 20% glycerol, 4% SDS and 0.2% bromophenol blue). Proteins were resolved by SDS-PAGE and transferred to polyvinylidine difluoride membrane. Membranes were blocked in 5% BSA-TBST (TRIS-0.05% Tween20), followed by overnight incubation with primary antibodies and 45 minutes incubation with HRP-conjugated secondary antibodies. Chemiluminescence was detected with a Typhoon 9400 imager (GE Healthcare).

Cell viability and caspase3/7 activity. Cells were processed using the ATPlite 1Step kit (Perkin Elmer) according to the manufacturer's instructions, followed by luminescence measurement on a plate reader. Caspase 3/7 activity was assessed with Caspase-Glo® 3/7 from Promega (Leiden, The Netherlands) according to manufacturer's protocol, and luminescence measurement on a plate reader.

3D culture assay. MOS and U2OS cells were cultured in 384-well plates (Greiner µclear) in a hydrogel containing Matrigel (Beckton Dickinson) and collagen I, supporting invasive growth of both cell lines. Cells in culture were trypsinized and directly added to the cooled gel solution. Using a robotic liquid handler (CyBio Selma 96/60), 14.5µL of gel-cell suspension was transferred to each well of a 384-well plate (2000 cells/well). After polymerization for 30 minutes at 37°C in an atmosphere of 5% CO_2, growth medium was added on top of the gel. After 24 hours, the cells were exposed to the compounds in quadruplicate for a period of 72 hours. For measuring cell viability in 3D, ATPlite was used as indicated by the manufacturer and luminescence was measured using a FluoroStar plate reader. Percentage viability was thereafter calculated by normalization of all conditions to DMSO. Results are presented as means ± SD. Images of 3D cultures were taken with a BD Pathway 855 (BD Biosciences).

Pathway analysis. We used a previously published data of mRNA expression of 19 osteosarcoma cell lines[Namlos et al PLoSOne 7, e48086, 2012] and performed a LIMMA analysis(Smyth, 2004) of sensitive (MOS, U2OS and 143b) versus resistant (KPD, ZK58 and Saos-2) cell lines(Kuijjer *et al*, 2012). We then ran a pre-ranked gene set enrichment analysis(Subramanian *et al*, 2005) using MSigDb v5.0 BioCarta (www.biocarta.com) signatures on the Benjamini and Hochberg False Discovery Rate corrected p-values obtained from LIMMA. Statistically significant signatures were defined as signatures with FDR<0.25.

Statistical analysis. Dose response curve fitting and statistical analyses were performed with GraphPad Prism 5.0 (GraphPad Software, La Jolla, CA).

RESULTS

Kinase inhibitor screen for inhibition of osteosarcoma cell viability identifies MEK inhibitors

A library composed of 273 kinase inhibitors was used to screen for inhibitors that, as a single agent, decreased viability of osteosarcoma cells. MOS and U2OS were exposed to a concentration of 1µM for 72 hours and viability was determined by measuring ATP production. Each screen was performed in duplicate with a goodness of fit (R^2) of 0.8501 for the screen in MOS and 0.7981 in U2OS (Fig. 1A). All values were normalized to DMSO condition, and the candidates that exhibited less than 50% viability were considered a hit (Fig. 1B). Under this criterium, we identified 16 inhibitors in common for MOS and U2OS of which, six targeted the PI3K/mTOR pathway (BEZ235, GSK2126458, AZD8055, Torin 2, INK-128, PIK-75), six targeted the cell cycle (AT9283, BI2536, SNS-032, CHIR-124, dinaciclib and flavopiridol HCl), one targted Src (KX-391), one targeted Syk and Flt (R406 free base), and two were MEK1/2 inhibitors (Fig. 2A,B). The PI3K/mTOR pathway has been implicated in osteosarcoma cell survival and proliferation in vivo(Gobin *et al*, 2014). Dinaciclib and flavoripirol were previously reported to induce apoptosis in osteosarcoma cells(Fu *et al*, 2011; Li *et al*, 2007). Plk1 inhibition has been shown to cause cell death in osteosarcoma cells and its expression correlates with overall survival in osteosarcoma patients(Duan *et al*, 2010; Morales *et al*, 2011; Yamaguchi *et al*, 2009). Here we focused on three MEK1/2 inhibitors: Trametinib and AZD8330, which were common in MOS and U2OS, and TAK-733, which was a hit in U2OS (in MOS treatment with TAK-733 showed 71% remaining viability).

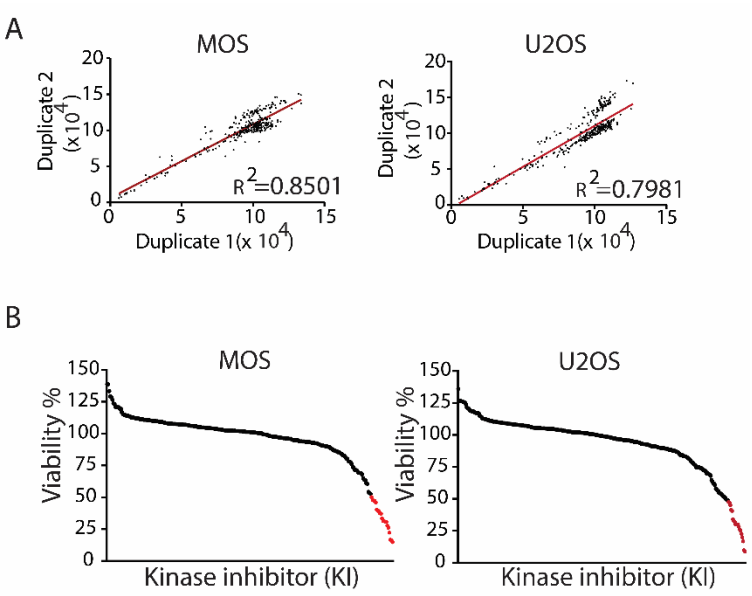

Figure 1. Kinase inhibitor screen in two human osteosarcoma cell lines. A) The screen was performed in MOS and U2OS cell lines in duplicate. The graphs represent the goodness of fit of the screens. **B)** All results were normalized to DMSO and hits are defined by <50% viability (red).

A

KI	Target	KI	Target
AT9283	**Jak2/3, AuroraA/B**	NVP-BGT226	PI3K
AZD2014	mTOR	**INK 128**	**mTOR**
IMD 0354	IKK	**BI2536**	**Plk1**
BEZ235	**mTOR, PI3K**	**SNS-032**	**CDK**
GSK2126458	**mTOR, PI3K**	**R406 free base**	**Syk, Flt**
KX2-391	**Src**	**Torin 2**	**mTOR**
Trametinib	**MEK**	**CHIR-124**	**Chk1**
AZD8055	**mTOR**	**PIK-75**	**PI3K, DNA-PK**
AZD8330	**MEK**	**Dinaciclib**	**CDK**
Torin 1	mTOR	**Flavopiridol HCl**	**CDK**
GSK1059615	mTOR, PI3K	Ly2603618	Chk1
PD0325901	MEK	TAK-733	MEK
PF-03814735	AuroraA,B	ON-01910	Plk1
Hesperadin	AuroraB		

B

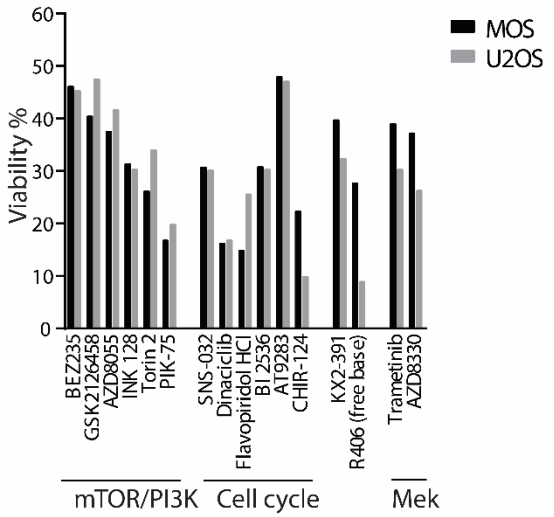

Figure 2. Selection of hits in two human osteosarcoma cell lines. A) List of hits common to both cell lines (bold blue), only in MOS (green) and only in U2OS cells (black). **B)** Bar graphs representing the hits common to both cell lines, their viability score relative to DMSO, and known biological activity.

MEK1/2 inhibition leads to apoptosis in cells with constitutive ERK activation

The activity of these three inhibitors was tested using concentration ranges in six osteosarcoma cell lines: MOS, U2OS, KPD, ZK58, 143b and Saos-2 (Fig. 3A). All three inhibitors decreased viability of MOS and U2OS and strongly affected 143b. By contrast, viability of KPD, ZK58 and Saos-2 was not affected by any of the three inhibitors. A capase3/7 activity assay confirmed that exposure to 0.5µM of each of the drugs induced apoptosis in MOS and U2OS, but not in KPD and ZK58 cells (Fig. 3B).

Next, we asked if the observed differences in the response to MEK inhibition was related to the status of MEK activity, as measured by phosphorylation of the MEK target, ERK. Indeed, 143b, which was the most sensitive cell line, is Ki-*ras*+ transformed (Sero *et al*, 2014) and showed the most prominent ERK phosphorylation, followed by the other two sensitive cell lines, MOS and U2OS (Fig. 4A). The resistant cell lines KPD, ZK58 and Saos-2 showed no

constitutive ERK activation. Exposing MOS, U2OS and 143b to a concentration of 0.5µM of Trametinib, AZD8330 or TAK-733 for 6 hours, led to loss of ERK phosphorylation indicating effective MEK inhibition (Fig. 4B).

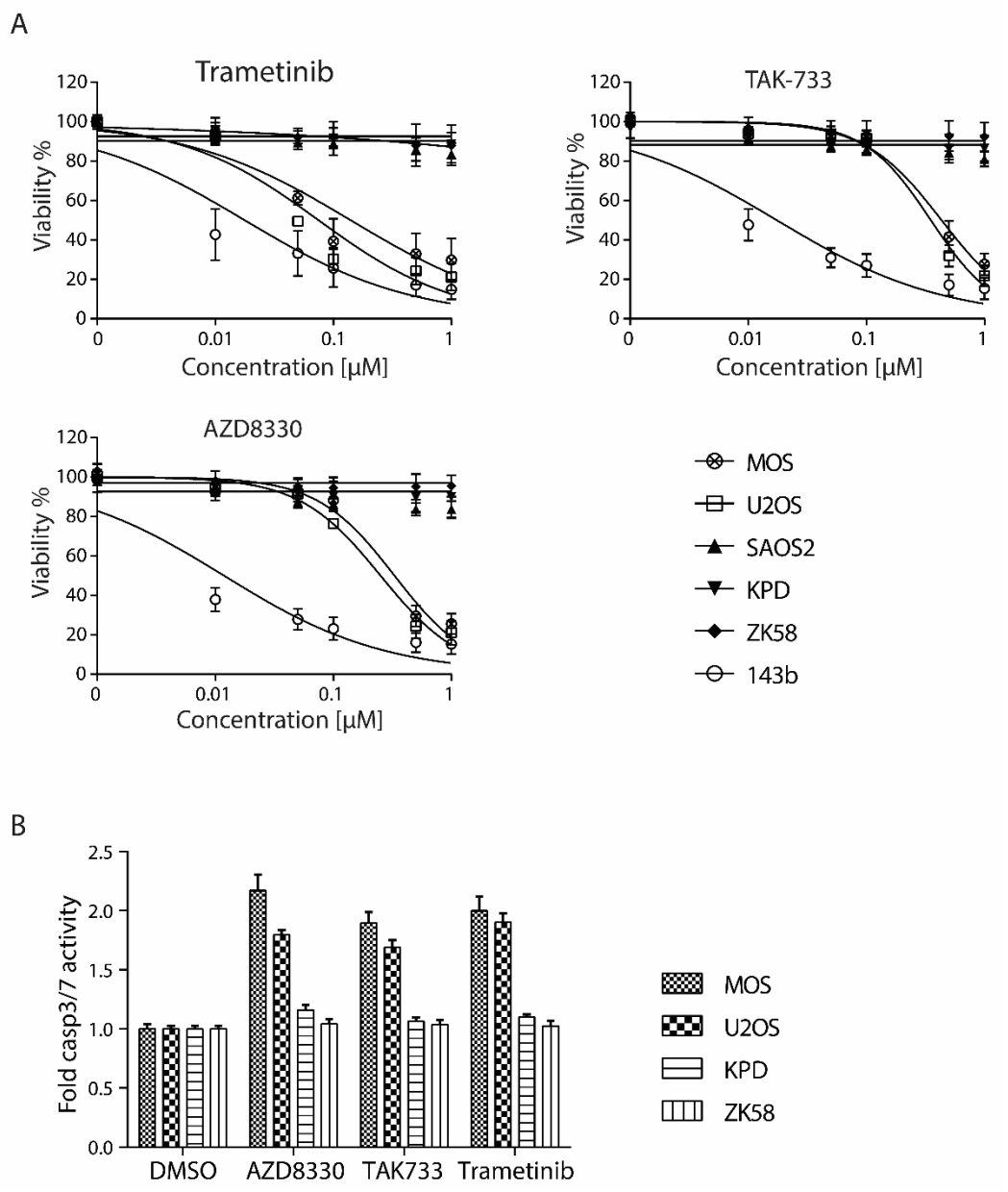

Figure 3. Validation of three MEK inhibitors in 6 osteosarcoma cell lines. A) Dose response curves for Trametinib, AZD8330 and TAK-733 in 6 osteosarcoma cell lines as indicated. Cells were exposed for 72 hours. Each graph represents mean±s.e.m. of three replicates. **B)** Caspase 3/7 activity in presence of indicated inhibitors relative to DMSO in 4 osteosarcoma cell lines. The graph is a representative experiment of 3 independent experiments, each performed in triplicate. Mean±s.d. is shown.

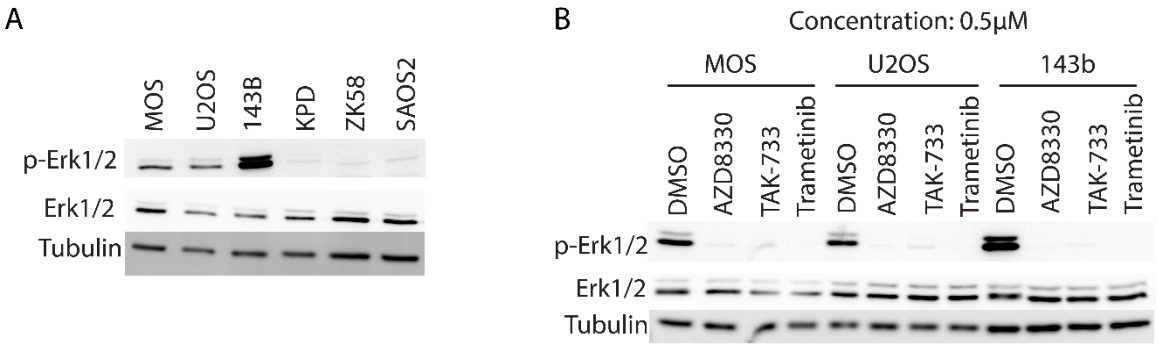

Figure 4. Western blot analysis of ERK phosphorylation in 6 osteosarcoma cell lines and effect of MEK inhibition. A) Western blot analysis of total ERK and phospho-ERK in 6 osteosarcoma cell lines. **B)** Western blot analysis of total ERK and phospho-ERK in MOS, U2OS and 143b osteosarcoma cell lines after 6 hours treatment with DMSO or 0.5µM of the indicated MEK inhibitors.

Validation of MEK inhibition in a 3D cell culture system

We made use of 3D cultures of identified sensitive and resistant cell lines to further validate the effect of Trametinib, AZD8330 and TAK-733. MOS, U2OS, KPD, and ZK58 were suspended in a collagen-matrigel mixture, and exposed 24 hours later to 0.5µM of each inhibitor for a period of 72 hours. As observed in 2D cultures, MOS and U2OS cells died in the presence of each of the three inhibitors whereas KPD and ZK58 were not affected (Fig. 5A,B).

Potential mechanisms of resistance in cell lines not sensitive to MEK inhibition Our data indicated that MEK1/2 inhibition could be used to treat osteosarcomas that present with constitutive ERK activation but not in cases where MEK activity is low. *Ras/Raf* mutations are strong predictors for sensitivity to MEK inhibition(Jing *et al*, 2012; Solit *et al*, 2006) explaining sensitivity of 143b. We searched for mutations in exons or splice sites in the genes *MEK1, MEK2, A-Raf, B-Raf, C-Raf, EGFR, FGFR, IGFR1, K-Ras, H-Ras* and *N-Ras* in all cell lines used, employing a previously published method(van Eijk *et al*, 2011) but could not identify mutations that may explain high constitutive ERK phosphorylation in MOS or U2OS (data not shown).

Next, we performed a pathway analysis on gene expression differences in sensitive (MOS, U2OS and 143b) versus resistant (KPD, ZK58 and Saos-2) cell lines(Kuijjer *et al*, 2012). This analysis revealed 7 signatures with enrichment of differentially expressed genes (Fig 6A). One of the signatures was the AKT pathway, which had positive fold change for 15/22 genes

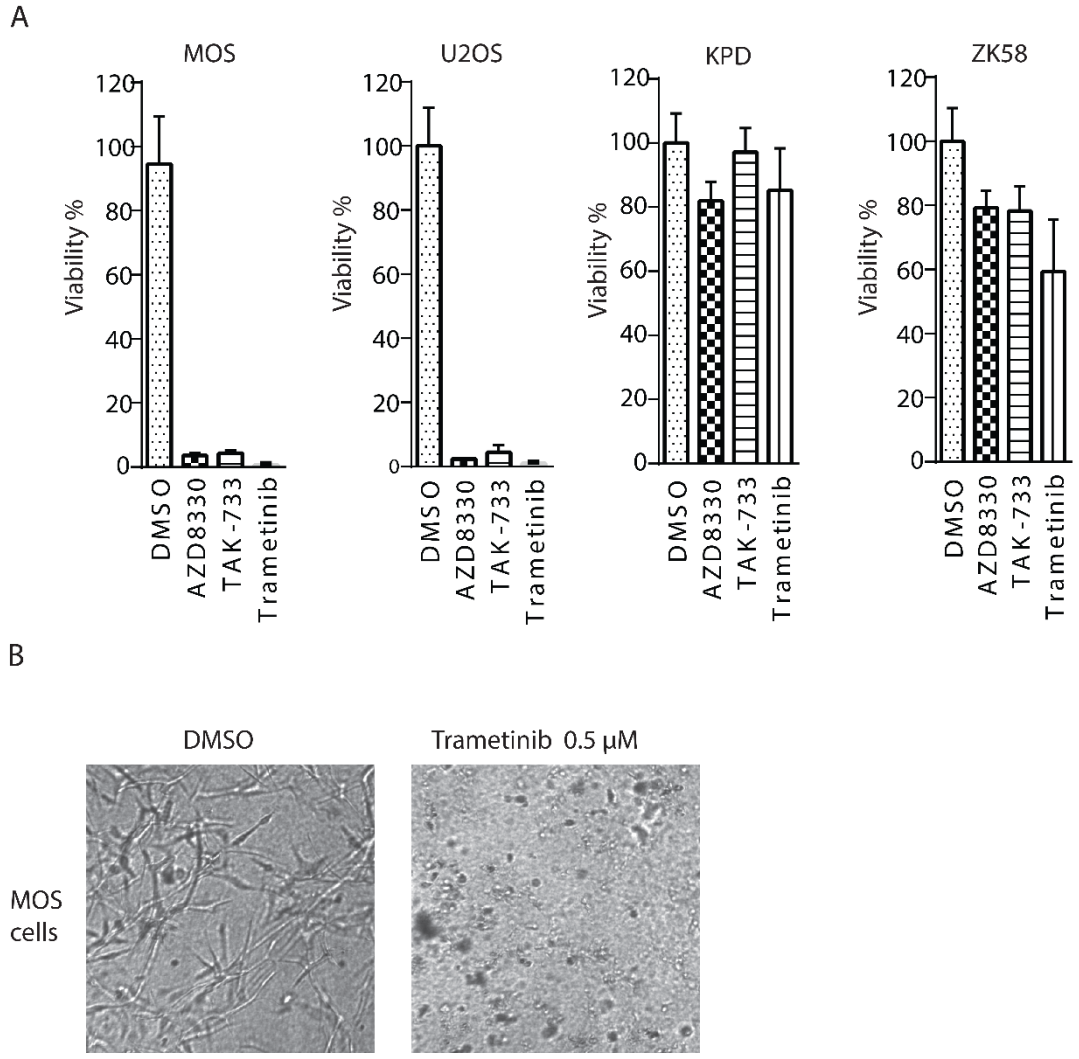

Figure 5. Validation of sensitivity to MEK inhibitors in a 3D culture system. A) MOS, U2OS, KPD and ZK58 cells were re-suspended in a collagen-matrigel mix and 3D cultures were subsequently exposed to 0.5µM of the MEK inhibitors for 72 hours. Graphs are a representative experiment of two replicates, each performed in quadruplicate. Mean±s.d is shown. **B)** Representative images of 3D MOS cultures in absence or presence of Trametinib.

upregulated in the resistant cell lines (Fig. 6B). However, Western blot analysis of phospho-AKT(Ser473) showed active AKT in all cell lines except ZK58 (Fig. 6B). Similarly, mTOR, a downstream target of AKT signaling, was not differentially activated between sensitive and resistant cell lines (Fig. 6C). In agreement, all cell lines responded similarly to inhibition of AKT signaling using A674563 (inhibits AKT1 selectively) or AT7867 (inhibits AKT1/2/3) and were highly sensitive to a dual PI3K/mTOR inhibitor, BEZ235 (Fig. 6D). These data indicate that other differentially activated signaling pathways, rather than the predicted difference in AKT activity underlie differential sensitivity of the osteosarcoma cell lines to MEK inhibition.

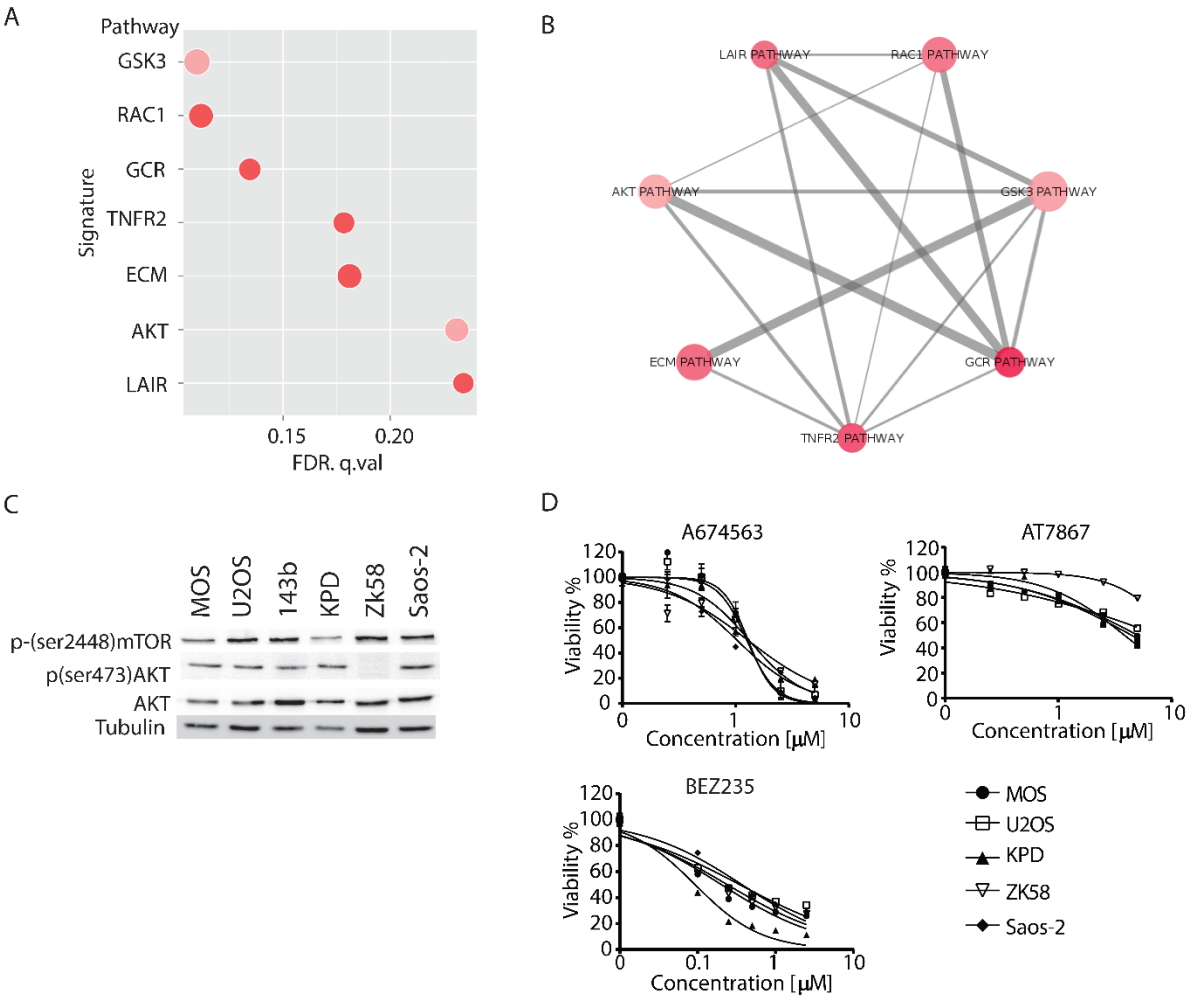

Figure 6. Analysis of AKT pathway and its pharmacological inhibition. A) Plot representing the 7 signatures that were significantly enriched (FDR< 0.25) in the cell lines resistant to MEK inhibition based on gene expression data. Pink/red represents the enrichment score (red>pink), and size represents the gene set size of the signature. **B)** Schematic representation of similarity between the 7 signatures. Pink/red represents the enrichment score (red>pink), and the line width represents the number of genes shared between signatures. **C)** Western blot analysis of total AKT, phosho(Ser473)-AKT and phospho-(Ser2448)-mTOR in the indicated osteosarcoma cell lines. **D)** Dose response curves for the indicated AKT-mTOR inhibitors in the indicated osteosarcoma cell lines. Mean±s.d for experiment performed in triplicate is shown.

DISCUSSION

To identify new candidate avenues for therapeutic intervention for osteosarcoma we performed a kinase inhibitor screen in two human osteosarcoma cells lines. Our screen confirms previously reported findings (e.g. PI3K-AKT-mTOR inhibition), thereby validating

our screen. It also identifies new drugs in the context of osteosarcoma that are in the clinic for other malignancies and hence may be candidates for repurposing.

PI3K-Akt-mTOR pathway is a network that controls many cellular processes such as cell proliferation, survival, metabolism and genomic integrity(Fruman & Rommel, 2014). It has been shown that osteosarcoma strongly depends on this pathway for cell survival and proliferation and pathway inhibition triggers cell death(Gupte *et al*, 2015; Perry *et al*, 2014). The expression of mTOR is correlated with event-free survival and cancer progression in osteosarcoma(Zhou *et al*, 2010). Our screen confirms mTOR signaling as a potential target to treat osteosarcoma.

The main characteristic of tumor cells is uncontrolled cell proliferation and cell cycle regulators are key players in cancer growth. Our screen identifies several inhibitors targeting this hallmark of cancer, including inhibitors of cyclin-dependent kinases and spindle checkpoints. Cyclin-dependent kinases 2,4 and 6 are altered in 80-90% of tumors(Malumbres & Barbacid, 2001). In osteosarcoma, the Rb/p16/CDK4 axis is often deregulated with mutations or deletions in these genes(Mohseny *et al*, 2010; Wei *et al*, 1999). Aurora and polo-like kinases are critical regulators of the mitotic spindle and have been implicated in various cancers(Fu *et al*, 2007). Several studies have shown that inhibition of Aurora kinases leads to cell death in osteosarcoma(Jiang *et al*, 2014; Tavanti *et al*, 2013). The Aurora kinase A inhibitor Alisertib (not present in our library) is undergoing testing in a phase II clinical trial of refractory solid tumors (NCT01154816). Inhibition of polo like kinase (Plk) 1 causes growth inhibition in various cancers(Bu *et al*, 2008; Reagan-Shaw & Ahmad, 2005). In osteosarcoma, Plk1 show higher expression in tumor samples compared to normal tissue, and its inhibition with NMS-P397 (not present in our library) leads to growth arrest and apoptosis(Sero *et al*, 2014).

The Ras-Raf-MEK-ERK mitogen activated protein kinase cascade is known to be involved in cell proliferation, apoptosis, differentiation and development. It integrates signals from cell surface receptors to activate ERK, which in turn enters the nucleus and activates transcription factors such as c-Myc, c-Fos, Ets, and Elk-1(Zhang & Liu, 2002). This pathway is often deregulated in tumors due to mutations or overexpression of upstream signaling components. *B-Raf* and *Ras* are frequently mutated in melanoma, colorectal cancer, ovarian cancer, lung cancer and pancreatic cancer among others (McCubrey *et al*, 2007; Roberts & Der, 2007). In osteosarcoma, ERK pathway activity was reported to occur in 67% of the cases analyzed, and mutations in B-RAF were only found in 13% of the

cohort(Pignochino *et al*, 2009). We identify three MEK inhibitors in the osteosarcoma cell viability screen: Trametinib is a selective allosteric inhibitor of MEK1/2 designed to treat tumor with overactive MEK-ERK pathway, which is found in tumors with *B-Raf* mutations(Abe *et al*, 2011). It was approved for melanoma, and it has also been tested in patients with pancreatic cancer, colorectal cancer and other solid tumors with *B-Raf* mutations(Wright & McCormack, 2013). AZD8330 and TAK-733 are two selective allosteric MEK1/2 inhibitors(Cohen *et al*, 2013; Dong *et al*, 2011). TAK-733 has shown good antitumor activity in melanoma cells(von Euw *et al*, 2012) as well as in human lung cancer(Ishino *et al*, 2015).

Our findings imply that MEK1/2 inhibition is a candidate approach to treat osteosarcomas harboring high ERK activity. Strikingly, while ERK phosphorylation status predicts sensitivity to MEK inhibition, mutation analysis of upstream components of this pathway does not identify candidate predictive mutations. Hence, ERK phosphorylation in tumor tissue as identified by immunohistochemistry may be a more accurate biomarker predicting sensitivity to MEK1/2 inhibitors than genomic analyses. We have not identified an alternative pathway selectively driving viability/growth of cell lines that are resistant to MEK inhibition. An enriched set of genes in the lines points to differential activation of the AKT pathway but based on AKT and mTOR phosphorylation status this pathway is active in all lines and, in agreement, all cell lines are similarly sensitive to AKT-mTOR inhibition. Interestingly, this indicates that three independent cell lines showing strong activity of MEK as well as AKT depend on the activity of both pathways. I.e., inhibition of either pathway is sufficient to cause loss of viability rather than these pathways compensating for each other.

To our knowledge, we are the first to describe the efficacy of MEK inhibition in osteosarcoma cells with high ERK phosphorylation. Recently, a Phase I clinical trial (NCT02124772) started enrolling patients with solid tumors, including osteosarcoma, to study the efficacy of trametinib in combination with dabrafenib. In this setting, such association between ERK phosphorylation status and response to trametinib may be investigated.

CONFLICT OF INTEREST:

L.S. Price is founder and co-owner of OcellO B.V. a contract research company that offers screening services using 3D tissues. This role has had no bearing on the content of the manuscript.

REFERENCES

Abe H, Kikuchi S, Hayakawa K, Iida T, Nagahashi N, Maeda K, Sakamoto J, Matsumoto N, Miura T, Matsumura K, Seki N, Inaba T, Kawasaki H, Yamaguchi T, Kakefuda R, Nanayama T, Kurachi H, Hori Y, Yoshida T, Kakegawa J, Watanabe Y, Gilmartin AG, Richter MC, Moss KG, Laquerre SG (2011) Discovery of a Highly Potent and Selective MEK Inhibitor: GSK1120212 (JTP-74057 DMSO Solvate). *ACS Med Chem Lett* **2**(4)**:** 320-4

Anninga JK, Gelderblom H, Fiocco M, Kroep JR, Taminiau AH, Hogendoorn PC, Egeler RM (2011) Chemotherapeutic adjuvant treatment for osteosarcoma: where do we stand? *European journal of cancer* **47**(16)**:** 2431-45

Bu Y, Yang Z, Li Q, Song F (2008) Silencing of polo-like kinase (Plk) 1 via siRNA causes inhibition of growth and induction of apoptosis in human esophageal cancer cells. *Oncology* **74**(3-4)**:** 198-206

Buddingh EP, Anninga JK, Versteegh MI, Taminiau AH, Egeler RM, van Rijswijk CS, Hogendoorn PC, Lankester AC, Gelderblom H (2010) Prognostic factors in pulmonary metastasized high-grade osteosarcoma. *Pediatric blood & cancer* **54**(2)**:** 216-21

Cohen RB, Aamdal S, Nyakas M, Cavallin M, Green D, Learoyd M, Smith I, Kurzrock R (2013) A phase I dose-finding, safety and tolerability study of AZD8330 in patients with advanced malignancies. *European journal of cancer* **49**(7)**:** 1521-9

Dong Q, Dougan DR, Gong X, Halkowycz P, Jin B, Kanouni T, O'Connell SM, Scorah N, Shi L, Wallace MB, Zhou F (2011) Discovery of TAK-733, a potent and selective MEK allosteric site inhibitor for the treatment of cancer. *Bioorganic & medicinal chemistry letters* **21**(5)**:** 1315-9

Duan Z, Ji D, Weinstein EJ, Liu X, Susa M, Choy E, Yang C, Mankin H, Hornicek FJ (2010) Lentiviral shRNA screen of human kinases identifies PLK1 as a potential therapeutic target for osteosarcoma. *Cancer letters* **293**(2)**:** 220-9

Fruman DA, Rommel C (2014) PI3K and cancer: lessons, challenges and opportunities. *Nature reviews Drug discovery* **13**(2)**:** 140-56

Fu J, Bian M, Jiang Q, Zhang C (2007) Roles of Aurora kinases in mitosis and tumorigenesis. *Molecular cancer research : MCR* **5**(1)**:** 1-10

Fu W, Ma L, Chu B, Wang X, Bui MM, Gemmer J, Altiok S, Pledger WJ (2011) The cyclin-dependent kinase inhibitor SCH 727965 (dinacliclib) induces the apoptosis of osteosarcoma cells. *Mol Cancer Ther* **10**(6)**:** 1018-27

Gobin B, Battaglia S, Lanel R, Chesneau J, Amiaud J, Redini F, Ory B, Heymann D (2014) NVP-BEZ235, a dual PI3K/mTOR inhibitor, inhibits osteosarcoma cell proliferation and tumor development in vivo with an improved survival rate. *Cancer letters* **344**(2)**:** 291-8

Gupte A, Baker EK, Wan SS, Stewart E, Loh A, Shelat AA, Gould CM, Chalk AM, Taylor S, Lackovic K, Karlstrom A, Mutsaers AJ, Desai J, Madhamshettiwar PB, Zannettino AC, Burns C, Huang DC, Dyer MA, Simpson KJ, Walkley CR (2015) Systematic Screening Identifies Dual PI3K and mTOR Inhibition as a Conserved Therapeutic Vulnerability in Osteosarcoma. *Clinical cancer research : an official journal of the American Association for Cancer Research*

Ishino S, Miyake H, Vincent P, Mori I (2015) Evaluation of the therapeutic efficacy of a MEK inhibitor (TAK-733) using F-fluorodeoxyglucose-positron emission tomography in the human lung xenograft model A549. *Ann Nucl Med*

Jiang Z, Jiang J, Yang H, Ge Z, Wang Q, Zhang L, Wu C, Wang J (2014) Silencing of Aurora kinase A by RNA interference inhibits tumor growth in human osteosarcoma cells by inducing apoptosis and G2/M cell cycle arrest. *Oncology reports* **31**(3)**:** 1249-54

Jing J, Greshock J, Holbrook JD, Gilmartin A, Zhang X, McNeil E, Conway T, Moy C, Laquerre S, Bachman K, Wooster R, Degenhardt Y (2012) Comprehensive predictive biomarker analysis for MEK inhibitor GSK1120212. *Mol Cancer Ther* **11**(3)**:** 720-9

Kuijjer ML, Rydbeck H, Kresse SH, Buddingh EP, Lid AB, Roelofs H, Burger H, Myklebost O, Hogendoorn PC, Meza-Zepeda LA, Cleton-Jansen AM (2012) Identification of osteosarcoma driver genes by integrative analysis of copy number and gene expression data. *Genes Chromosomes Cancer* **51**(7)**:** 696-706

Li Y, Tanaka K, Li X, Okada T, Nakamura T, Takasaki M, Yamamoto S, Oda Y, Tsuneyoshi M, Iwamoto Y (2007) Cyclin-dependent kinase inhibitor, flavopiridol, induces apoptosis and inhibits tumor growth in drug-resistant osteosarcoma and Ewing's family tumor cells. *Int J Cancer* **121**(6)**:** 1212-8

Malumbres M, Barbacid M (2001) To cycle or not to cycle: a critical decision in cancer. *Nature reviews Cancer* **1**(3)**:** 222-31

McCubrey JA, Steelman LS, Chappell WH, Abrams SL, Wong EW, Chang F, Lehmann B, Terrian DM, Milella M, Tafuri A, Stivala F, Libra M, Basecke J, Evangelisti C, Martelli AM, Franklin RA (2007) Roles of the Raf/MEK/ERK pathway in cell growth, malignant transformation and drug resistance. *Biochimica et biophysica acta* **1773**(8)**:** 1263-84

Mohseny AB, Machado I, Cai Y, Schaefer KL, Serra M, Hogendoorn PC, Llombart-Bosch A, Cleton-Jansen AM (2011) Functional characterization of osteosarcoma cell lines provides representative models to study the human disease. *Lab Invest* **91**(8)**:** 1195-205

Mohseny AB, Tieken C, van der Velden PA, Szuhai K, de Andrea C, Hogendoorn PC, Cleton-Jansen AM (2010) Small deletions but not methylation underlie CDKN2A/p16 loss of expression in conventional osteosarcoma. *Genes Chromosomes Cancer* **49**(12)**:** 1095-103

Morales AG, Brassesco MS, Pezuk JA, Oliveira JC, Montaldi AP, Sakamoto-Hojo ET, Scrideli CA, Tone LG (2011) BI 2536-mediated PLK1 inhibition suppresses HOS and MG-63 osteosarcoma cell line growth and clonogenicity. *Anti-cancer drugs* **22**(10)**:** 995-1001

Ottaviano L, Schaefer KL, Gajewski M, Huckenbeck W, Baldus S, Rogel U, Mackintosh C, de Alava E, Myklebost O, Kresse SH, Meza-Zepeda LA, Serra M, Cleton-Jansen AM, Hogendoorn PC, Buerger H, Aigner T, Gabbert HE, Poremba C (2010) Molecular characterization of commonly used cell lines for bone tumor research: a trans-European EuroBoNet effort. *Genes Chromosomes Cancer* **49**(1)**:** 40-51

Perry JA, Kiezun A, Tonzi P, Van Allen EM, Carter SL, Baca SC, Cowley GS, Bhatt AS, Rheinbay E, Pedamallu CS, Helman E, Taylor-Weiner A, McKenna A, DeLuca DS, Lawrence MS, Ambrogio L, Sougnez C, Sivachenko A, Walensky LD, Wagle N, Mora J, de Torres C, Lavarino C, Dos Santos Aguiar S, Yunes JA, Brandalise SR, Mercado-Celis GE, Melendez-Zajgla J, Cardenas-Cardos R, Velasco-Hidalgo L, Roberts CW, Garraway LA, Rodriguez-Galindo C, Gabriel SB, Lander ES, Golub TR, Orkin SH, Getz G, Janeway KA (2014) Complementary genomic approaches highlight the PI3K/mTOR pathway as a common vulnerability in osteosarcoma. *Proc Natl Acad Sci U S A* **111**(51)**:** E5564-73

Pignochino Y, Grignani G, Cavalloni G, Motta M, Tapparo M, Bruno S, Bottos A, Gammaitoni L, Migliardi G, Camussi G, Alberghini M, Torchio B, Ferrari S, Bussolino F, Fagioli F, Picci P, Aglietta M (2009) Sorafenib blocks tumour growth, angiogenesis and metastatic potential in preclinical models of osteosarcoma through a mechanism potentially involving the inhibition of ERK1/2, MCL-1 and ezrin pathways. *Mol Cancer* **8:** 118

Reagan-Shaw S, Ahmad N (2005) Silencing of polo-like kinase (Plk) 1 via siRNA causes induction of apoptosis and impairment of mitosis machinery in human prostate cancer cells: implications for the treatment of prostate cancer. *FASEB journal : official publication of the Federation of American Societies for Experimental Biology* **19**(6)**:** 611-3

Roberts PJ, Der CJ (2007) Targeting the Raf-MEK-ERK mitogen-activated protein kinase cascade for the treatment of cancer. *Oncogene* **26**(22)**:** 3291-310

Rosenberg AE, Cleton-Jansen A-M, Pinieux Gd, Deyrup AT, Hauben E, Squire J (2013) Conventional osteosarcoma. In *WHO Classification of Tumours of Soft Tissue and Bone*, pp 282-288. Lyon: IARC

Sero V, Tavanti E, Vella S, Hattinger CM, Fanelli M, Michelacci F, Versteeg R, Valsasina B, Gudeman B, Picci P, Serra M (2014) Targeting polo-like kinase 1 by NMS-P937 in osteosarcoma cell lines inhibits tumor cell growth and partially overcomes drug resistance. *Invest New Drugs* **32**(6)**:** 1167-80

Smyth GK (2004) Linear models and empirical bayes methods for assessing differential expression in microarray experiments. *Stat Appl Genet Mol Biol* **3:** Article3

Solit DB, Garraway LA, Pratilas CA, Sawai A, Getz G, Basso A, Ye Q, Lobo JM, She Y, Osman I, Golub TR, Sebolt-Leopold J, Sellers WR, Rosen N (2006) BRAF mutation predicts sensitivity to MEK inhibition. *Nature* **439**(7074)**:** 358-62

Subramanian A, Tamayo P, Mootha VK, Mukherjee S, Ebert BL, Gillette MA, Paulovich A, Pomeroy SL, Golub TR, Lander ES, Mesirov JP (2005) Gene set enrichment analysis: a knowledge-based approach for interpreting genome-wide expression profiles. *Proc Natl Acad Sci U S A* **102**(43)**:** 15545-50

Tavanti E, Sero V, Vella S, Fanelli M, Michelacci F, Landuzzi L, Magagnoli G, Versteeg R, Picci P, Hattinger CM, Serra M (2013) Preclinical validation of Aurora kinases-targeting drugs in osteosarcoma. *British journal of cancer* **109**(10)**:** 2607-18

van Eijk R, Licht J, Schrumpf M, Talebian Yazdi M, Ruano D, Forte GI, Nederlof PM, Veselic M, Rabe KF, Annema JT, Smit V, Morreau H, van Wezel T (2011) Rapid KRAS, EGFR, BRAF and PIK3CA mutation analysis of fine needle aspirates from non-small-cell lung cancer using allele-specific qPCR. *PLoS One* **6**(3)**:** e17791

von Euw E, Atefi M, Attar N, Chu C, Zachariah S, Burgess BL, Mok S, Ng C, Wong DJ, Chmielowski B, Lichter DI, Koya RC, McCannel TA, Izmailova E, Ribas A (2012) Antitumor effects of the investigational selective MEK inhibitor TAK733 against cutaneous and uveal melanoma cell lines. *Mol Cancer* **11:** 22

Wei G, Lonardo F, Ueda T, Kim T, Huvos AG, Healey JH, Ladanyi M (1999) CDK4 gene amplification in osteosarcoma: reciprocal relationship with INK4A gene alterations and mapping of 12q13 amplicons. *Int J Cancer* **80**(2)**:** 199-204

Wright CJ, McCormack PL (2013) Trametinib: first global approval. *Drugs* **73**(11)**:** 1245-54

Yamaguchi U, Honda K, Satow R, Kobayashi E, Nakayama R, Ichikawa H, Shoji A, Shitashige M, Masuda M, Kawai A, Chuman H, Iwamoto Y, Hirohashi S, Yamada T (2009) Functional genome screen for therapeutic targets of osteosarcoma. *Cancer science* **100**(12)**:** 2268-74

Zhang W, Liu HT (2002) MAPK signal pathways in the regulation of cell proliferation in mammalian cells. *Cell research* **12**(1)**:** 9-18

Zhou Q, Deng Z, Zhu Y, Long H, Zhang S, Zhao J (2010) mTOR/p70S6K signal transduction pathway contributes to osteosarcoma progression and patients' prognosis. *Medical oncology* **27**(4)**:** 1239-45

5

Dasatinib Src inhibitor selectively triggers apoptosis and loss of invasive potential in human osteosarcoma cells

Zuzanna Baranski, Tijmen H. Booij, Anne-Marie Cleton-Jansen, Leo Price, Bob van de Water, Judith V. M. G. Bovée, Pancras C.W. Hogendoorn, Erik H.J. Danen

Manuscript in preparation

ABSTRACT

Conventional high-grade osteosarcoma is the most common primary bone malignancy with relatively high incidence in young people. About 40% of the patients develop metastases and have a very poor prognosis. New insights into osteosarcoma growth and progression that may lead to new therapeutic strategies are needed. Expression and activity of the Src cytoplasmic tyrosine kinase has been correlated with clinical stage and survival. Here, we studied the effect of pharmacological inhibitors of Src activity, including dasatinib, bosutinib and saracatinib in MOS and U2OS human osteosarcoma cell lines in 2D and 3D. All inhibitors decreased viability with an IC50 in the micromolar range. Likewise, treatment with each of the inhibitors reduced the IC50 of doxorubicin. However, only dasatinib treatment triggered caspase3/7 activation pointing to apoptosis. The selective activity of dasatinib correlated with its capacity to reduce Src activity. Next, the effects of the inhibitors were studied in MOS and U2OS cultures in 3D extracellular matrix (ECM) scaffolds. Under these conditions, all three inhibitors reduced viability but formation of branched networks in 3D ECM was selectively inhibited by dasatinib in presence of doxorubicin. The activity of focal adhesion kinase (FAK), a Src substrate that is important for cell migration, was exclusively sensitive to dasatinib. Indeed, in 3D ECM-embedded spheroid cultures dasatinib blocked cell migration capacity whereas the other inhibitors had no or partial effects. Together, these findings point to the use of dasatinib as a candidate drug to enhance apoptosis in response to chemotherapy and to reduce metastatic spread in patients with osteosarcoma.

INTRODUCTION

Osteosarcoma is the most common primary malignant bone tumor that arises from mesenchymal stem cells that are capable of producing osteoid[1]. It has an overall incidence of 3 cases per million annually occurring predominantly in children and adolescents, with a second peak in people above 50 years of age[2]. At the moment of diagnosis, 10-20% of the patients present with metastasis, and about 30-40% of the patients with localized osteosarcoma will relapse mainly by presenting lung metastasis. Patients with relapsed disease have very poor prognosis with 23-33% 5-year overall survival[3].

Src is a nonreceptor tyrosine kinase that belongs to a family of 11 members, and it is widely expressed in a most tissues. Src acts as signal transducer from cell membrane receptors to downstream substrates. Src activity regulates cell morphology, adhesion, and migration, as well as survival and proliferation through activation of PI3K-Akt, Ras-Raf-MEK-ERK, and Jak-Stat and a cell-extracellular matrix (ECM) adhesion-signaling platform including the Src substrate focal adhesion kinase (FAK) [4,5]. Activation and expression of Src in colon cancer is associated with late tumor stage[6] and ability to metastasize[7]. Furthermore, Src activity and expression is also implicated in other malignancies such as breast cancer[8,9], ovarian cancer[10], lung cancer[11] and chondrosarcoma[12]. Notably, despite the fact that Src is overexpressed or constitutively active in many malignancies, mutations are rare in this gene. Therefore, in most cancers Src does not appear to drive tumor initiation or tumor formation, but may rather play a role in aspects of tumor progression[13,14].

As mentioned above, Src transduces signal from cell receptors among which is IGFR. This receptor was reported to be highly expressed in high grade conventional osteosarcoma[15], and its inhibition with antibodies proofed to increase event free survival duration[16]. Additionally,, in osteosarcoma Src expression and activity has been shown to correlate with clinical stage and patient survival, making Src a potential aiding marker to determine prognosis in osteosarcoma[17]. All together, these findings leads us to investigate the inhibition of Src as potential treatment for patients with osteosarcoma.

Dasatinib and bosutinib are two Src/Bcr-Abl inhibitors approved by the FDA for chronic myelogenous leukemia resistant to prior therapy[18-21]. Saracatinib, is a Src inhibitor that is currently in clinical trial for patients with recurrent osteosarcoma localized to the lung (NCT00752206), other cancers including melanoma (NCT00669019), prostate cancer (NCT01267266), and Alzheimer's disease (NCT01864655). The compounds have been tested as single agents in solid tumors with no evident clinical activity[22-26]. Here, we assessed the capacity of these inhibitors to attenuate human osteosarcoma cell survival and migration in 2D and 3D environments. The inhibitors were tested alone or in combination with the clinically relevant chemotherapeutic compound, doxorubicin.

MATERIALS AND METHODS

Reagents and antibodies. Doxorubicin was obtained from the Department of Clinical Pharmacology at LUMC, bosutinib, dasatinib and saracatinib were from SelleckChem (Huissen, Netherlands). Antibodies against ERK1/2(clone137F5), phospho-ERK(42/44) (#4695), AKT(9272), and phospho-AKT(Ser473) (#9271), were from Cell Signalling (Bioké, Leiden, The Netherlands). Antibodies against Src (clone GD11) and phospho-Src(Tyr418) (#44660G) were from Millipore (Amsterdam, The Netherlands) and Invitrogen (Bleiswijk, The Netherlands), respectively. Antibody against FAK (clone4.47) was from BioConnect (Huissen, The Netherlands). Antibodies against phospho-FAK(Tyr925) (**#**MBS8507066) and phospho-FAK(Tyr861) (#MBS8507535) were from Biosourse (California, U.S.A.). Antibody against tubulin (T-9026) was from Sigma-Aldrich (Zwijndrecht, Netherlands).

Cell culture. Human osteosarcoma cell lines MOS, U2OS were previously described[27,28]. Cells were grown in RPMI1640 medium supplemented with 10% fetal bovine serum and 25 U/mL penicillin and 25 μg/mL of penicillin-streptomycin. All cells were cultured in a humidified incubator at 37°C with 5% CO_2.

Western blotting. Cells were lysed with SDS protein buffer (125mM Tris/HCl pH 6.8, 20% glycerol, 4% SDS and 0.2% bromophenol blue). Proteins were resolved by SDS-PAGE and transferred to polyvinylidine difluoride membrane. Membranes were blocked in 5% BSA-TBST (TRIS-0.05% Tween20), followed by overnight incubation with primary antibodies and 45 minutes incubation with HRP-conjugated secondary antibodies. Chemoluminescence was detected with a bioimager, LAS400 (GE Healthcare).

Measuring cell viability and apoptosis in 2D cultures. For cell viability, cells were processed using the ATPlite 1Step kit (Perkin Elmer) according to the manufacturer's instructions, followed by luminescence measurement. Apoptosis was measured by assessing caspase3/7 activity with CaspaseGlo 3/7 (Promega). The cells were exposed to the drug for 24 hours after which the reagent was added 1:1. Luminescence was measured in a Fluostar Optima plate reader.

3D collagen/matrigel culture assay. U2OS and MOS cells were cultured in 384-well plates (Greiner µclear) in a hydrogel containing Matrigel (Beckton Dickinson) and collagen I, supporting invasive growth of both cell lines. Cells in culture were trypsinized and directly added to the cooled gel solution. Using a robotic liquid handler (CyBio Selma 96/60), 14.5µL of gel-cell suspension was transferred to each well of a 384-well plate (2000 cells/well). After polymerization for 30 minutes at 37°C in an atmosphere of 5% CO_2, growth medium was added on top of the gel. After three days, when the cells had formed a network structure, compounds were diluted and added in quadruplicate wells for a period of 72 hours.

For measuring cell viability in 3D, a solution of 7g/L WST-1 (Serva Electrophoresis) and 8mg/L phenazinium methylsulfate (PMS; Sigma Aldrich) in 1x PBS were mixed in a 1:1 ratio and 5µL was added to each well. Plates were placed at 37°C for 5 hours, after which the absorbance at 450nm was measured using a FluoStar Optima late reader. Percentage viability was thereafter calculated by robust normalization (median) of the plates between positive control (no cells; 0% viability) and negative control (solvent; 100% viability) conditions.

For imaging, cells were fixed using 3.7% Formaldehyde (Sigma-Aldrich), permeabilized with 0.1% Triton-X100 and stained for F-actin using 50nM Rhodamine-Phalloidin (Sigma Aldrich) for 12 hours at 4˚C. Subsequently, the plates were washed in PBS for at least 24 hours at 4˚C. The plates were then imaged on a BD Pathway 855 inverted fluorescence microscope (BD Biosciences) using a 4x lens to capture Rhodamine-Phalloidin staining at focal planes spaced 50µm throughout the gel, capturing approximately 70% of a well. Subsequently, maximum intensity projections of the in-focus information of the Z-stacks was made using OcellO (OcellO B.V., Leiden, The Netherlands) image analysis tools.

3D collagen spheroid assay. Cell suspensions were injected into collagen scaffolds using automated injection as previously described[29,30]. 1 mg/ml rat tail collagen was prepared in complete growth medium supplemented with 1:5 dilution of 0.44M $NaHCO_3$ and 1:10 dilution of 1M Hepes pH 7.4. 60µL was added to each well of a 96-well µ-clear plate (Corning) and incubated for 1 hour at 37ºC to allow polymerization. Cells were collected in medium containing 2% PVP, transferred to a needle and droplets of ~8nL were injected into the collagen gels resulting in spheroids of ~300µm diameter, using injection robotics from Life Science Methods, Leiden NL (http://www.lifesciencemethods.com). For DIC imaging of spheroids, a Nikon confocal microscope was used.

Statistical analysis. Dose response curve fitting and all statistical analyses were performed with GraphPad Prism 5.0 (GraphPad Software, La Jolla, CA). The unpaired two-tailed *t*-test

was used to compare between groups. Significant difference between groups in the 3D assay was calculated using 2way ANOVA with Bonferroni posttest.

RESULTS

Reduced human osteosarcoma cell viability in presence of bosutinib, dasatinib and saracatinib and selective Src kinase inactivation by dasatinib

We determined the effect of dasatinib, bosutinib and saracatinib on cell viability in MOS and U2OS human osteosarcoma cells. Responses to these inhibitors were highly similar for MOS and U2OS cells but differed considerably between the different inhibitors (Fig. 1A). Both cell lines showed no response to bosutinib concentrations <1 μM and a rapid decline in viability was observed as the bosutinib concentration increased from 1 to 5 μM. Instead, viability gradually decreased in response to 0.1-10 μM dasatinib and a similar trend, albeit less effective, was observed for saracatinib. IC50 for bosutinib and dasatinib was ~5 μM and IC50 was >10 μM for saracatinib (Fig 1B).

PI3K/AKT and Raf-MEK-ERK MAP kinase signaling pathways represent important drivers of survival and proliferation in many different cancer types. These two pathways are regulated by Src activity[31,32]. We tested if treatment of MOS and U2OS cells with the Src inhibitors affected these pathways. However, treatment with up to 2.5μM bosutinib, dasatinib, or saracatinib did not affect phosphorylation of ERK (Fig 1C). In fact, treatment with saracatinib increased the levels of ERK phosphorylation particularly in U2OS. On the other hand, dasatinib and saracatinib suppressed AKT phosphorylation at 2.5μM whereas bosutinib had no effect. Moreover, while 1μM dasatinib effectively attenuated Src phosphorylation at Y418 in both cell lines, indicating attenuated Src kinase activity, bosutinib and saracatinib failed to do so even at 2.5μM.

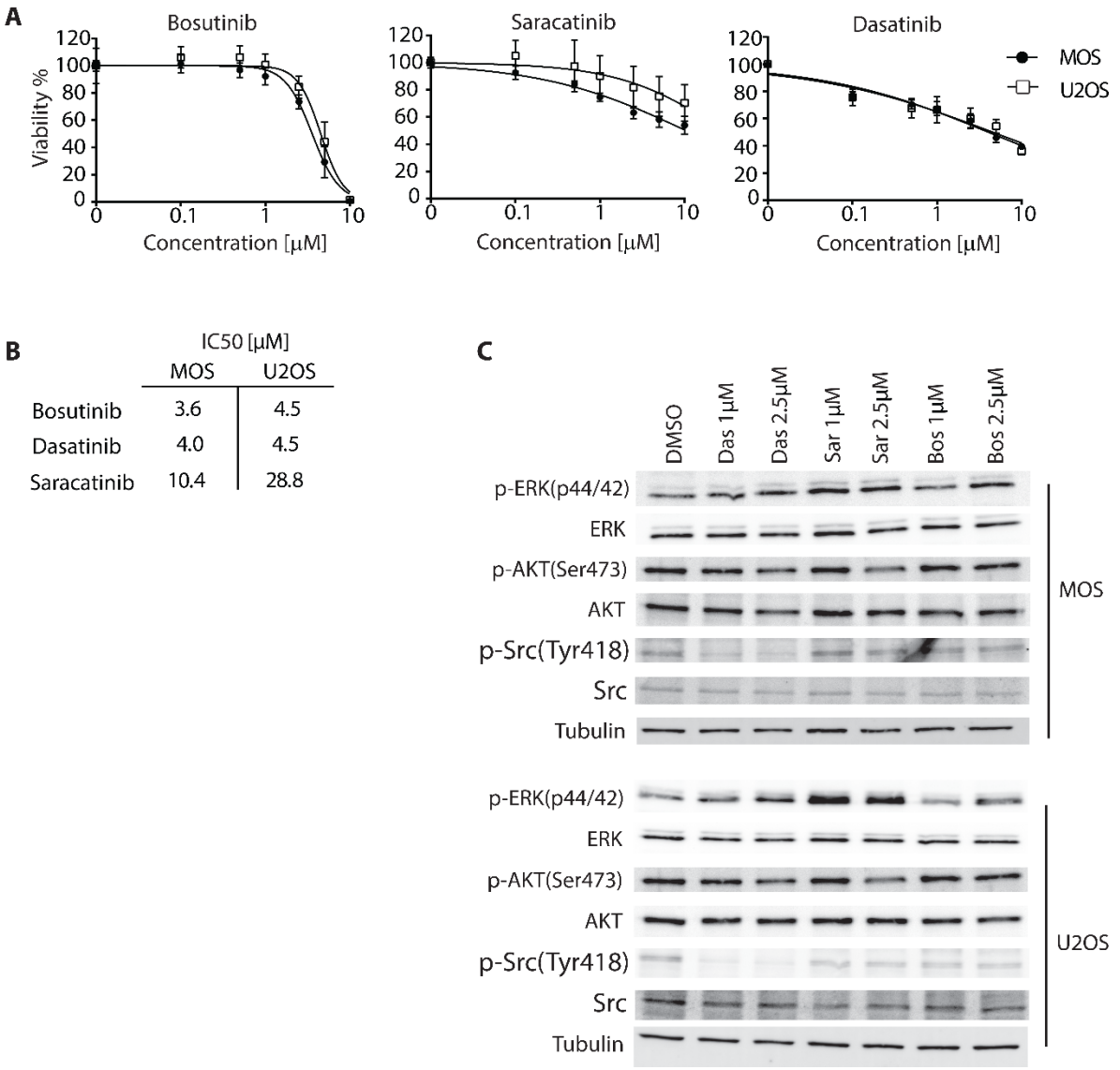

Figure 1. Effect of dasatinib, bosutinib and saracatinib in human osteosarcoma cells.
A) Dose response curves for dasatinib, bosutinib and saracatinib in two human osteosarcoma cell lines. Error bars represent the standard deviation of three experiments performed in triplicate. Cells were exposed for 72 hours. **B)** Table with IC50 values of bosutinib, dasatinib and saracatinib in MOAS and U2OS cells. **C)** Western blot analysis of phospho-ERK(p44/42), total ERK, phospho-AKT(Ser473), total AKT, phospho-Src(Tyr418), total Src, and tubulin loading control in MOS and U2OS cells under control (DMSO) conditions or after 48 hours treatment with 1 or 2.5μM of the indicated inhibitors.

Sensitization to doxorubicin in presence of bosutinib, dasatinib and saracatinib and selective induction of apoptosis by dasatinib

Src kinase activity may not be a bona fide cancer driver and mono therapy using either of these inhibitors may be ineffective. However, as Src stimulates pro-survival and proliferation

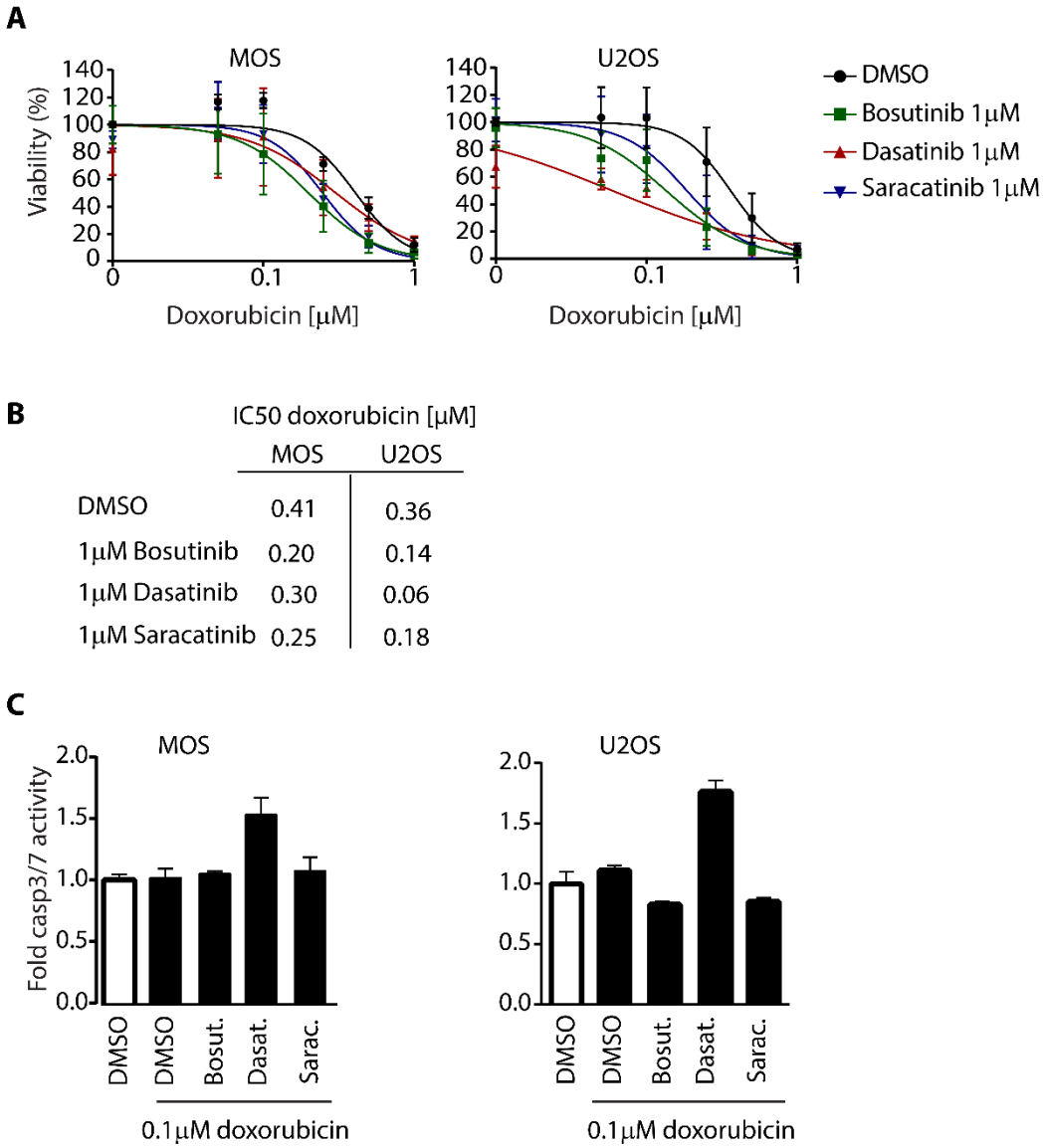

Figure 2. Effect of dasatinib, bosutinib and saracatinib in human osteosarcoma cells in the context of doxorubicin. A). Dose response curves for doxorubicin in two human osteosarcoma cell lines in absence (black) or presence of 1μM of dasatinib (red), bosutinib (green) or saracatinib (blue). Cells were exposed for 72 hours. Error bars represent mean ± SEM of three experiments **B)**. Table with IC50 values for doxorubicin alone (DMSO) or in combination with 1μM bosutinib, dasatinib or saracatinib in MOS and U2OS cells. **C)** Caspase 3/7 activity in two human osteosarcoma cell lines under control conditions (white bars) or upon exposure for 24 hours to 0.1μM doxorubicin (black bars) in the presence of DMSO or 1μM dasatinib, bosutinib and saracatinib as indicated. Mean ± S.D is shown for one representative experiment of 3 performed in triplicate.

signaling pathways[13,14]. Its inhibition may render tumor cells more sensitive to chemotherapy. To investigate this, MOS and U2OS cells were exposed to 1μM of the inhibitor together with a dose range of doxorubicin for 72 hours. Indeed, both cell lines showed a reduction in viability already at lower doses of doxorubicin in presence of

dasatinib, bosutinib, or saracatinib, as compared to the response to doxorubicin alone (Fig. 2A). For MOS cells, the IC50 for doxorubicin was reduced by 30-50%, and for U2OS cells a reduction of 50-80% was observed (Fig 2B). In order to assess whether decreased viability was related to apoptosis, we determined caspse3/7 activity. Interestingly, only treatment with dasatinib led to apoptosis either alone (not shown) or in combination with doxorubicin (Fig. 2C).

Reduced human osteosarcoma cell viability in 3D cultures in presence of bosutinib, dasatinib and saracatinib and selective morphological effects induced by dasatinib.

Next, we analyzed the effect of the panel of Src inhibitors in a 3D in vitro culture model. MOS and U2OS cells were suspended in a collagen-matrigel mixture and allowed to form a multicellular network for 72 hours. Subsequently cells were exposed to 1μM of dasatinib, bosutinib, or saracatinib alone or combined with a concentration range of doxorubicin. Inhibition of cell viability by the inhibitors alone as measured biochemically, was more pronounced compared to effects measured in 2D. All three inhibitors by themselves caused a reduction in viability of 40-50% (Fig 3A). Additional treatment with doxorubicin further decreased viability but no synergy was observed between doxorubicin and any of the inhibitors.

Next we used imaging and image analysis algorithms to measure “branch length” and “solidity” or roundness of the multicellular structures; parameters correlated cell migration [33]. Low concentrations of doxorubicin up to 0.1μM did not affect these parameters (Fig 3B). Exposure to 1μM of the Src inhibitors alone led to decreased branch length and increased solidity. However, in the presence of dasatinib MOS and U2OS cells were selectively responsive to low concentrations of doxorubicin; showing a decrease in branch length and a concomitant increase in solidity of the multicellular structures (Fig. 3B-D).

Selective inhibition of FAK activity and 3D osteosarcoma cell migration by dasatinib

To further investigate morphological effects caused by these inhibitors that may impact on osteosarcoma progression we made use of a 3D spheroid model. MOS and U2OS cells were injected as nL droplets into collagen gels as described before[29,30], and resulting spheroids

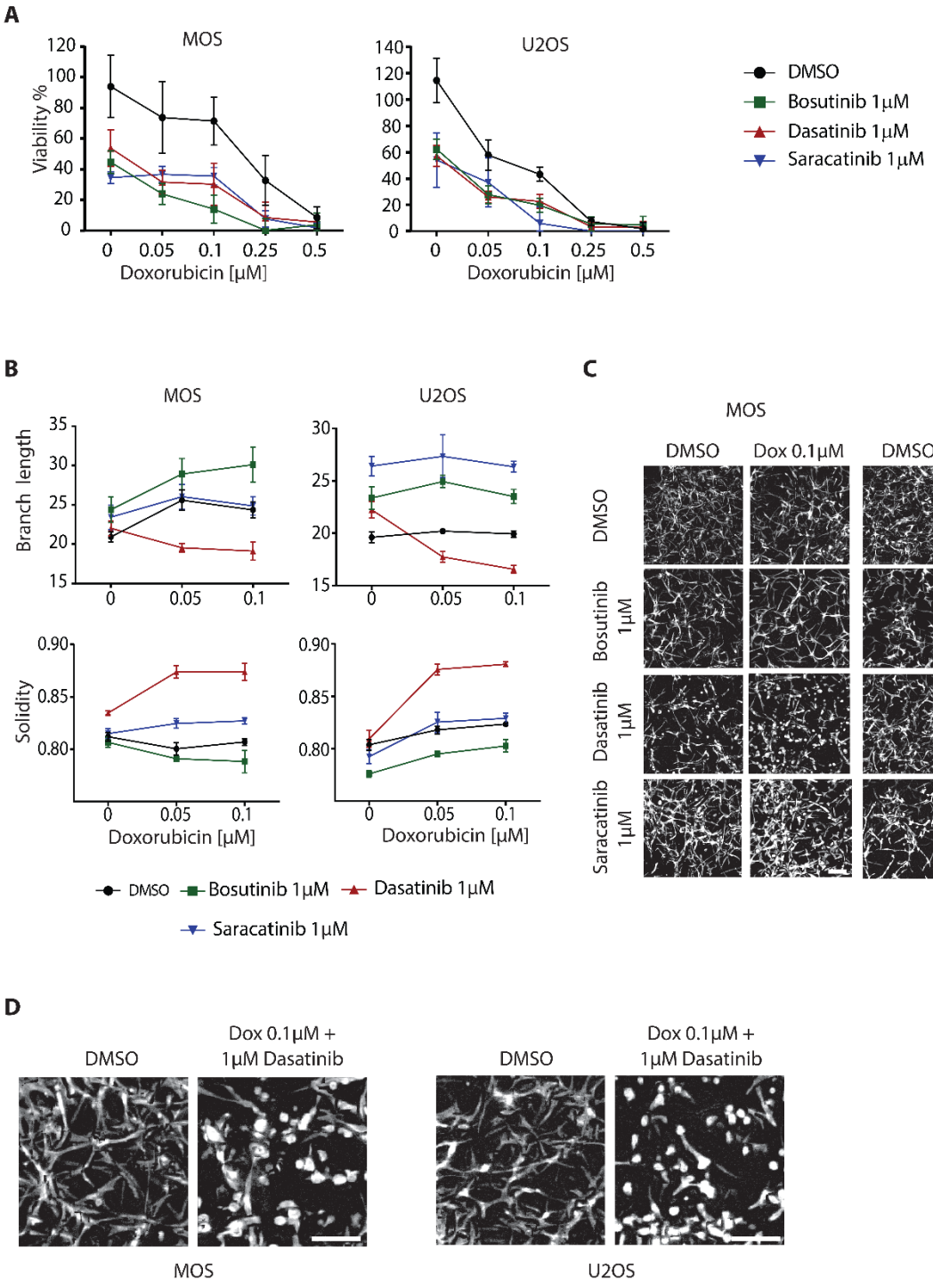

Figure 3. **Effect of dasatinib, bosutinib and saracatinib in human osteosarcoma cells in the context of doxorubicin in 3D cultures. A,B)** Doxorubicin dose response curve for human osteosarcoma cells grown in collagen/matrigel mixture under control conditions (DMSO; black line) or in presence of 1μM dasatinib (red), bosutinib (green), or saracatinib (blue). Cells were exposed for 72 hours. **A)** Viability was assessed using WST/PMS absorbance. Error bars represent mean ± SEM of three experiments. Values were normalized to median of DMSO. **B)** Image analysis was used to assess average branch length (top graphs) and solidity (bottom graphs). Error bars represent mean±s.d of one representative experiment done in quadruplicate. **C)** Representative images such as those used

for graphs in B. Each image is a compression of 11stacks of the 3D culture. **D)** Zoom-in of selected areas from images in C, showing marked effect of doxorubicin/dasatinib combination.

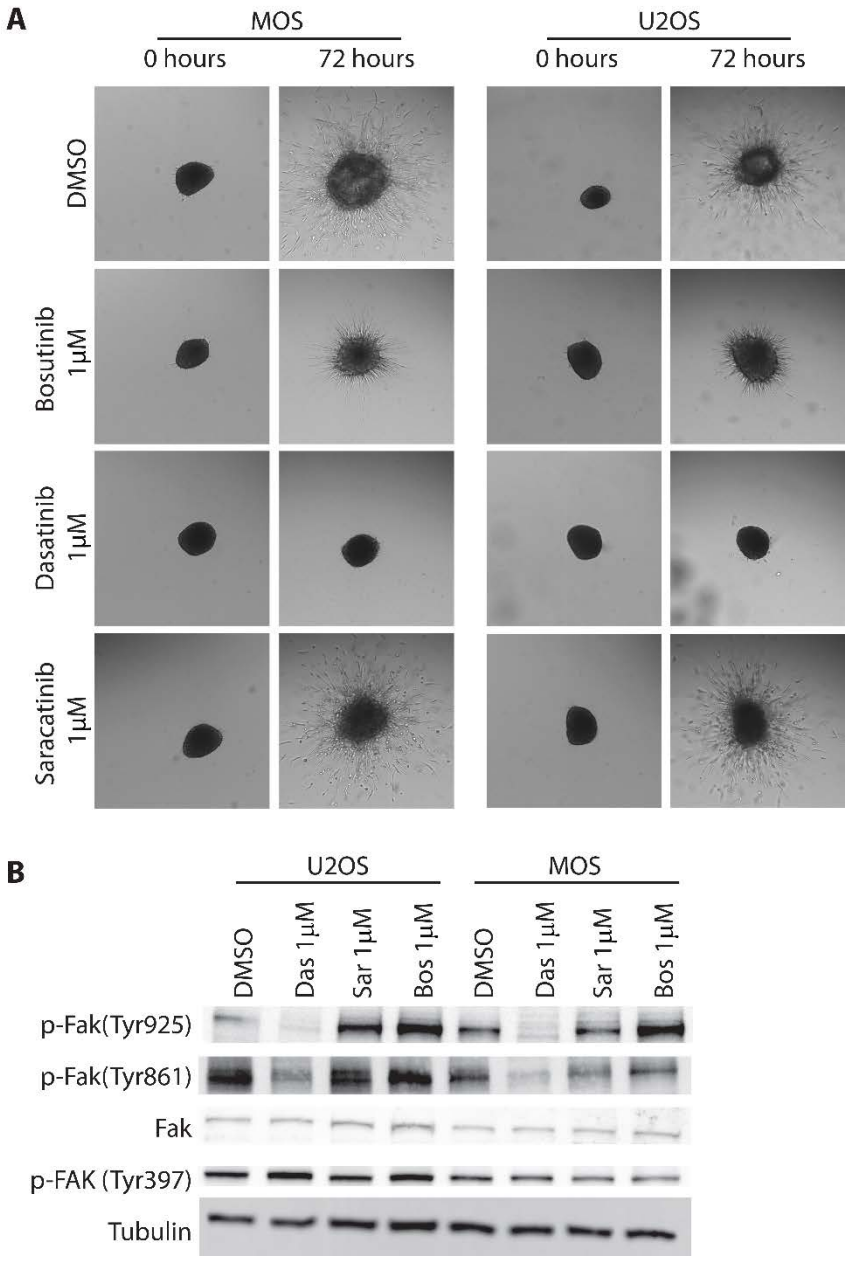

Figure 4. Dasatinib inhibits Fak activation and stops collagen invasion in osteosarcoma. A) U2OS and MOS cell-derived collagen-embedded spheroids directly after cell-injection (0 hours) and after 72 hours incubation under control conditions (DMSO) or in presence of 1µM of the indicated inhibitors. Images were obtained using a Nikon confocal microscope. **B)** Western blot analysis of total FAK and phospho-Fak(Tyr397), (Tyr861), (Tyr925), and tubulin loading control for U2OS and MOS cells maintained for 48 hours under control conditions (DMSO) or in presence of 1µM of the indicated inhibitors.

were exposed to DMSO or 1µM bosutinib, dasatinib and saracatinib for 72hours. Saracatinib did not affect spheroid outgrowth or 3D cell migration and bosutinib had an intermediate effect while dasatinib treatment completely blocked outgrowth and collagen invasion of MOS and U2OS cells in this model (Fig 4A).

Src promotes invasion and metastasis and plays a key role as a regulator of cell-ECM adhesions containing the Src substrate FAK. The Src/FAK complex integrates signals from the extracellular environment and controls and coordinates adhesion dynamics and cell migration[34,35]. FAK is autophosphorylated at Tyr397 upon integrin-mediated adhesion creating a binding site for Src, which subsequently phosphorylates FAK at Tyr407, 576, 577, 861 and 925[34,36]. We analyzed FAK phosphorylation after 48hour treatment with 1µM dasatinib, bosutinib or saracatinib. The FAK autophosphorylation site was not affected by any of the inhibitors. However, in agreement with its selective inhibition of cell migration through 3D ECM scaffolds, phosphorylation of FAK at Src substrates Tyr861 and Tyr925 was selectively inhibited by dasatinib. Whereas Saracatinib and bosutinib had no apparent effect (Fig 4B).

DISCUSSION

It this study we investigated the effect of Src inhibitors dasatinib, bosutinib, and saracatinib in two human osteosarcoma cell lines. Impacts on cell viability and migration were tested as single agent as well as in combination with the chemotherapeutic compound doxorubicin, which is used in the clinic for treatment of osteosarcoma. Src activity regulates the PI3K-Akt, Ras-Raf-ERK, Jak-Stat and FAK-Paxillin pathways. In osteosarcoma, none of the inhibitors interfered with ERK and AKT phosphorylation, and only dasatinib inhibited Src and Fak activation in MOS and U2OS cell lines. Notably, the inhibitors have other targets such as other members of the Src family, Bcr-Abl, MAPK kinases, Eph receptors, cKit, STK6, PDGFR and TEC family kinases[37,38]. An interesting study that mapped the target profile of bosutinib in chronic myeloid leukemia cells identified new targets and to what extent targets were inhibited[39]. The MAPK family was found to be a major target, but MEK1 and MEK2 were not significantly inhibited[39,40]. These results may explain why ERK activation was not inhibited by any of the inhibitors in our study. Furthermore, the fact these inhibitors do not completely inhibit the activity of a kinase, can explain why saracatinib and bosutinib did not show appreciable inhibition of Fak phosphorylation, and failed to affect cell migration. The autophosphorylation site (Tyr397) of Fak causes a conformational change allowing Src binding and further Fak phosphorylation in Tyr576/577, Tyr861 and Tyr925. The phosphorylation of these sites is important for the interaction with integrins and E-cadherin[34]. While bosutinib has been reported to inhibit Fak-(Y925) phosphorylation in breast cancer cells, in the two osteosarcoma cell lines used only dasatinib inhibited Src-mediated phosphorylation of Fak Tyr861 and Tyr925[41].

To study the effect of dasatinib, bosutinib or saracatinib on the migratory behavior of osteosarcoma cells, we used 3D cell culture systems. 3D cultures may better reflect the tumor microenvironment as compared to 2D cultures and cell matrix adhesions and migratory behavior are closer to the in vivo situation [42-45]. In the two 3D systems we used, including mixture of cells in collagen/matrigel and microinjection of cells to examine migration from spheroids in collagen gels, collagen type I is the major ECM component and this is also the main component (90%) of the ECM of bones[46]. Our finding that dasatinib selectively blocks osteosarcoma cell migration in this environment correlates its selective inhibition of Src-mediated Fak phosphorylation. Thus, dasatinib treatment likely interferes with the Src/Fak signaling platform to prevent cell migration and may thus interfere with metastatic capacity.

In addition, dasatinib selectively triggers apoptosis and causes morphological alterations in 3D cultures in the presence of doxorubicin. It was previously reported that dasatinib has the capacity to sensitize chondrosarcoma cells to doxorubicin (jolieke refe). Furthermore, a new Src inhibitor, A-770041, was shown to increase sensitivity to doxorubicin in osteosarcoma cells (refDuan et al. BMC Cancer 2014, 14:681). Notably, a decrease in the IC50 of doxorubicin is observed when combined with each the inhibitors indicating that dasatinib selectively affects some, but not all aspects of these inhibitors. Several studies have hown that these three inhibitors do not have an effect as single agents in solid tumors. For example, dasatinib inhibits activation of Src and Fak *in vi*tro and *in vivo*, but it does not induce apoptosis or prevent tumor metastasis to the lungs in a xenograft osteosarcoma mice[47]. However, others showed that for biliary tract carcinomas saracatinib was effective in a preclinical model, and both dasatinib and saracatinib are effective in leukemia[48-51] indicating that the therapeutic effect of these inhibitors is cancer type-dependent. Despite the lack of activity as a single agent, the combination of dasatinib, bosutinib or saracatinib with doxorubicin in breast cancer or pancreatic cancer cells did lead to a synergistic effect *in vitro* and *in vivo*[52-54].

Altogether, we find that dasatinib selectively inhibits activity of the Src/Fak signaling complex in osteosarcoma cells and, most likely as a consequence of this, migration in collagen scaffolds. Furthermore, while all three inhibitors decreased the IC50 of doxorubicin, dasatinib selectively triggers apoptosis and morphological changes in the context of doxorubicin. Our findings point to the combination of dasatinib and doxorubicin as a potential therapy for osteosarcoma to prevent or minimize metastasis.

CONFLICT OF INTEREST

L.S. Price is founder and co-owner of OcellO B.V. a contract research company that offers screening services using 3D tissues. This role has had no bearing on the content of the manuscript.

REFERENCES

1. Mohseny AB, Szuhai K, Romeo S, *et al.* Osteosarcoma originates from mesenchymal stem cells in consequence of aneuploidization and genomic loss of Cdkn2. *J Pathol* 2009; **219**: 294-305.
2. Rosenberg AE, Cleton-Jansen A-M, Pinieux Gd, *et al.* Conventional osteosarcoma. In: WHO Classification of Tumours of Soft Tissue and Bone. (ed)^(eds). IARC: Lyon, 2013; 282-288.
3. Buddingh EP, Anninga JK, Versteegh MI, *et al.* Prognostic factors in pulmonary metastasized high-grade osteosarcoma. *Pediatric blood & cancer* 2010; **54**: 216-221.
4. Amundson SA, Myers TG, Scudiero D, *et al.* An informatics approach identifying markers of chemosensitivity in human cancer cell lines. *Cancer research* 2000; **60**: 6101-6110.
5. Yeatman TJ. A renaissance for SRC. *Nature reviews Cancer* 2004; **4**: 470-480.
6. Talamonti MS, Roh MS, Curley SA, *et al.* Increase in activity and level of pp60c-src in progressive stages of human colorectal cancer. *The Journal of clinical investigation* 1993; **91**: 53-60.
7. Jones RJ, Avizienyte E, Wyke AW, *et al.* Elevated c-Src is linked to altered cell-matrix adhesion rather than proliferation in KM12C human colorectal cancer cells. *British journal of cancer* 2002; **87**: 1128-1135.
8. Biscardi JS, Ishizawar RC, Silva CM, *et al.* Tyrosine kinase signalling in breast cancer: epidermal growth factor receptor and c-Src interactions in breast cancer. *Breast cancer research : BCR* 2000; **2**: 203-210.
9. Hynes NE. Tyrosine kinase signalling in breast cancer. *Breast cancer research : BCR* 2000; **2**: 154-157.
10. Wiener JR, Windham TC, Estrella VC, *et al.* Activated SRC protein tyrosine kinase is overexpressed in late-stage human ovarian cancers. *Gynecologic oncology* 2003; **88**: 73-79.
11. Leung EL, Tam IY, Tin VP, *et al.* SRC promotes survival and invasion of lung cancers with epidermal growth factor receptor abnormalities and is a potential candidate for molecular-targeted therapy. *Molecular cancer research : MCR* 2009; **7**: 923-932.
12. van Oosterwijk JG, van Ruler MA, Briaire-de Bruijn IH, *et al.* Src kinases in chondrosarcoma chemoresistance and migration: dasatinib sensitises to doxorubicin in TP53 mutant cells. *British journal of cancer* 2013; **109**: 1214-1222.
13. Frame MC. Src in cancer: deregulation and consequences for cell behaviour. *Biochimica et biophysica acta* 2002; **1602**: 114-130.
14. Summy JM, Gallick GE. Src family kinases in tumor progression and metastasis. *Cancer metastasis reviews* 2003; **22**: 337-358.
15. Hassan SE, Bekarev M, Kim MY, *et al.* Cell surface receptor expression patterns in osteosarcoma. *Cancer* 2012; **118**: 740-749.
16. Kim SY, Toretsky JA, Scher D, *et al.* The role of IGF-1R in pediatric malignancies. *Oncologist* 2009; **14**: 83-91.
17. Hu C, Deng Z, Zhang Y, *et al.* The prognostic significance of Src and p-Src expression in patients with osteosarcoma. *Medical science monitor : international medical journal of experimental and clinical research* 2015; **21**: 638-645.
18. Kantarjian H, Jabbour E, Grimley J, *et al.* Dasatinib. *Nature reviews Drug discovery* 2006; **5**: 717-718.

19. Stansfield L, Hughes TE, Walsh-Chocolaad TL. Bosutinib: a second-generation tyrosine kinase inhibitor for chronic myelogenous leukemia. *Ann Pharmacother* 2013; **47**: 1703-1711.
20. Shah NP, Tran C, Lee FY, *et al.* Overriding imatinib resistance with a novel ABL kinase inhibitor. *Science* 2004; **305**: 399-401.
21. Boschelli F, Arndt K, Gambacorti-Passerini C. Bosutinib: a review of preclinical studies in chronic myelogenous leukaemia. *European journal of cancer* 2010; **46**: 1781-1789.
22. Reddy SM, Kopetz S, Morris J, *et al.* Phase II study of saracatinib (AZD0530) in patients with previously treated metastatic colorectal cancer. *Invest New Drugs* 2015; **33**: 977-984.
23. Mackay HJ, Au HJ, McWhirter E, *et al.* A phase II trial of the Src kinase inhibitor saracatinib (AZD0530) in patients with metastatic or locally advanced gastric or gastro esophageal junction (GEJ) adenocarcinoma: a trial of the PMH phase II consortium. *Invest New Drugs* 2012; **30**: 1158-1163.
24. Gucalp A, Sparano JA, Caravelli J, *et al.* Phase II trial of saracatinib (AZD0530), an oral SRC-inhibitor for the treatment of patients with hormone receptor-negative metastatic breast cancer. *Clin Breast Cancer* 2011; **11**: 306-311.
25. Schilder RJ, Brady WE, Lankes HA, *et al.* Phase II evaluation of dasatinib in the treatment of recurrent or persistent epithelial ovarian or primary peritoneal carcinoma: a Gynecologic Oncology Group study. *Gynecologic oncology* 2012; **127**: 70-74.
26. Taylor JW, Dietrich J, Gerstner ER, *et al.* Phase 2 study of bosutinib, a Src inhibitor, in adults with recurrent glioblastoma. *J Neurooncol* 2015; **121**: 557-563.
27. Mohseny AB, Machado I, Cai Y, *et al.* Functional characterization of osteosarcoma cell lines provides representative models to study the human disease. *Lab Invest* 2011; **91**: 1195-1205.
28. Ottaviano L, Schaefer KL, Gajewski M, *et al.* Molecular characterization of commonly used cell lines for bone tumor research: a trans-European EuroBoNet effort. *Genes Chromosomes Cancer* 2010; **49**: 40-51.
29. Truong HH, de Sonneville J, Ghotra VP, *et al.* Automated microinjection of cell-polymer suspensions in 3D ECM scaffolds for high-throughput quantitative cancer invasion screens. *Biomaterials* 2012; **33**: 181-188.
30. Truong HH, Xiong J, Ghotra VP, *et al.* beta1 integrin inhibition elicits a prometastatic switch through the TGFbeta-miR-200-ZEB network in E-cadherin-positive triple-negative breast cancer. *Science signaling* 2014; **7**: ra15.
31. Dhillon AS, Hagan S, Rath O, *et al.* MAP kinase signalling pathways in cancer. *Oncogene* 2007; **26**: 3279-3290.
32. Martini M, De Santis MC, Braccini L, *et al.* PI3K/AKT signaling pathway and cancer: an updated review. *Annals of medicine* 2014; **46**: 372-383.
33. Di Z, Klop MJ, Rogkoti VM, *et al.* Ultra high content image analysis and phenotype profiling of 3D cultured micro-tissues. *PLoS One* 2014; **9**: e109688.
34. McLean GW, Carragher NO, Avizienyte E, *et al.* The role of focal-adhesion kinase in cancer - a new therapeutic opportunity. *Nature reviews Cancer* 2005; **5**: 505-515.
35. Mitra SK, Schlaepfer DD. Integrin-regulated FAK-Src signaling in normal and cancer cells. *Current opinion in cell biology* 2006; **18**: 516-523.
36. Westhoff MA, Serrels B, Fincham VJ, *et al.* SRC-mediated phosphorylation of focal adhesion kinase couples actin and adhesion dynamics to survival signaling. *Molecular and cellular biology* 2004; **24**: 8113-8133.
37. Zarbock A. The shady side of dasatinib. *Blood* 2012; **119**: 4817-4818.

38. Shi H, Zhang CJ, Chen GY, *et al.* Cell-based proteome profiling of potential dasatinib targets by use of affinity-based probes. *J Am Chem Soc* 2012; **134**: 3001-3014.
39. Remsing Rix LL, Rix U, Colinge J, *et al.* Global target profile of the kinase inhibitor bosutinib in primary chronic myeloid leukemia cells. *Leukemia* 2009; **23**: 477-485.
40. Winter GE, Rix U, Carlson SM, *et al.* Systems-pharmacology dissection of a drug synergy in imatinib-resistant CML. *Nat Chem Biol* 2012; **8**: 905-912.
41. Vultur A, Buettner R, Kowolik C, *et al.* SKI-606 (bosutinib), a novel Src kinase inhibitor, suppresses migration and invasion of human breast cancer cells. *Molecular cancer therapeutics* 2008; **7**: 1185-1194.
42. Ravi M, Paramesh V, Kaviya SR, *et al.* 3D cell culture systems: advantages and applications. *J Cell Physiol* 2015; **230**: 16-26.
43. Thoma CR, Zimmermann M, Agarkova I, *et al.* 3D cell culture systems modeling tumor growth determinants in cancer target discovery. *Advanced drug delivery reviews* 2014; **69-70**: 29-41.
44. Cukierman E, Pankov R, Stevens DR, *et al.* Taking cell-matrix adhesions to the third dimension. *Science* 2001; **294**: 1708-1712.
45. Baker EL, Srivastava J, Yu D, *et al.* Cancer cell migration: integrated roles of matrix mechanics and transforming potential. *PLoS One* 2011; **6**: e20355.
46. Boskey AL. Bone composition: relationship to bone fragility and antiosteoporotic drug effects. *Bonekey Rep* 2013; **2**: 447.
47. Hingorani P, Zhang W, Gorlick R, *et al.* Inhibition of Src phosphorylation alters metastatic potential of osteosarcoma in vitro but not in vivo. *Clinical cancer research : an official journal of the American Association for Cancer Research* 2009; **15**: 3416-3422.
48. Cavalloni G, Peraldo-Neia C, Sarotto I, *et al.* Antitumor activity of Src inhibitor saracatinib (AZD-0530) in preclinical models of biliary tract carcinomas. *Molecular cancer therapeutics* 2012; **11**: 1528-1538.
49. Cortes JE, Kantarjian HM, Brummendorf TH, *et al.* Safety and efficacy of bosutinib (SKI-606) in chronic phase Philadelphia chromosome-positive chronic myeloid leukemia patients with resistance or intolerance to imatinib. *Blood* 2011; **118**: 4567-4576.
50. Apperley JF, Cortes JE, Kim DW, *et al.* Dasatinib in the treatment of chronic myeloid leukemia in accelerated phase after imatinib failure: the START a trial. *J Clin Oncol* 2009; **27**: 3472-3479.
51. Yu EY, Wilding G, Posadas E, *et al.* Phase II study of dasatinib in patients with metastatic castration-resistant prostate cancer. *Clinical cancer research : an official journal of the American Association for Cancer Research* 2009; **15**: 7421-7428.
52. Pichot CS, Hartig SM, Xia L, *et al.* Dasatinib synergizes with doxorubicin to block growth, migration, and invasion of breast cancer cells. *British journal of cancer* 2009; **101**: 38-47.
53. Beeharry N, Banina E, Hittle J, *et al.* Re-purposing clinical kinase inhibitors to enhance chemosensitivity by overriding checkpoints. *Cell Cycle* 2014; **13**: 2172-2191.
54. Liu KJ, He JH, Su XD, *et al.* Saracatinib (AZD0530) is a potent modulator of ABCB1-mediated multidrug resistance in vitro and in vivo. *Int J Cancer* 2013; **132**: 224-235.

6

Summary and General Discussion

Osteosarcoma is the most common primary malignant bone sarcoma occurring predominantly in children and adolescents, and a second peak at middle age. It is characterized for being highly metastatic and resistant to chemotherapy, which gives these patients very poor prognosis.[1,2]

Before the introduction of chemotherapy, patients with osteosarcoma had a low chance of surviving this tumor. Once it was introduced, their prognosis increased dramatically, however, it has reached plateau. To address this challenge, there have been many clinical trials with the goal to find the best combination of chemotherapeutic agents that can increase the overall survival rate.[3,4] However, until now, there has been no further improvement. New efforts are being made to find new drug targets such as kinases or signaling pathways of the immune system. Many clinical trials testing these new molecules have shown that single agent therapies are not effective.

The aim of this thesis was to find new strategies to reduce osteosarcoma viability or that could potentiate the effect of doxorubicin. These findings, if translated to the clinic, would allow the use of lower doses of doxorubicin and avoid serious side effects that compromise the patient's life. I used a variety of techniques including high-throughput screening using siRNA and inhibitor libraries, which led to the discovery of new potential treatments.

Cell lines

Cancer cell lines derived from tumors are the most common tumor used in cancer research, and it has been of tremendous value in the field. There are doubts about how representative they are of the tumors they came from, and many research groups have made efforts to identify cell lines which are most represent the type of tumor they come from.[5–7] However, it has been also been shown for 127 cancer cell lines, that when injected in nude mice, they all formed a tumor which resembled histologically the cancer type.[8] Additionally, cancer cell lines retain the genotype of the original tumor such as mutations and expression of a characteristic gene.[9]

In this thesis I used osteosarcoma cell lines that have fully characterized by Mohseny A, et al. All of the cell lines had the capacity to differentiate *in vitro* into at least one of the three histological subtypes of osteosarcoma. However, not all of them had the capacity to form tumor in nude mice.[10] The cell lines employed in these studies, were chosen based on the genetic profile of p53 and CDKN2A, which are two of the well-known altered genes in osteosarcoma.[11] Additionally, the identity of cell lines was confirmed using the Cell ID

GenePrint 10 system (Promega Benelux BV, Leiden, The Netherlands) before and after completion of the experiments, and mycoplasma tests were performed on a regular basis.

Targeting the cell cycle

The DNA Damage Response (DDR) is evolutionary conserved and essential to ensure the faithful maintenance and replication of the genome. This signaling cascade senses DNA damage and triggers repair, cell cycle arrest and, in case of severe damage, cell death.[12] Chemotherapeutic drugs such as doxorubicin cause DNA double strand breaks, DNA alkylation, topoisomerase inhibition II among many other mechanisms.[13] This type of DNA lesions activate the DDR which lead to cell cycle arrest allowing the tumor cells to repair the damage and continue dividing. In **Chapter 2**, I proposed Aven to be a new regulator of DNA damage response showing that it is a key regulator of ATR-Chk1 axis. Subsequently, I investigated the effect of CHK1 inhibition in combination with doxorubicin. For the first time in osteosarcoma, these findings indicate that abrogation of Chk1 signaling using clinically relevant drugs may be combined with chemotherapy to treat osteosarcoma more effectively. Cancer cell cycle deregulation is often caused by altered CDK activity.[14] Furthermore, osteosarcoma is characterized by alterations in Rb protein and CDK4, which leads to uncontrolled cell cycle progression. In **Chapter 3** a screen of kinase inhibitors revealed that osteosarcoma cells are sensitive to inhibitors targeting kinases that regulate the cell cycle among others. Overall, I show that osteosarcoma is highly dependent on the cell cycle kinases to proliferate, and this signaling network is a potential therapeutic target.

3D cultures

Tumors are a complex disease that is governed by many intracellular signals such as gain of function of oncogenes, loss of function of tumor suppressors and mutations in key proteins. However, tumor cells are also influenced by the extracellular environment such as cell-matrix and cell-cell interactions. 2D mono-layer cultures have been a powerful tool but it was shown that the cells divide abnormally, change shape and physiological behavior.[15,16] 3D culture models provide a platform in which the tumor cells can behave more like the real tumor, and can be used to study cell viability and metastatic behavior after treatment with inhibitors.

Throughout the whole thesis I set out to find approved or preclinical inhibitors, which were effective alone or in combination with doxorubicin. In **Chapter 2,4,5** I assessed viability

of the treated cells in 2D monolayer cultures, and validated these results in 3D culture models.

Importance of inhibiting migration

Ostesarcoma is a highly metastatic tumor and at the moment of diagnosis, 10-20% of the patients already present with metastasis. About 30-40% of the patients with localized osteosarcoma will relapse mainly by presenting lung metastasis. Patients with recurrence have very poor prognosis with 23-33% 5-year overall survival.[17,18]

Tumor cell migration to distant locations has already occurred in patients with metastases implicating that cell migration is not a therapeutically relevant aspect of tumor progression. However, it has been shown that short range-migration (dispersal) to adjacent sites affects tumor topology and growth rates. This is the case in primary tumors and metastatic tumors. Although the tumor origin is genetically homogeneous, clonal variations arise that change the fate of these cells leading to resistance to treatment, and regrowth of the tumor after months of the treatments. Recent modeling approaches have shown that short-range dispersal contributes to cell mixing inside the tumor and targeting cell migration could in fact considerably suppress tumor growth.[19] In **Chapter 5** I used two 3D models to study the inhibition of migration using dasatinib, saracatnib and bosutinib. Using the spheroid collagen injection model, dasatinib was the only inhibitor capable of containing the cells in the spheroid; it inhibited migration completely. In the other 3D model employed here, the cells were re-suspended as single cells in a collagen-matrigel mix allowing me to study their morphology under treatment conditions. In this case I exposed these cells to doxorubicin in combination with the inhibitors mentioned above. Strikingly, only the combination of dasatinib and doxorubicin induced the retraction of branches and a round shape morphology. These two experiments confirm each other, and indicate that dasatinib in combination with doxorubicin is an effective targeted therapy that may avoid recurrence. Doxorubicin together with dasatinib is a potential candidate for further clinical studies.

Signaling pathways involved in osteosarcoma cell survival

PI3K-Akt-mTOR pathway is a network that controls many cellular processes such as cell proliferation, survival, metabolism and genomic integrity.[20] The expression of mTOR is correlated with event-free survival and cancer progression in osteosarcoma[21]. A kinase

inhibitor screen described in **chapter 4** indicated PI3K/mTOR pathway as crucial: 37% of the hits were inhibitors that targeted this pathway. Another relevant signaling network for osteosarcoma is the cell cycle with 37% of the hits inhibiting kinases in this pathway, such as aurora kinases, Chk1, CDKs and Plk1.

The Ras-Raf-MEK-ERK mitogen activated protein kinase cascade is known to be involved in cell proliferation, survival, differentiation and development. It integrates signals from cell surface receptors that activate MEK, which will activate ERK. Once ERK is activated, it enters the nucleus and activates transcription factors such as c-Myc, c-Fos, Ets, and Elk-1.[22] In osteosarcoma, ERK pathway activity was reported to occur in 67% of the cases analyzed.[23] In **chapter 4**, I identified three MEK inhibitors in a screen, which led me to further investigate this pathway. Although no genomic or transcriptomic changes in the MEK pathway discriminated sensitive from insensitive cell lines, I could show that MEK inhibitors are only effective in cells where relatively high ERK activity can be detected. Thus, active, phosphorylated ERK (that may be detected by immunohistochemistry in clinical samples) may serve as a biomarker for treatment with MEK inhibitors.

In **Chapter 3** I investigated the anti-apoptotic protein Bcl-xL. The expression of Bcl-xL did not correlate with survival, but in osteosarcoma cells the inhibition of Bcl-xL did potentiate the effect of doxorubicin. Furthermore, it has been shown that Bcl-xL expression is dependent on ERK activity.[24,25] Strikingly, the osteosarcoma cell lines sensitive to MEK inhibition were also the ones with highest Bcl-xL expression and more sensitive to Bcl-xL inhibition. These results suggest that ERK expression could also be used as a marker for this strategy, pointing to a more personalized treatment.

Future perspectives

In this thesis I described several possible therapies to treat patients with osteosarcoma. These results come from *in vitro* studies, and must be tested in osteosarcoma animal models to be translated to the clinic. Mouse models are commonly used because of the close genetic and physiological resemblance to that of humans, and the ease with which they can be genetically modified to facilitate tumor formation.[26,27] Genetically engineered mouse models with *p53* and *Rb* deletions in the osteoblasts effectively induce osteosarcoma formation that resembles human osteosarcomas.[28] Another possible mouse model involves overexpression of *c-fos* and *c-jun* proto-oncogenes, which induces the formation of osteosarcoma.[29] This model allows the spontaneous formation of osteosarcomas that can be

used to validate novel treatments. Alternatives to genetic mouse models for further investigation of drugs and drug combinations used in this thesis include mouse or zebrafish xenografts with patient materials or patient-derived osteosarcomas cultured in a 3D collagen matrix. Such strategies allow testing of treatment options for specifically for a given patient.

REFERENCES

1. Luetke, A., Meyers, P. A., Lewis, I. & Juergens, H. Osteosarcoma treatment - where do we stand? A state of the art review. *Cancer Treat. Rev.* **40,** 523–32 (2014).

2. Rosenberg, A. . *et al.* in *WHO Classification of Tumours of Soft Tissue and Bone* (eds. Fletcher, C. D. M., Bridge, J. A., Hogendoorn, P. C. W. & Mertens, F.) 282–288 (2013).

3. Whelan, J. S. *et al.* EURAMOS-1, an international randomised study for osteosarcoma: results from pre-randomisation treatment. *Ann. Oncol.* **26,** 407–14 (2015).

4. Isakoff, M. S., Bielack, S. S., Meltzer, P. & Gorlick, R. Osteosarcoma: Current Treatment and a Collaborative Pathway to Success. *J. Clin. Oncol.* **33,** 3029–35 (2015).

5. Sandberg, R. & Ernberg, I. The molecular portrait of in vitro growth by meta-analysis of gene-expression profiles. *Genome Biol.* **6,** R65 (2005).

6. Ross, D. T. *et al.* Systematic variation in gene expression patterns in human cancer cell lines. *Nat. Genet.* **24,** 227–35 (2000).

7. Sinha, R., Schultz, N. & Sander, C. *Comparing cancer cell lines and tumor samples by genomic profiles*. *bioRxiv* (Cold Spring Harbor Labs Journals, 2015). doi:10.1101/028159

8. Fogh, J., Fogh, J. M. & Orfeo, T. One hundred and twenty-seven cultured human tumor cell lines producing tumors in nude mice. *J. Natl. Cancer Inst.* **59,** 221–6 (1977).

9. Masters, J. R. Human cancer cell lines: fact and fantasy. *Nat. Rev. Mol. Cell Biol.* **1,** 233–6 (2000).

10. Mohseny, A. B. *et al.* Functional characterization of osteosarcoma cell lines provides representative models to study the human disease. *Lab. Invest.* **91,** 1195–205 (2011).

11. Ottaviano, L. *et al.* Molecular characterization of commonly used cell lines for bone tumor research: a trans-European EuroBoNet effort. *Genes. Chromosomes Cancer* **49,** 40–51 (2010).

12. Kurz, E. U. & Lees-Miller, S. P. DNA damage-induced activation of ATM and ATM-dependent signaling pathways. *DNA Repair (Amst).* **3,** 889–900

13. Gewirtz, D. A. A critical evaluation of the mechanisms of action proposed for the antitumor effects of the anthracycline antibiotics adriamycin and daunorubicin. *Biochem. Pharmacol.* **57,** 727–41 (1999).

14. Malumbres, M. & Barbacid, M. Cell cycle, CDKs and cancer: a changing paradigm. *Nat. Rev. Cancer* **9,** 153–66 (2009).

15. Baker, B. M. & Chen, C. S. Deconstructing the third dimension: how 3D culture microenvironments alter cellular cues. *J. Cell Sci.* **125,** 3015–24 (2012).

16. Thoma, C. R., Zimmermann, M., Agarkova, I., Kelm, J. M. & Krek, W. 3D cell culture systems modeling tumor growth determinants in cancer target discovery. *Adv. Drug Deliv. Rev.* **69-70,** 29–41 (2014).

17. Buddingh, E. P. *et al.* Prognostic factors in pulmonary metastasized high-grade osteosarcoma. *Pediatr. Blood Cancer* **54,** 216–21 (2010).

18. Gelderblom, H. *et al.* Survival after recurrent osteosarcoma: data from 3 European Osteosarcoma Intergroup (EOI) randomized controlled trials. *Eur. J. Cancer* **47,** 895–902 (2011).

19. Waclaw, B. *et al.* A spatial model predicts that dispersal and cell turnover limit intratumour heterogeneity. *Nature* **525,** 261–4 (2015).

20. Perry, J. A. *et al.* Complementary genomic approaches highlight the PI3K/mTOR pathway as a common vulnerability in osteosarcoma. *Proc. Natl. Acad. Sci. U. S. A.* **111,** E5564–73 (2014).

21. Zhou, Q. *et al.* mTOR/p70S6K signal transduction pathway contributes to osteosarcoma progression and patients' prognosis. *Med. Oncol.* **27,** 1239–45 (2010).

22. Zhang, W. & Liu, H. T. MAPK signal pathways in the regulation of cell proliferation in mammalian cells. *Cell Res.* **12,** 9–18 (2002).

23. Pignochino, Y. *et al.* Sorafenib blocks tumour growth, angiogenesis and metastatic potential in preclinical models of osteosarcoma through a mechanism potentially involving the inhibition of ERK1/2, MCL-1 and ezrin pathways. *Mol. Cancer* **8,** 118 (2009).

24. Boucher, M. J. *et al.* MEK/ERK signaling pathway regulates the expression of Bcl-2, Bcl-X(L), and Mcl-1 and promotes survival of human pancreatic cancer cells. *J. Cell. Biochem.* **79,** 355–69 (2000).

25. Iwasawa, M. *et al.* The antiapoptotic protein Bcl-xL negatively regulates the bone-resorbing activity of osteoclasts in mice. *J. Clin. Invest.* **119,** 3149–59 (2009).

26. Waterston, R. H. *et al.* Initial sequencing and comparative analysis of the mouse genome. *Nature* **420,** 520–62 (2002).

27. Emes, R. D., Goodstadt, L., Winter, E. E. & Ponting, C. P. Comparison of the genomes of human and mouse lays the foundation of genome zoology. *Hum. Mol. Genet.* **12,** 701–9 (2003).

28. Walkley, C. R. *et al.* Conditional mouse osteosarcoma, dependent on p53 loss and potentiated by loss of Rb, mimics the human disease. *Genes Dev.* **22,** 1662–76 (2008).

29. Wang, Z. Q., Liang, J., Schellander, K., Wagner, E. F. & Grigoriadis, A. E. c-fos-induced osteosarcoma formation in transgenic mice: cooperativity with c-jun and the role of endogenous c-fos. *Cancer Res.* **55,** 6244–51 (1995).

SUMMARY

Osteosarcoma: searching for new treatment options

Osteosarcoma is the most frequent high-grade primary malignant bone tumor that is thought to arise from mesenchymal stem cells with the capacity to produce osteoid. The overall incidence is of three cases per million annually, and it occurs predominantly in children and adolescents as well as in people over 50 years of age.

Currently, the treatment consists of preoperative chemotherapy followed by resection of the tumor. The most effective systemic chemotherapeutics are cisplatin, doxorubicin and methotrexate. Despite extensive studies aimed at finding optimal combined chemotherapeutic strategies, overall 5-year survival rates have not increased above 70%, and around 35-45% of the patients have tumors that do not respond to chemotherapy.

The aim of this thesis was to discover new therapeutic options for osteosarcoma patients. I focused on finding candidate targets and pharmaceutical inhibitors for killing human osteosarcoma cells or for sensitizing osteosarcoma cells to doxorubicin. In **Chapter 2** I studied Aven, an adaptor protein that has been implicated in anti-apoptotic signaling and in DNA damage response signaling. The expression of Aven is inversely correlated with metastasis-free survival in osteosarcoma patients, and is increased in metastases compared to primary tumours. In tumour cells, silencing Aven triggered a G2 cell cycle arrest. Chk1 protein levels were attenuated and ATR-Chk1 DNA damage response signaling in response to chemotherapy was abolished in Aven-depleted osteosarcoma cells while ATM, Chk2, and p53 activation remained intact. It is not possible to target Aven, therefore I examined whether pharmacological inhibition of the Aven-controlled ATR-Chk1 response could sensitize osteosarcoma cells to doxorubicin. For this purpose, I tested pharmacological inhibitors targeting Chk1/Chk2 or selectively Chk1 in 2D and 3D cultures. Co-treatments in both culture systems led to effective sensitization to chemotherapy. Together, these findings implicate Aven in ATR-Chk1 signaling and point towards Chk1 inhibition as a strategy to sensitize human osteosarcomas to chemotherapy.

An siRNA screen targeting members of the Bcl-2 family in human osteosarcoma cell lines to identify critical regulators of osteosarcoma cell survival was performed in **chapter 3**. Silencing the anti-apoptotic family member Bcl-xL but also the pro-apoptotic member Bak caused loss of viability. Loss of Bak impaired cell cycle progression and triggered autophagy. Instead, silencing Bcl-xL induced apoptotic cell death. Clinical osteosarcoma samples showed expression of Bcl-xL, but mRNA or protein levels did not significantly correlate with therapy response or survival. Nevertheless, pharmacological inhibition of Bcl-xL synergistically

enhanced the response to the chemotherapeutic agent, doxorubicin. Indeed, in osteosarcoma cells strongly expressing Bcl-xL, the Bcl-xL-selective BH3 mimetic, WEHI-539 potently enhanced apoptosis in the presence of low doses of doxorubicin. Our results identify Bcl-xL as a candidate drug target for sensitization to chemotherapy in patients with osteosarcoma.

In **Chapter 4** I performed a kinase inhibitor screen in two osteosarcoma cell lines, which identified MEK1/2 inhibitors: Trametinib, AZD8330 and TAK-733. These inhibitors were further validated in a panel of six osteosarcoma cell lines of which three were sensitive and three resistant to these inhibitors. Western blot analysis revealed that sensitive lines had high constitutive ERK activity. Furthermore, experiments in which the cell lines were cultured in a 3D culture system and exposed to the inhibitors, validated the effect seen in 2D monolayer cultures. A gene expression analysis was performed to identify differentially expressed gene signatures in sensitive and resistant cell lines, and indicated an activation of the AKT signaling network in the resistant cell lines. In conclusion, MEK1/2 inhibition represents a candidate treatment strategy for osteosarcomas displaying high MEK activity as determined by ERK phosphorylation status.

Chapter 5, focuses on elucidating the effect of three Src inhibitors, dasatinib, bosutinib and saracatinib, on osteosarcoma viability and cell migration using 2D cultures and validation in 3D culture systems. Expression and activity of the Src cytoplasmic tyrosine kinase has been correlated with clinical stage and survival. All inhibitors were tested in combination with doxorubicin showing a reduction of the IC50 of this chemotherapeutic. However, only dasatinib treatment triggered caspase3/7 activation, and decreased Src activity. The effects of the inhibitors were studied in 3D extracellular matrix (ECM) scaffolds. Under these conditions, all three inhibitors reduced viability but formation of branched networks in 3D cultures was selectively inhibited by dasatinib in presence of doxorubicin. The activity of focal adhesion kinase (FAK), a Src substrate that is important for cell migration, was exclusively sensitive to dasatinib. Additionally, in 3D ECM-embedded spheroid cultures dasatinib blocked cell migration capacity whereas the other inhibitors had no or partial effects. Together, these findings point to the use of dasatinib as a candidate drug to enhance apoptosis in response to chemotherapy and to reduce metastatic spread in patients with osteosarcoma.

In summary, the work presented in this thesis provides four new candidate treatment options for osteosarcoma. These studies provide the basis to continue this research in animal models, which may then be translated to the clinic.

SAMENVATTING

Osteosarcoom: de zoektocht naar nieuwe behandelingen

Osteosarcoom is de meest voorkomende hooggradige primaire kwaardaardige bot tumor. De tumor ontstaat waarschijnlijk uit mesenchymale stamcellen die de mogelijkheid hebben tot vorming van botweefsel. De incidentie is jaarlijks drie gevallen op één miljoen mensen, voornamelijk kinderen, adolescenten en mensen ouder dan 50 jaar.
Op dit moment bestaat de behandeling uit pre-operatieve chemotherapie gevolgd door chirurgische verwijdering van de tumor. De meest effectieve chemotherapeutica die systemisch werken zijn cisplatine, doxorubicine en methotrexaat. Ondanks intensieve studies naar de optimale strategie om chemotherapeutica te combineren, zijn de algemene vijfjaarsoverlevingskansen niet boven de 70% gestegen. Daarbij hebben 30-45% van de patiënten tumoren die niet reageren op chemotherapie.

Het doel van deze thesis was om nieuwe therapeutische opties voor osteosarcoom patienten te ontdekken. Ik heb me daarbij gericht op het vinden van mogelijke genen en farmaceutische remmers die humane osteosarcoom cellen kunnen doden of gevoeliger maken voor doxorubicine.

In **Hoofdstuk 2** heb ik Aven bestudeerd, een adapter eiwit waarvan gedacht wordt dat het een rol speelt in anti-apoptotische signalering en DNA schade respons. De expressie van Aven is omgekeerd gecorreleerd met metastasevrije overleving in osteosarcoom patiënten, en is verhoogd in metastases vergeleken met primaire tumoren. In tumorcellen induceert het uitschakelen van Aven een G2 celcyclus arrest. De hoeveelheid Chk1 eiwit is verlaagd en na chemotherapie en het uitschakelen van Aven was de ATR-Chk1 DNA schade respons volledig verdwenen. Dit terwijl de activering van ATM, Chk2 en p53 intact bleef. Omdat het niet mogelijk is om de functie van Aven te remmen, heb ik onderzocht of farmacologische remming van de Aven-gecontroleerde ATR-Chk1 respons osteosarcoom cellen gevoeliger kon maken voor doxorubicine. Om dit te bereiken heb ik in 2D en 3D kweeksystemen farmacologische remmers getest die zich richten op de functie van Chk1/Chk2 of selectief zijn voor Chk1. Gelijktijdige behandeling in beide kweeksystemen leidde tot effectieve sensitivering voor chemotherapie. Gezamenlijk impliceren deze vindingen dat Aven een rol speelt in ATR-Chk1 signalering en wijzen naar inhibitie van Chk1 functie als een strategie om humane osteosarcomen gevoeliger te maken voor chemotherapie.

Om essentiële regulatoren van cel overleving te identificeren heb ik een siRNA screen uitgevoerd, die zich richtte op de Bcl2 eiwitfamilie, in **Hoofdstuk 3**. Het uitschakelen van het anti-apoptotische eiwit Bcl-xL, maar ook het uitschakelen van het pro-apoptotische eiwit Bak zorgde voor minder levensvatbaarheid van de cellen. Het uitschakelen van Bak blokkeerde het proces van de celcyclus en induceerde autofagie. Daarentegen induceerde het uitschakelen van Bcl-xL apoptotische celdood. Klinische osteosarcoom samples lieten expressie van Bcl-xL zien, maar de hoeveelheid mRNA of eiwit correleerde niet significant met de respons op therapie of overlevingskans. Desalniettemin, farmaceutische inhibitie van Bcl-xL verhoogt op een synergistische manier de respons op doxorubicine. Inderdaad, in osteosarcoma cellen met sterke expressie van Bcl-xL, verhoogde een selective Bcl-xL BH3 mimetic (WEHI-539) in combinatie met lage doses doxorubicine apoptose sterk. Deze resultaten identificeren Bcl-xL als kandidaat target gen voor nieuwe medicijnen, die in combinatietherapie de osteosarcoom in patienten gevoeliger zou kunnen maken voor de chemotherapie.

In **hoofdstuk 4** heb ik een kinase remmer screen in twee osteosarcoom cellijnen uitgevoerd waaruit drie MEK1/2 remmers (Trametinib, AZD8330 & TAK-733) interessant bleken te zijn. Deze remmers werden verder gevalideerd door gebruik te maken van zes osteosarcoom cellijnen, waaronder drie gevoelige cellijnen en drie ongevoelige cellijnen. Western Blot analyse liet zien dat met name in de gevoelige cellijnen ERK-activering verhoogd was. Bovendien bevestigden experimenten waarin de cellijnen in een 3D system werden gekweekt en vervolgens blootgesteld werden aan de remmers het effect dat aanvankelijk in 2D celkweek systemen werd gezien. Om verschillen in genexpressie tussen gevoelige en ongevoelige cellijnen te identificeren, werd een genexpressie analyse uitgevoerd. Daaruit bleek dat activering van de AKT signaalcascade vooral bij ongevoelige cellijnen voorkwam. Ten slotte, het remmen van MEK1/2 vormt een mogelijk behandelingstrategie bij osteosarcomen die een hoog niveau van MEK activatie hebben, wat bepaald kan worden door de fosforyleringsstatus van ERK.

Hoofdstuk 5 richt zich op de effecten van drie Src-remmers (Dasatinib, Bosutinib & Saracatinib) op de levensvatbaarheid en migratie van osteosarcomen in 2D, en voor validatie ookin 3D kweeksystemen. De expressie en activiteit van de cytoplasmatische kinase Src is gecorreleerd met klinische fase en overlevingskans. Alle remmers werden in combinatie met doxorubicine getest, wat tot een vermindering van de IC50 voor doxorubicine leidde. Desalniettemin, alleen behandeling met dasatinib leidde tot activatie van caspase3/7 en verminderde activering van Src. In 3D extracellulaire matrix (ECM) kweeksystemen verhinderden alledrie de remmers levensvatbaarheid, maar het vormen van netwerken van vertakkingen werd uitsluitend geremd door dasatinib in combinatie met doxorubicine. De

activiteit van focal adhesion kinase (FAK), een substraat van Src dat belangrijk is voor celmigratie, toonde uitsluitend gevoeligheid voor dasatinib. Daarbovenop werd celmigratie in 3D ECM-ingebedde sferoïde kweeksystemen alleen geremd door dasatinib terwijl de andere remmers er geen of alleen gedeeltelijk effect op hadden. Als geheel wijzen deze resultaten erop dat dasatinib ertoe in staat is om apoptose in combinatie met chemotherapie te verhogen en wellicht metastatische verspreiding in osteosarcoom patiënten te verhinderen.

Samengevat, het hier beschreven onderzoek heeft vier potentiele mogelijkheden voor de behandeling van osteosarcoom opgeleverd. Deze studies vormen de basis voor eventuele dierproeven, die uiteindelijk naar een klinisch relevante oplossing kunnen worden vertaald.

LIST OF PUBLICATIONS

Aven-mediated checkpoint kinase control regulates proliferation and resistance to chemotherapy in conventional osteosarcoma

***Zuzanna Baranski**, Tijmen H. Booij, Anne-Marie Cleton-Jansen, Leo Price, Bob van de Water, Judith V. M. G. Bovée, Pancras C.W. Hogendoorn, Erik H.J. Danen. J Pathol* **236**:348-359, 2015

Pharmacological inhibition of Bcl-xL sensitizes osteosarcoma to doxorubicin

***Zuzanna Baranski**, Yvonne de Jong, Trayana Ilkova, Elisabeth F.P. Peterse, Anne-Marie Cleton-Jansen, Bob van de Water, Pancras C.W. Hogendoorn, Judith V. M. G. Bovée, Erik H.J. Danen. Oncotarget* **6**:36113-36125, 2015

MEK inhibition induces apoptosis in osteosarcoma cells with constitutive ERK1/2 phosphorylation

***Zuzanna Baranski**, Tijmen H. Booij, Marieke L. Kuijjer, Yvonne de Jong, Anne-Marie Cleton-Jansen, Leo S. Price, Bob van de Water, Judith V. M. G. Bovée, Pancras C.W. Hogendoorn, Erik H.J. Danen. Genes and Cancer*, **in press** 2015

SYK Is a Candidate Kinase Target for the Treatment of Advanced Prostate Cancer

*Ghotra VP, He S, van der Horst G, Nijhoff S, de Bont H, Lekkerkerker A, Janssen R, Jenster G, van Leenders GJ, Hoogland AM, Verhoef EI, **Baranski Z**, Xiong J, van de Water B, van der Pluijm G, Snaar-Jagalska BE, Danen EH. Cancer Research* **75**:230-240, 2015

Dasatinib Src inhibitor selectively triggers apoptosis and loss of invasive potential in human osteosarcoma cells

***Zuzanna Baranski**, Tijmen H. Booij, Anne-Marie Cleton-Jansen, Leo Price, Bob van de Water, Judith V. M. G. Bovée, Pancras C.W. Hogendoorn, Erik H.J. Danen.* Manuscript in preparation

CURRICULUM VITAE

Zuzanna Baranski Madrigal was born on the 21st of March of 1981 in San Jose, Costa Rica. She studied Pharmacy at the University of Costa Rica from 2000 to 2006. After obtaining her degree, she worked as a pharmacist in Costa Rica from 2006 to 2008. After this period, she travelled to The Netherlands to obtain her Master degree in Biopharmaceutical Sciences at Leiden University. She obtained her degree in 2011.

In 2011 she started as a PhD student at the department of Toxicology at LACDR Institute in Leiden University, under the supervision of Dr. Erik Danen. The project was part of the Translational Drug Discovery and Development grant: Identification and validation of novel kinase drug targets for sarcoma growth & therapy resistance.

She started a postdoctoral fellowship with Dr. Erik Danen the 1st of February, 2016.